Norwegian
University of
Life Sciences

Master's Thesis 2026 30 ECTS
Faculty of Science and Technology

Pathways to a Net-Zero Nordic Power System: A Large-Scale 2050 Optimization Study Using PyPSA-Eur

Jonas Jortveit Andresen
Environmental Physics and Renewable Energy

Abstract

The Nordic power system is currently undergoing a crucial transformation to align with the European Union's target of net-zero emissions by 2050. To achieve this, high integration of renewable energy sources and significant expansion of the transmission network are necessary. This study explores cost-optimal development pathways of this transition under varying constraints for renewable energy deployment. Utilizing the PyPSA-Eur modeling framework, four distinct scenarios are simulated to quantify the dynamics between domestic renewable capacity limits, regional system costs, and the necessity of power trade interconnections with continental Europe.

The results indicate that significant transmission expansion is required regardless of scenario, with the capacity of AC lines increasing by 42.1% to 72.8%, and HVDC interconnectors by up to 662%. When capacity expansion is constrained to align with official projections, the model installs a total renewable capacity of 251.5 GW at an annualized Nordic system cost of 14.0 BEUR/year. In contrast, when the system is allowed to freely optimize renewable integration without policy bounds, it deploys 423.7 GW of renewable capacity. However, the associated wind power expansion relies on sector-coupled hydrogen demands that significantly exceed official projections, indicating potential over-estimation. While the latter configuration provides the cost-optimal solution for the broader European power system, it implies an increase of Nordic costs to 15.6 BEUR/year. To ensure stability in the Nordic power system, the model favors an expansion of power trade capabilities with continental Europe and the UK over heavily investing in domestic storage facilities such as batteries and hydrogen.

This study demonstrates that a reliable and cost-efficient carbon-neutral Nordic power system by 2050 is feasible through large-scale expansion of renewable generation capacity, coupled with an integrated European transmission network. The cost mismatch between regional and continental optimization highlights that realizing these optimal pathways will require trans-national cost-sharing agreements, rather than relying solely on isolated Nordic investments. Future research should also account for factors such as multi-year weather variations and socio-political constraints, to provide a more accurate prediction of the Nordic energy transition.

Sammendrag

Det nordiske kraftsystemet gjennomgår en viktig omstilling for å møte EUs mål om netto nullutslipp innen 2050. For å klare dette er det nødvendig med en sterk utbygging av fornybar energi og en betydelig oppgradering av kraftnettet. Denne studien undersøker kostnadsoptimale utviklingsløsninger for denne overgangen, gitt varierende begrensninger for fornybar utbygging. Fire ulike scenarioer blir simulert ved bruk av modelleringsverktøyet PyPSA-Eur, og sammen identifiserer scenarioene samspillet mellom ulike nivåer av fornybar produksjonskapasitet i Norden, regionale systemkostnader og avhengighet av tilkobling og krafthandel med resten av Europa.

Resultatene viser at en betydelig oppgradering av kraftnettet er nødvendig, med en utvidelse av transmisjonsnettet som går fra 42,1 % til 72,8 %, og HVDC-utenlandskabler utvides med opptil 662 %. Når utbyggingen av fornybar energi er satt til å følge offisielle prognoser, installeres en fornybar effekt på 251,5 GW, noe som gir en årlig systemkostnad på 14,0 mrd.EUR/år. Derimot blir en fornybar effekt på 423,7 GW installert når systemet er fritt til å kostnadsoptimaliseres, uten hensyn til offisielle tall. Den tilhørende veksten i vindkraft avhenger imidlertid av en sektorkoblet hydrogenetterspørsel som er betydelig større enn i offisielle prognoser, og indikerer en mulig overestimering. Selv om dette scenarioet resulterer i den laveste totalkostnaden for det europeiske kraftsystemet, øker den nordiske kostnaden til 15,6 mrd.EUR/år. For å sikre stabilitet i det nordiske systemet favoriserer modellen utvidelse av muligheten for krafthandel med resten av Europa, fremfor omfattende investeringer i interne lagringssystemer som batterier og hydrogen.

Denne studien viser at et stabilt og kostnadseffektivt kraftsystem i Norden kan oppnå karbonnøytralitet innen 2050. Dette forutsetter en storskala utbygging av fornybar produksjonskapasitet kombinert med et integrert europeisk overføringsnett. Det økonomiske avviket mellom regional og kontinental optimalisering understreker at realisering av disse scenarioene krever internasjonale avtaler for kostnadsdeling, fremfor en isolert avhengighet av nordiske investeringer. Videre forskning bør ta høyde for værvariasjoner over flere år, samt sosio-politiske begrensninger, for å gi en mer nøyaktig vurdering av den nordiske energiomstillingen.

Acknowledgements

The submission of this thesis marks the finish-line of my five years as a student at NMBU. These years have brought me both new friendships, hobbies, and a greater love for physics. I will forever be grateful of my years as a student in Oslo and Ås.

A big thank you is due to my great supervisor, Leonardo Rydin Gorjão. You have provided fantastic support and discussions, nudged me in the right directions, and enabled me to complete a thesis far beyond what I expected. I also want to thank Vetle Malum, who did some initial heavy lifting in this research area, giving me the opportunity to further build on his work.

An honorable mention also goes to my favorite person in the whole world, my lovely wife Johanne. You are my greatest support in all my adventures in life, including this one. Thank you for standing by my side through good and rough times, you rock!

Lastly, before it's time for me to enjoy both some road biking and traveling, I would like to acknowledge the Great Creator of this wonderful universe, and His systematic creation of math and physics for me to enjoy. The more I learn, the more I realize that this all simply cannot be a coincidence.

> *In the beginning God created the heavens and the earth. Now the earth was formless and empty, darkness was over the surface of the deep, and the Spirit of God was hovering over the waters. And God said, "Let there be light," and there was light.*
> (Genesis 1:1-3)

Contents

List of Figures

List of Tables

List of Acronyms

AC	Alternating Current
AI	Artificial Intelligence
BODF	Branch Outage Distribution Factor
BEUR	Billion Euros (10^9)
CCS	Carbon Capture and Storage
DAC	Direct Air Capture
DLR	Dynamic Line Rating
EU	European Union
ENS	Energy Not Served
ENTSO-E	European Network of Transmission System Operators for Electricity
ENTSO-G	European Network of Transmission System Operators for Gas
GHG	Greenhouse Gas
HSAT	Horizontal Single-Axis Tracker
HVDC	High-voltage Direct Current
IEA	International Energy Agency
IRENA	International Renewable Energy Agency
KVL	Kirchhoff's Voltage Law
OSM	OpenStreetMap
PEID	Power Electronic Interfaced Devices
PHS	Pumped Hydro Storage
PPM	Powerplantmatching
PV	Photovoltaic
PyPSA	Python for Power System Analysis
RoR	Run of River

SOC State of Charge

TMY Typical Meteorological Year

TSO Transmission System Operator

TYNDP Ten Year Network Development Plan

UN United Nations

vRES Variable Renewable Energy Sources

1 Introduction

1.1 Motivation

The usage of fossil fuels for energy generation releases significant amounts of CO_2 and other greenhouse gases into the atmosphere, which is a major cause of climate change [1]. In an effort to limit the consequences of fossil fuel burning, the European and Nordic power systems are currently undergoing a major transition towards clean energy supply, which is necessary to meet the European Union's target of net-zero emissions by 2050 [2]. In order to achieve this, a key effort is to shift electricity production from fossil-fueled sources to renewable energy generation like wind, solar photovoltaics (PV) and hydropower. The Nordic countries play a central part in this development, and face both opportunities and challenges in doing so. Combined, the energy generation capacity from fossil-free sources within the Nordics is projected to nearly triple by 2050, rising from roughly 125 GW in 2023 to 340 GW by 2050 [3]. With such a significant expansion, it is clear that an efficient, stable and secure power grid must be developed within the Nordic region [4].

However, this transformation introduces several challenges. The power output from renewable energy sources, such as wind and solar, is highly dependent on the weather. This dependency leads to unstable and variable generation, which complicates their integration into the power system. Unlike the inherent stability provided by conventional generators, this variability can lead to imbalances and instability in the grid. To address these complexities, large-scale models that account for both spatial distribution of power generation and its temporal variability can be used to explore different pathways for power system development. Such models allow for analysis of how renewable resources affect the grid by identifying highly loaded components, finding ways to minimize expansion costs, and exploring storage and power trade as solutions for balancing the system in a carbon-neutral future [5].

Within the Nordic context, navigating these integration complexities requires modeling tools that accurately reflect the physical and economic properties of the region. While previous expansion studies have analyzed the Nordics as an isolated system [6,7], this simplification overlooks the significant impact of cross-border power trade. Integrating HVDC interconnections to Continental Europe and the UK is therefore necessary, as these components are able to manage energy surpluses and deficits in the Nordics, in addition to enabling clean power supply from the Nordic system to the broader European grid. Consequently, by incorporating these external connections and aligning with the latest Nordic grid development plans [3], the PyPSA-Eur framework can be utilized to simulate realistic 2050 transition pathways. Analyzing such pathways identifies the necessary balance of renewable power generation, energy storage, and grid reinforcements required to achieve a cost-efficient transition to a carbon-neutral Nordic power system.

1.2 Research Question

To provide a more comprehensive assessment of the future Nordic power system, this study aims to address the following question:

> How do varying capacity constraints on renewable energy expansion in cost-optimal modeling of power system technologies impact the configuration of a carbon-neutral Nordic system by 2050?

To answer this question, the PyPSA-Eur modeling framework is utilized to simulate the capacity expansion of the Nordic power system towards 2050. By exploring different development pathways, the study identifies the grid reinforcements required to meet growing electricity demand and enable cross-border power trade. It also explores cost-optimal generation mixes of renewable energy sources across the different scenarios. Furthermore, the research evaluates the flexibility and storage mechanisms required to balance variable renewable generation, ensuring reliable power delivery. Together, these elements provide a comprehensive projection of the overall system configuration required to achieve a carbon-neutral Nordic grid.

2 Background

This chapter provides an overview of the Nordic power system and its associated transmission grid development projections. Section 2.1 presents the goal of reaching net-zero emissions by 2050. Section 2.2 presents the Nordic power system, while Section 2.3 summarizes Statnett's current development plan for Norway. Section 2.4 explores the integration and price-linking between the Nordic and European systems, before the impacts of variable generation are detailed in Section 2.5. Lastly, optimization modeling of energy systems is presented in Section 2.6, before relevant literature to this thesis is presented in Section 2.7.

2.1 The Goal of Net Zero Emission

The usage of fossil fuels is the single biggest contributor to emissions of greenhouse gases (GHGs), such as CO_2, worldwide [8]. In 2024, fossil fuels accounted for 79% of the global energy mix. This comprises all energy sectors, such as electricity, heat and transportation. In terms of electricity generation alone, fossil fuels accounted for nearly 60% of the worldwide generation in 2024, whereas the European share was slightly below 30%. The remaining electricity generation in Europe came from *low-emission sources* that have very low to no GHG emissions, consisting of renewable energy (48%) and nuclear power (23%) [9]. While low-emission sources dominate the electricity mix in Europe, these numbers illustrate a continued dependence on fossil fuels, which is not compatible with the goal of limiting further global warming.

In 2015, the United Nations (UN) adopted the Paris Agreement, which set out to limit the rise in global average temperature to well below 2 °C compared to pre-industrial levels, with the additional aim of keeping the increase close to 1.5 °C [10]. While 2024 was recorded as the first individual year to surpass the 1.5 °C mark [11], this single-year anomaly does not constitue a definitive failure of the agreement. However, according to the latest report from the International Energy Agency (IEA) [9], exceeding the 1.5 °C target as a sustained, multi-year average is now considered inevitable. Nevertheless, limiting the long-term increase to 2 °C remains achievable, and staying below this limit is recognized as vital in order to limit extreme, irreversible changes to the global climate.

In order to align with the Paris Agreement, the European Union (EU) has set a goal of reaching net-zero emissions by 2050 [2]. Alongside various initiatives across economic sectors in the EU, achieving the net-zero target will require a substantial transformation and expansion of the European energy sector. A key element is the rapid replacement of fossil fuels with renewable energy as a source of electricity generation. This becomes especially important in light of the expected rise in electricity demand driven by the electrification of energy-intensive industry and transport [2,9]. Growth of electricity demand is also expected in the Nordic countries, which means that the Nordic power system must be expanded to align with the net-zero goal of the EU.

2.2 The Nordic Power System

The Nordic power system is an interconnected synchronous region spanning Norway, Sweden, Finland, and the region of Sjælland in Denmark. Within this region, the Nordic power system operates as an alternating current (AC) network with a nominal frequency of 50 Hz, primarily maintained by synchronous generators in hydropower and nuclear facilities [12]. While other European systems depend heavily on fossil-fuel-based thermal generation, the Nordic system has a higher share of low-emission sources in its generation mix [13]. In 2023, renewable energy sources accounted for 78% of electricity generation in the Nordic region, with nuclear power contributing a further 18% to the overall mix. Thus, 96% of the Nordic production was fossil-free and emitted no GHGs. This number far exceeds the EU average of 64%, while fossil fuels accounted for 34% of electricity generation [13,14].

In Norway, hydropower plays a key part in the power mix. The many water reservoirs act as natural storage units that can store energy and generate electricity when needed [15]. In 2024, hydropower alone supplied 89% of Norway's total electricity generation [16]. Finland's electricity mix is dominated by nuclear generation at a 40% share, which provides a stable baseload supply to the Nordic region [17]. Denmark's Sjælland depends largely on wind and solar power, which together account for 69% of electricity generation, introducing variability to the system and increasing its complexity [18]. Lastly, Sweden has the most balanced mix of the Nordic countries, with hydro, nuclear, and wind contributing approximately 38%, 29%, and 24%, respectively, in 2024 [19]. Together, these energy sources comprise the majority of the Nordic electricity supply profile.

Being an interconnected, synchronous region, the Nordic countries are internally connected through a high-voltage AC grid. Within the region, the system is divided into *bidding areas*, which are geographical market zones with distinct electricity prices [12]. These bidding areas are used as a tool to ensure that the power market reflects the physical grid limitations [3]. Furthermore, the system is complemented by high-voltage direct current (HVDC) links to neighboring European countries. These interconnections support cross-border electricity trade and enhance system reliability [12]. Key HVDC connections from Norway are NorNed to the Netherlands, North Sea Link to the UK, NordLink to Germany, and Skagerrak to Denmark. SwePol and NordBalt connect Sweden to Poland and Lithuania, respectively, while Estlink connects Finland to Estonia [12]. Figure 2.1 displays a simplified representation of this structure, including the bidding areas and HVDC interconnections.

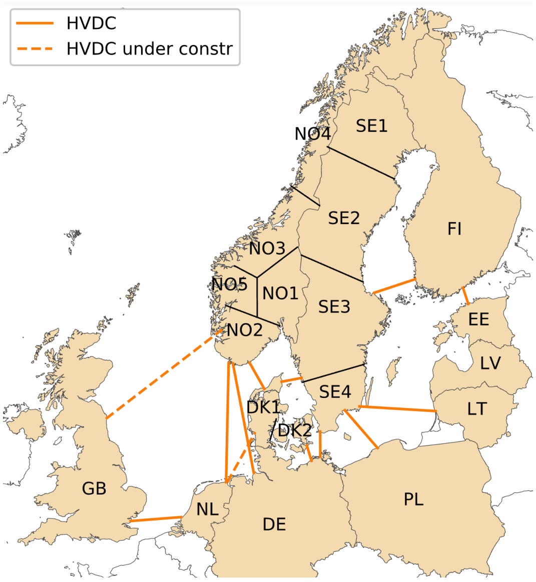

Figure 2.1: A simple representation map of the Nordic power system, with interconnections to European countries included. Note that North Sea Link is no longer under construction [20]. The figure shows a rough outline of the bidding areas of Norway, Sweden, and Denmark, and includes the Baltic countries, Poland, Germany, the Netherlands, and Great Britain in addition to the Nordic countries. Reused with permission from [21].

2.2.1 Nordic Grid Development Perspective

European and Nordic power systems are currently in the middle of a significant transformation. Statnett is reporting rising power generation from wind and solar, growth in grid expansion projects and increasingly volatile power prices [22]. The transition to a carbon-neutral energy system by 2050 requires an extensive renewal of the infrastructure. Official projections forecast an aggressive, parallel expansion of both electricity consumption and renewable generation capacity across the region [3].The growth in consumption is mainly driven by the electrification of industry, expansion of energy-intensive industry, and data centers, but is partly restricted by how much generation increases. New electricity generation will mostly come from variable wind and solar power, also backed up by storage units such as hydrogen stores and battery-provided power.

Figure 2.2 shows the Nordic mix of electricity production capacity in 2023, and the development of this mix towards 2050 as projected by the Nordic Transmission System Operators (TSOs). In 2023, the Nordic power system had a combined production capacity of approximately 125 GW. Within 2050, this is projected to nearly triple, reaching around 340 GW.

It is expected that the most significant growth in generation capacity will come from variable renewable energy sources (vRES), such as solar PV, onshore wind, and off-

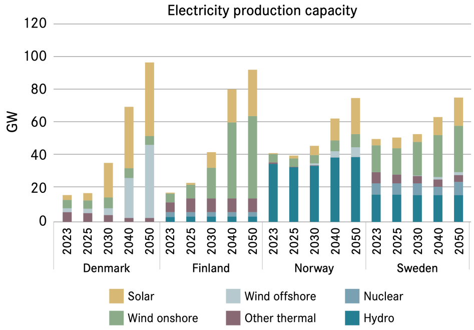

(a) Projection of electricity production capacity in the Nordic countries from 2023 to 2050, measured in GW. Capacity is split by country and color-coded by generation sources. Across all Nordic countries, solar and wind production increase, while nuclear power, hydropower, and thermal power remain constant or decrease.

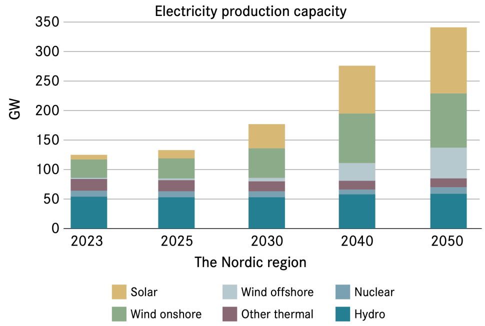

(b) Projection of electricity production capacity in the Nordic countries from 2023 to 2050, measured in GW. Capacity is aggregated for the whole region and color-coded by generation sources. Production from hydro and nuclear remain constant, thermal decrease slightly, while solar and wind generation increase significantly.

Figure 2.2: Projected expansion of electricity production in the Nordic countries, from the Nordic TSOs' grid development plan. (a) shows the production split by country, while (b) shows the aggregated projection for the whole Nordic region. Figure reused from [3].

shore wind power. Hydropower and nuclear power generation are projected to remain constant, which indicates no further development of these generation carriers. Additionally, a decrease in production from other thermal sources is expected due to the effort of phasing out fossil fuels for electricity production [3]. These projections are a part of the *Nordic Grid Development Perspective 2025*, made in a joint effort between the four Nordic TSOs, namely Svenska Kraftnät, Energinet, Fingrid, and Statnett. This report identifies necessary actions in the Nordics to meet rising electricity demand and ensure a reliable transmission system, including grid expansion and renewal of over 16 800 km of transmission lines, alongside the near tripling of generation capacity to roughly 340 GW. Such investments are required to maintain a strong and reliable Nordic power system, while keeping up with rising demand and reaching net-zero by 2050. In Norway, a major effort is Statnett's investment of roughly 12.5 billion euros (BEUR) in the national grid, mainly going towards upgrading the existing 300 kV network to 420 kV [3].

In recent years, geopolitical shifts, global competition, and high costs of selected technologies such as offshore wind and nuclear power have increased the Nordic TSOs' uncertainty regarding system development. Furthermore, the Nordic TSOs have intensified their cooperation on security and preparedness, primarily due to Russia's war in Ukraine and changes in the international order [3]. Although existing cross-border connections allow for the sharing of complementary energy resources, where flexible hydropower from Norway and Sweden can balance variable wind and solar generation in Denmark and Finland, the TSOs aim to expand these cross-border transmission capacities. Expanding this cooperation will strengthen the security of supply beyond current national capabilities and reduce the need for domestic reserve capacities. Such a deeply integrated Nordic system, where interconnectors allow countries to rely on each other's generation mixes, is projected to further improve resource use and reduce overall system costs [3].

An increasing share of solar PV and wind power, and thus Power Electronic Interfaced Devices (PEID), is expected to rapidly change the technical characteristics of the Nordic power system. PEIDs are devices that traditionally connect vRES to the power system by converting their output in real time to match the characteristics of the grid [23]. Higher shares of these devices will affect the system's reliability, due to their fundamental difference from synchronous generators that carry inertia, as further presented in Section 2.5. In response, the Nordic TSOs are coordinating efforts on common guidelines and monitoring frameworks to manage converter-related stability issues. This includes the development of a joint guideline for grid-forming functionality, a technology that allows PEIDs to actively contribute to the stabilizing of the grid's voltage and frequency. These guidelines will ensure that grid-forming capabilities are implemented in a consistent way across the Nordics, strengthening system flexibility and supporting stable operation as the system develops.

Beyond these challenges following PEID integration, the utilization of the grid is further limited by fixed and conservative transmission capacity ratings, which are in place due to thermal constraints. This limitation highlights the need for new solutions and operational practices [3]. An example of such operational practices is the implementation of Dynamic Line Rating (DLR), which is a tool that dynamically determines the capacity limit for a line based on actual weather conditions, allowing for increased utilization of existing lines [24].

2.3 Grid Development Plan from Statnett

The Norwegian transmission grid is facing an increase in both electricity demand and new generation requests, with over 8000 MW of consumption capacity already reserved in the Norwegian grid [22]. To address the necessary expansion, Statnett plans to invest up to 200 billion NOK in grid development over the next decade [4]. These investments will enable increased grid capacity by upgrading existing transmission lines as well as building new ones. Key priorities include reinforcing capacity between domestic bidding areas, as well as enhancing cross-border interconnections with Sweden and Finland [22]. Figure 2.3 shows the planned developments within Norway by 2050, primarily consisting of voltage upgrades from 300 kV to 420 kV [4].

Statnett has established clear strategies for the planned grid development. Some transmission paths which are currently creating bottlenecks in the Norwegian system are being prioritized and are expected to be fully upgraded by 2040. These

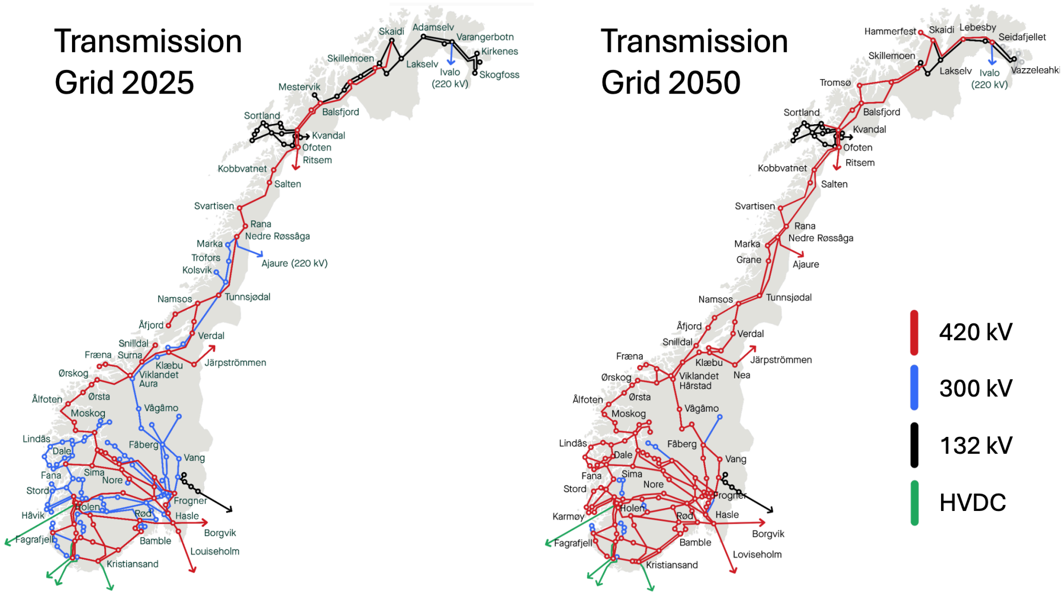

Figure 2.3: The left map shows the current Norwegian transmission grid in 2025. The right map shows the target grid, according to Statnett's grid development plan. Note that while the figure states 2050, Statnett aims to reach the target grid in roughly 20 years from 2025, indicating the realization might be done by 2045. The target shows a widespread upgrade of existing 300 kV lines to 420 kV. Red lines are 420 kV, blue lines are 300 kV, black lines are 132 kV, and green lines are interconnecting HVDC cables. Reproduced with changes from [4].

include the connections between Northern and South-Western Norway, Southern and Eastern Norway, Mid-Norway to Oslo, and Helgeland to Sweden [4]. All of these paths will have lines upgraded from 300 kV to 420 kV, and some supplemented with new 420 kV lines.

Another priority for Statnett is the development of a more reliable and flexible power system. As of 2024, renewable energy accounted for 48% of the electricity mix in Europe, and towards 2050 it is expected that production growth will mainly come from wind and solar power [22]. Alongside fossil fuel generation being phased out, this development yields an expected power deficit during hours with low wind and irradiance, thus calling for smart solutions in energy storage and grid flexibility. During such power deficit situations, meeting the system demand can be enabled through storage solutions, such as batteries, hydrogen storage and pumped hydro storage (PHS). These technologies are able to store excess energy during periods of low demand, and dispatch that energy when the system needs it [25]. For their part, Statnett addresses the challenge by expanding and upgrading the transmission grid. This effectively brings the system components closer together from an electrical standpoint, increasing capacity, flexibility, and overall system strength [4].

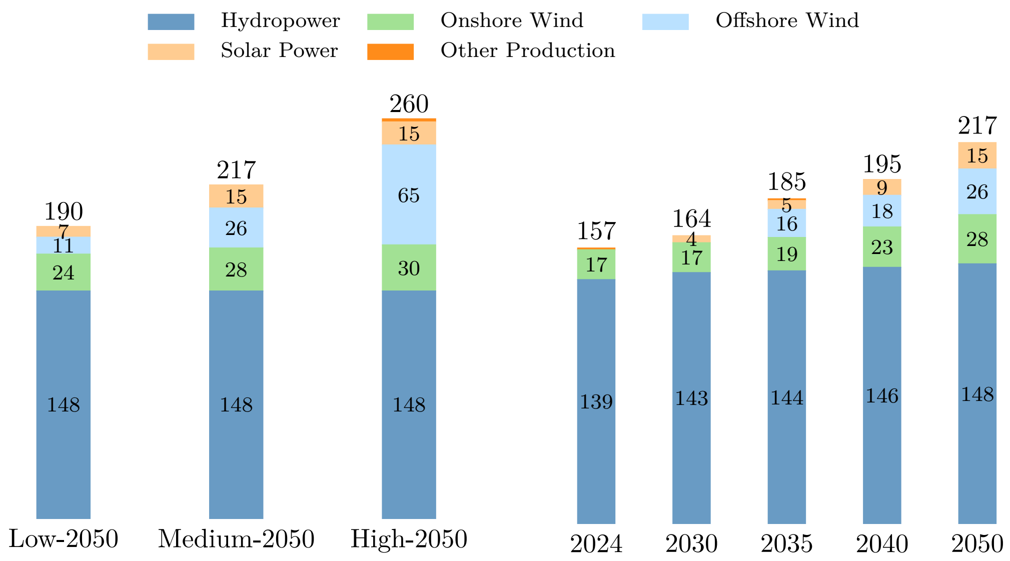

(a) Projected development of electricity production [TWh] in Norway in 2050, for three scenarios. Production is color-coded by source. The medium scenario is based on achieving net-zero emissions by 2050, while low and high scenarios assume lower or higher growth in both demand and production, respectively.

(b) Projected development of electricity production [TWh] in Norway from 2024 to 2050, based on the Medium scenario. Production is color-coded by source. Production from hydro and onshore wind increase slightly each 5-year period, while a substantial increase is seen for offshore wind and solar.

Figure 2.4: Projected increase in electricity production in Norway, from Statnett's long-term market analysis. (a) shows three 2050 scenarios, while (b) shows the development of production in the medium scenario. Reproduced with changes from [22].

2.3.1 Projections for Low-Emission Generation

Statnett's development plans include comprehensive integration of wind and solar power, which will enable the Norwegian grid to meet the demand of an expected doubling of national electricity consumption [4]. In their long-term system analysis, three development scenarios for the Norwegian electricity generation and consumption towards 2050 have been modeled: *Low*, *Medium*, and *High*. All three scenarios assume a balanced development between consumption and generation, but differ in the extent of growth. In the Medium scenario, which is additionally aligned with achieving net-zero emissions, solar power is expected to grow by 16 GW, while onshore and offshore wind are projected to increase by 3 GW and 6 GW, respectively. Additionally, an increase of 5 GW is expected from hydropower, primarily due to the upgrading and modernization of existing power plants. Figure 2.4 illustrates the annual electricity production in TWh, across all three scenarios. For the middle scenario, the development is shown in five-year intervals leading up to 2050.

While these scenarios give a promising outlook for the expansion of the Norwegian power system, several challenges remain regarding the development of new fossil-fuel-free generation. The expected growth in wind power, both onshore and offshore, is particularly beneficial as production peaks during the winter months when Norwegian electricity consumption is at its highest. Although Norway possesses significant offshore wind potential, rising costs in recent years have created uncertainty regarding further development [4]. In order to facilitate further expansion, Statnett is currently exploring hybrid grid solutions in collaboration with other North Sea operators. Additionally, solar PV has a strong potential to supply power to the Nordic system. The increased electricity demand that comes from data centers and the electrification of industry can be partially met by solar power, which peaks in production during the summer months, when wind power is less available. Furthermore, localized solar production, such as rooftop solar installations, is a key contributor for reaching the Norwegian government's target of reducing grid-based electricity consumption in buildings by 10 TWh by 2030 [26].

Beyond renewables, other energy sources, such as biomass and thermal stores, can be used for electricity production. However, expansion of these technologies is expected to be minimal in Norway, and are seen as less relevant [26]. Nuclear power, on the other hand, is also being considered and has lately gained increased public support [27]. While it is currently not seen as a viable addition to the energy mix due to high and unpredictable costs, large-scale, standardized development could make this technology a feasible option for the Norwegian power system in the long term. To further explore this, the Norwegian government has appointed a committee to evaluate nuclear power as a domestic energy source, with a final report due in April 2026 [4].

2.4 Coupling of the Nordic Power System to Europe

The Nordic power system operates at a different frequency from the Continental Europe Synchronous Area, necessitating the use of non-synchronous HVDC interconnectors for physical coupling [12]. Introduced in section 2.2, these links facilitate the coupling of the Nordic and European power systems, which are both geographically and technically distinct. Beyond simple connectivity, these interconnectors provide a stabilizing operational function by linking flexible Nordic hydropower to the broader European grid. Specifically, they enable the use of hydro reservoirs to balance the higher levels of vRES across the European continent [26]. By providing bidirectional exchange, these interconnectors enable the Nordic system to export surplus low-carbon power while importing energy during periods of high local demand or low hydrological inflow [3].

As a result of these interconnections, power prices within Nordic bidding areas are fundamentally linked to the price dynamics of the broader European power market. Nordic hydropower producers manage this link by using water values, which represent the calculated value of stored water based on both current and future market outlooks [28]. Producers continuously calibrate these values against expected continental price signals, minimizing the risk of energy rationing or water overflow. This mechanism is a central reason why European price fluctuations have such a significant impact on Nordic price levels, as seen in 2022–2023 when the war in Ukraine led to high prices in Europe [22,29]. While the interconnectors facilitate long-term price convergence, they also introduce significant short-term volatility, which can lead to unstable loads and rapid changes in the supply and demand in the systems. During periods when production cannot meet internal demand, Nordic prices often align with the high costs of Continental European thermal peak-load plants. Conversely, solar surpluses in neighboring countries lead to the import of zero or negative price hours into the Nordic system [26].

The coupling of the Nordic grid to Europe is projected to deepen through 2050, both via asset renewal and targeted capacity expansions [3]. Even as rising domestic consumption reduces total surplus volumes, the Nordic region is anticipated to expand solar and wind generation, thereby maintaining a positive net electricity balance through 2050 [22]. The variability of these production sources will lead to a change in how the interconnectors are used. Instead of serving primarily as channels for steady exports, the interconnectors will become more important for managing rapid fluctuations in supply and demand [3]. Consequently, Nordic power prices are expected to settle between 50 EUR/MWh and 55 EUR/MWh by 2040, far below the Norwegian average of 130 EUR/MWh in the 4th quarter of 2025 [22,30]. However, the expansion of vRES in Europe will likely lead to more frequent hours with zero or negative prices during the summer. Despite these fluctuations, the interconnectors will remain valuable as they allow for trading based on price differences and help balance the power supply across the European market [22,31].

2.5 The Impact of vRES on the Nordic Power System

While wind and solar offer significant potential for the expansion of electricity generation in the Nordic power system, integrating them into the power grid presents challenges [3]. Traditionally, the Nordic power system has relied on synchronous generators, primarily within hydropower and nuclear facilities. These machines provide rotational inertia, a physical property that allows the grid to naturally resist frequency deviations by absorbing or releasing kinetic energy during disturbances [22,32]. In contrast, vRES typically connect to the grid asynchronously via PEIDs, which convert the output to align with the grid [23]. Since solar PV produces DC and wind turbines often operate at variable frequencies, power electronic converters are required to synchronize and interface these sources with the fixed-frequency AC grid [23]. Unlike traditional synchronous machines, PEIDs lack a direct mechanical link to the grid's frequency, thereby contributing little to no inherent inertia to the system [33].

This shift from mechanical to electronic coupling reduces system inertia, making the grid more sensitive to sudden imbalances, as there is less kinetic energy to naturally resist frequency changes. Although the fast control capabilities of PEIDs allow them to respond to disturbances quicker than traditional generators, their asynchronous nature means the grid can experience faster frequency fluctuations during contingencies, such as the loss of a large generator or load [23]. While these stability issues occur on a sub-second timescale, the integration of vRES also introduces challenges for the operational balancing of the grid over longer intervals.

Beyond volatile frequencies, the intermittent nature of wind and solar production makes it more difficult to ensure a long-term balance of supply and demand. To manage this variability, power systems must maintain sufficient reserve capacities that can be dispatched during periods of low renewable generation [12]. These reserves contribute to maintaining grid reliability over hours or days when wind and solar availability are limited. While the Nordic power system traditionally has relied on its hydro reservoirs and nuclear power to provide this balancing support, the increasing share of vRES necessitates a broader range of technical solutions that are capable of maintaining a balanced system [4,23]. Accurate forecasting also plays a central role in this process, as it allows operators to anticipate production shifts and effectively schedule access to flexible resources in advance [12]. Ultimately, the combination of variable production and the uncertainty of weather patterns makes the timing and volume of electricity supply harder to predict. This creates a need for power system flexibility, which offers the balancing mechanisms required to bridge generation gaps and ensure a reliable energy supply.

2.5.1 Flexibility in Power Systems

According to the International Renewable Energy Agency (IRENA) [34], "Power system flexibility is defined as the ability of a power system to reliably and cost-effectively manage the variability and uncertainty of demand and supply across all relevant timescales." This property of the grid is becoming increasingly important due to the rising integration of vRES, which introduces significant fluctuations in power generation. As established by the IRENA definition, this requirement addresses both the predictable variability of weather patterns and the inherent uncertainty of forecasting. Flexibility is therefore essential to ensure a continuous power supply, ranging from sub-second stability corrections to managing energy accessibility over several days [12,22].

Historically, flexibility was provided by adjustable power plants, such as hydropower or gas turbines, which can quickly adjust their output [34]. Modern flexibility, however, also relies on demand-side management and energy storage systems. These strategies involve controlling consumer loads to respond to grid imbalances, often by incentivising users to reduce or shift electricity usage during peak periods. When combined with smart systems, these adjustments can be performed automatically [25]. Furthermore, modern energy storage is characterized by a range of technologies that serve different functional needs. Short-duration assets like batteries provide the fast response required for frequency stability, while long-duration solutions such as hydrogen storage and PHS enable the energy security necessary to maintain a balance over several days [25]. By capturing excess energy and releasing it during load peaks, these systems are also able to perform peak load shaving. In this process, energy storages supply the lacking power and reduces the maximum power that the grid must supply at any single moment. This, in turn, ensures better grid utilization and minimizes the need for expensive infrastructure upgrades [4]. In the Nordic region, leveraging this full spectrum of flexibility is essential for integrating higher shares of vRES while maintaining the necessary system stability.

2.6 Optimization Modeling of Energy Systems

Modeling modern energy systems requires a transition from the continuous nature of the physical system to a discrete mathematical framework. Within this framework, the model is governed by an objective function designed to minimize total system costs, including both capital expenditures and operational expenses [35]. This minimization is performed under a collection of physical and policy-based constraints, such as energy balances, Kirchhoff's laws for power flow, and defined CO_2 emission limits [5]. However, because a mathematical continuum represents an infinite number of points, attempting to optimize system behavior directly would result in an undetermined problem. Consequently, to utilize these optimization algorithms and simulate supply, demand, and transmission, the physical system must be discretized into a finite dataset of spatial nodes and temporal windows [35,5].

Once the system is discretized into spatial nodes and temporal windows, the accuracy of the model relies on selecting an appropriate level of granularity to capture the physical dynamics of the grid. High spatial and temporal resolutions enable a precise representation of geographical boundaries, local constraints, and the temporal variability of renewable generation [5,36]. However, because finer resolutions exponentially increase the time and memory required to solve the optimization, this physical accuracy must be balanced against the computational demand. Consequently, relying on an overly coarse spatial resolution carries the risk of inaccurate component placement, as the model may fail to recognize geographical constraints, potentially siting solar PV or wind farms within protected nature reserves [5]. Furthermore, such high spatial aggregation can overlook regional dynamics by merging disparate production and consumption profiles into an average profile. As an example, modeling an entire country as a single node would fail to capture the local requirements for power transmission that arise when wind generation is concentrated in the west while solar potential is located in the east. Similarly, low temporal resolution leads to the averaging of data over long intervals. This smoothing effect fails to capture the inherent variability of renewable generation and consumption, which can lead to misleading simulations of the power flow within the system and its stability [36]. Configuring the model therefore requires an evaluation of the inherent trade-off between physical detail and computational demand, selecting the minimum resolutions necessary to accurately reflect system constraints while avoiding parameters that demand excessive computational resources and time.

Once such a balance has been established, the optimization of the system is achieved by simultaneously solving two interdependent problems known as capacity expansion and operational dispatch [35]. While capacity expansion is solved by determining the optimal investment strategy by identifying which infrastructure to build and where to locate it, operational dispatch uses technical and physical constraints in order to find the most efficient way to run the system. The model actively searches for a solution that satisfies the physical requirements of power flow alongside the economic objective of cost-efficiency [5,36]. By merging these technical and financial facets, the optimization process yields an integrated system design. This comprehensive approach ensures that all physical constraints are met at the lowest possible cost and provides a robust foundation for long-term energy planning [35].

2.7 Relevant Literature

This section reviews research central to the scope of this thesis. While the selected studies demonstrate a range of focus areas, they all employ modeling and system optimization to analyze future power systems. Notably, the majority of these studies utilize Python for Power System Analysis (PyPSA), aligning with the modeling framework chosen for this thesis.

2.7.1 PyPSA-Eur: An open optimisation model of the European transmission system

Hörsh et al. [37] present PyPSA-Eur, the first open-source dataset of the complete European power system, covering the whole European Network of Transmission System Operators for Electricity (ENTSO-E) area. It contains high-resolution details of transmission grids and power plants, a geo-referenced database of potential sites for wind and solar power, and time series of electrical demand. Furthermore, the model derives time series for wind and solar generation availability using re-analysis weather datasets, and estimates renewable capacity potentials constrained by land use. Validation of the complete dataset has been done by comparing key power system characteristics with official statistics. The combination of high spatial detail and continental coverage allows PyPSA-Eur to accurately represent the European power system, capturing both national grid constraints and cross-border interactions essential for analyzing renewable integration and system planning. Temporal and spatial resolution are customizable parameters in the setup, making this tool suitable for both dispatch and capacity expansion analysis. Since PyPSA-Eur is exclusively relying on freely available and open data, the paper encourages open exchange of developed datasets among European data holders, which would improve the quality and accuracy of the model.

2.7.2 Large-Scale Optimization of the Nordic Power System in Connection with Statnett's Grid Development Plans using PyPSA

Malum [6] performs a study that explores how carbon-neutrality can be achieved in the Nordic power system by 2050. PyPSA-Eur allows one to model such a carbon-neutral system, and can simulate different scenarios for 2050 in order to optimize the system. Specifically, the study tackles three main problems. The thesis focuses on identifying the necessary upgrades in transmission lines to enable expansion of renewable energy integration. Moreover it searches for the optimal mix of different renewable energy sources in the Nordic system, specifically among onshore wind, offshore wind and solar. Lastly, the thesis investigates the most effective options for energy storage, which are necessary to balance the system under variable generation from renewable energy sources, thus ensuring system stability.

The results show different scenarios resulting in a grid expansion varying from 3.66% to 4.97%, based on reasonably selected model setup and parameters. The most cost-effective scenario comes from the model being seemingly free of constraints, in which it prioritized onshore wind and solar. This scenario showed a system cost of 33.9 BEUR, with a total installed capacity of 130.4 GW. This was also the only scenario where methanol and EV-battery storage were absent, as the model for this scenario managed to balance supply and demand using the existing flexibility in hydropower.

While these results give clear indications on how the Nordic power system can be developed towards 2050, the selected modeling does not include power exchange with European countries outside the Nordic region, which is a significant simplification. The inclusion of these exchanges, in this case through HVDC-connections, would allow the model to simulate international power flow outside of the Nordics, thus yielding different and more realistic results for both the energy and economic aspects. This can easily be spotted in the methodology, where the thesis compares modeled capacities of the current Nordic power system to actual capacities in 2023, in which substantial deviations are found.

2.7.3 Exploring Offshore Wind Development in Norway Through Heuristic modeling

Saleem [7] provides relevant research within the field of PyPSA-Eur. This work focuses solely on Norway's target of building 30 GW of offshore wind power by 2040, and investigates the necessary developments in the Norwegian power system in order to achieve this goal. Similar to [6], Saleem models the Nordic power system consisting of Norway, Sweden, and Finland, without any inclusion of interconnections to

Europe. The results across multiple scenarios show a necessary transmission system expansion of 48.3%, compared to the current Nordic power system and assuming a 50% increase in electricity demand by 2040. The total system costs are estimated to be 27.1 BEUR/year, and are annualized for 2040. Furthermore, the research lacks inclusion of multiple, highly relevant considerations. Firstly, the model does not include hydropower as a power generator, although it by far is the biggest contributor of electricity generation in Norway [38]. The model does not take into account any coexistent development of other renewable energy sources, neither does it model any specific increase in energy-demanding industry in the Nordics. The exclusion of European connections is also a substantial simplification. Performing a similar study where these considerations are taken into account would likely yield a more realistic modeling of the necessary expansion of the power system. Comparing with [6], this work concludes on significantly higher numbers for transmission system expansion and the related costs.

2.7.4 The Impact of eCooking in the Tanzanian Power System: modeling eCooking transitions using PyPSA- Earth

Eide [39] performs a study that utilizes PyPSA Earth to explore the Tanzanian power system. The research explores how large-scale adoption of electrical home-cooking in Tanzania will affect the power system in 2040. This is done by analyzing the planned development of the Tanzanian power system, and assessing the additional upgrades required to supply future demand under different electric cooking adoption scenarios. The scenarios are based on different shares of the population using electricity for cooking, and ranges from 2% in the baseline all the way to 100% adoption within 2040. This work includes modeling of new renewable power generation to meet the increasing demand, and finds that the introduction of electrical cooking will reshape daily load curves across all scenarios. A full transition to electrical cooking was found to significantly increase the peak demand in the power system, exceeding the currently expected peaks from the development plans for the sector by 45%. One weakness of the model is that it isolates Tanzania's power system from neighboring countries, which is unrealistic. However, the transmission capacities in the grid are not affected by this, and the inclusion of external connections would likely yield a lower need for new power generation within the country. This was not the main scope of the study, and therefore the simplification is considered to have a minimal impact on the main results.

2.7.5 Modeling Power Disruption Scenarios and Assessing Resilience of a Power System

Bermejo et al. [40] provide research that applies PyPSA-Eur to assess power system resilience. The study models the power system of an anonymized EU-region consisting of three countries over a three-month period in 2025, and assesses the system's resilience under several disruption scenarios of interconnected power lines. The modeled region is necessarily well interconnected with neighboring countries, and the disruptions are modeled using PyPSA-Eur. 10 disruption scenarios are modeled and compared to a baseline scenario where no special disruptions occur. The results are presented in three main parameters: energy not served (ENS) due to the disruption, the average cost of electricity in the region, and a resilience score index. Overall, the study finds that disruptions on multiple interconnecting HVDC links are the most vulnerable scenarios, and these receive the lowest resilience scores. The worst rated scenario of two disrupted links show ENS of 226.5 GWh/month over the simulated months. The average electricity price reaches a maximum of 3886 EUR/MWh, based on an assumption that the cost of unsupplied energy is 10 000 EUR/MWh. A limitation of the model is that it does not account for the reduction in electricity demand due to high prices, which likely leads to an overestimation of the electricity price and ENS.

2.7.6 Pursuing decarbonization and competitiveness: a narrow corridor for European green industrial transformation

Bella et al. [41] examine trade-offs between decarbonizing the European industry sector while keeping competitiveness in global markets. This study utilizes PyPSA-Eur to model energy- and emission-intensive industry sectors. The main goal of the research is to find how European countries can decarbonize while preserving their industrial competitiveness. To answer that, the authors explore options for intra-European relocation of industry, selective import of low-carbon goods, and targeted subsidies to European industries. Unlike the typical application of PyPSA-Eur, which includes modeling of electrical power- and transmission-systems, this study focuses on policy-relevant strategies to decarbonize the European industry. The results show that deep industrial decarbonization is technically possible, heavily driven by electrification. However, maintaining competitiveness is highly sensitive to policy. Relocating production within Europe provides modest energy savings, while strategic imports of green goods can reduce system costs and carbon prices while preserving domestic production and employment. Subsidies are needed to prevent industrial relocation abroad, but are not sustainable under expansion of industrial activity. It is therefore suggested that potential subsidies take on a strategic focus, only supporting key sectors that allow for strong decarbonization.

2.7.7 Offshore power and hydrogen networks for Europe's North Sea.

Glaum et al. [42] present a study on the renewable energy potential in the European North Sea. This area has a great potential of providing clean electricity for Europe's energy transition. However, there is considerable uncertainty about the large scale integration possibilities of offshore wind power, and whether offshore hydrogen should be a part of the development. To address this, the authors model a carbon-neutral, sector-coupled European energy system using PyPSA-Eur. The model freely optimizes how much offshore wind is deployed, and which infrastructure is used to integrate the power. The results show that 310 GW of offshore wind can be deployed with the current infrastructure of point-to-point connectors, while 420 GW is possible if meshed networks and hydrogen are allowed, with potential cost savings of up to 15 BEUR/year. Additionally, 75 GW of floating offshore wind is only seen if offshore hydrogen production is available. In general the model calls for offshore wind integration through both electricity and hydrogen networks. Limitations of the study include an inaccurate representation of the meshed DC network, as the model does not incorporate the fundamental principle of Kirchhoff's voltage law. Moreover, AC connections from wind farms are not modeled, and ecological constraints as well as potential impacts on marine life are not considered.

2.7.8 Exploring Uncertainties in Future Power Systems: Methodology and Analysis for Italy 2040

Pampado et al. [43] perform a study on the development of the Italian power system towards 2040. To do so, a high-resolution PyPSA-Eur model of the South-European power system is used to assess uncertainties in the power system through scenario exploration. Seven scenarios, each exploring different technology expansions and emission targets, are modeled and compared to a baseline that corresponds to the development plans of the Italian TSO [44]. Results find that nuclear power development is not cost-competitive, as it is excluded even under zero emission constraints. Under these constraints the model instead favors generation expansion of biomass and hydrogen, sizing up to 33 GW and 2653 GW, respectively. This unrealistic expansion of hydrogen comes at the expense of decreasing wind and solar capacities, alongside a substantially increased power import from neighboring countries. In total this yields an electricity price of roughly 60 EUR/MWh across the zero-emission scenarios. A notable limitation of this study is the fact there are no realistic limits on the expansion of technologies. Although zero-emission by 2040 is hard to reach, the model would likely yield more realistic results if accurate limitations were applied to technologies like biomass and hydrogen.

2.7.9 Early cross-sector decarbonization for Europe's hard-to-abate sectors: Insights from Denmark's 2030 target

Fristed et al. [45] present a study that explores early decarbonization pathways in Denmark's hard-to-abate sectors, which will be essential for achieving the national target of a 70% reduction in GHG emissions by 2030. Using PyPSA-Eur to model 33 European countries, the study sets cross-sector carbon budgets based on national commitments and examines seven scenarios where specific sectors fail to meet targets, alongside a baseline scenario in which all targets are met. In each scenario, the model optimizes capacity expansion and dispatch of electricity, heating, transport, hydrogen and biomass, including carbon capture and storage (CCS). Denmark's carbon budget is extended to include *sectoral decarbonization trajectories*. Results indicate a total system cost of roughly 8 BEUR/year across all scenarios. Two key factors drive high carbon abatement costs. First, failure to decarbonize agriculture increases costs, since this would require near-zero or even negative emissions from all other sectors. Second, the increasing competition for biomass resources also raises costs, as biomass is projected to be in demand for low-cost carbon capture, carbon-neutral dispatchable heat, and renewable fuel production. Together, these factors could nearly double the expected carbon abatement cost to around $200-210$ EUR/tCO_2e. However, these results are constrained by fixed assumptions in sectors such as transport and industry, which may overlook more cost-effective or regionally feasible abatement options.

2.7.10 Hydrogen for harvesting the potential of offshore wind: A North Sea case study

Bødal et al. [46] address the challenge of high transmission costs for offshore wind power in the North Sea by evaluating the cost sensitivity of energy export via offshore H_2-electrolysis. Unlike other papers presented in this thesis, the authors use EnergyModelsX rather than PyPSA-Eur to model the integrated system. The modeling includes existing hydropower and its pumping capacity, alongside various export options such as HVDC cables, new hydrogen pipelines, tie-in to existing pipelines, and pipelines with line packaging. When analyzing the necessary conditions for offshore electrolysis to be cost efficient, results indicate a *window-of-opportunity* with respect to electricity prices. Electricity prices below 150% of the baseline price do not lead to sufficient available electricity to make the offshore electrolysis attractive, while prices exceeding this threshold lead to the electricity becoming more valuable than H_2, even at the cost of increased wind farm curtailment. However, linepacking is found to increase system resilience against both low prices of H_2 and high electricity prices, as the storage of excess energy allows for a more variable electrolyzer operation. A central limitation of the study is the likely overestimation of H_2-demand, due to this demand not being price-sensitive. Furthermore, the potential strengths of linepacking the H_2-pipelines are uncertain, as this technology is not currently utilized at scale, and depend on complex flow-computations not captured in the linear optimization of EnergyModelsX.

2.7.11 Summary of Research Gaps

Current studies, such as Malum [6] and Saleem [7], provide a good starting point for modeling the Nordic power system. However, the reviewed literature often treats this region as an isolated grid, which simplifies the reality of how the Nordic region interacts with the rest of Europe. Additionally, some studies lack the consideration of the need for reserve capacity to keep the grid stable in a carbon-neutral system. This thesis aims to fill these gaps by including the main interconnectors from the Nordics to continental Europe and the UK. By also exploring different solutions for reserve capacity, this study will provide a more realistic view of how the Nordic power system can be developed to achieve net-zero emissions by 2050.

3 Theory

This chapter establishes the theoretical foundation necessary for the thesis, and closely follows the theory section from [6]. It begins with an overview of electrical power grids in Section 3.1, followed by the principles of power system stability in Section 3.2. The chapter then covers power flow analysis in Section 3.3, before concluding with the presentation of PyPSA-Eur in Section 3.4.

3.1 Electrical Power Grids

Power grids provide the critical infrastructure required to transport electricity from power producers to consumers. This network of transmission lines and substations is managed by TSOs, who are responsible for the continuous balancing of the national power systems [47]. In the Nordic and European regions, these systems operate at a nominal frequency of 50 Hz [48]. Beyond balancing, the TSOs are responsible for the long-term quality and reliability of the grid. This includes grid developments to ensure the system is suited for increasing demand and the rising integration of renewable energy sources [3,49].

As an example, the Norwegian power grid is structured into three main voltage sections. At the top is the transmission grid, operating between 132 kV and 420 kV, and serving as the primary highway for long-distance electricity transport. Such high voltage levels are used to ensure that large amounts of energy can be transmitted efficiently with minimal losses, as high voltages yield low currents, and power loss is proportional to the square of the current [32]. The regional grid, with voltages between 33 kV and 132 kV, is the medium-voltage level that delivers electricity between the transmission lines and the local networks, though power-intensive industries and production plants may connect directly at this voltage level. Finally, the distribution grid operates at or below 22 kV, with the purpose of delivering electricity directly to end-consumers [50].

3.1.1 Components in Power Systems

A complete power system consists of a network of interconnected components, including generators, storage units, loads, and transmission lines [32]. Within power system analysis, these elements are connected at nodes referred to as *buses*. Depending on the spatial resolution, a bus can represent a specific high-voltage substation, an entire city, or an aggregated regional zone. Regardless of its geographical scale, a bus functions as a hub for energy exchange, where the power entering and leaving must at all times be balanced to satisfy the principle of energy conservation. Each bus in the network is defined by two primary variables, its voltage magnitude and phase angle. Together, these variables determine the direction and magnitude of power flows throughout the network. Ultimately, buses are a core element of power system analysis because they represent the specific points of energy exchange between all system components [32].

3.2 Power System Stability

According to [51], "Power system stability is the ability of an electric power system, for a given initial operating condition, to regain a state of operating equilibrium after being subjected to a physical disturbance, with most system variables bounded so that practically the entire system remains intact." Maintaining this stability is a dynamic process, as power systems are rarely in perfect equilibrium due to constant fluctuations in generation and load. Therefore, the system is actively monitored to ensure reliable power delivery. This includes ensuring that bus voltages are close to nominal values and preventing excessive phase angle differences across transmission lines. Furthermore, components like generators, transformers, and lines are monitored to avoid exceeding their thermal or physical limits, which could lead to equipment damage or widespread blackouts [32].

As discussed in Section 2.5, stability in conventional power systems is primarily maintained by synchronous generators. These machines operate at a rotational speed directly linked to the system frequency. Stability is preserved as long as all generators remain synchronized, meaning their rotor angles stay aligned relative to one another [32]. When a disturbance occurs, such as the loss of a generator or load, it causes deviations in these rotor angles and consequently the operating frequency. To resist such changes, synchronous generators provide inertia to the system, giving operators the time needed to restore balance. Since this requires a match between generation and consumption at all times, the frequency ultimately serves as a direct reflection of the instantaneous system balance [32,52].

Beyond the immediate dynamic stability that is governed by inertia, a reliable power system must also maintain a continuous balance between supply and demand over longer time horizons. This aspect of stability is often referred to as resource adequacy, and ensures that sufficient generation and transmission capacity is available to satisfy load requirements under varying conditions [12]. Unlike transient stability, which deals with both second and sub-second electromechanical dynamics, this perspective assesses the system stability by ensuring a set of steady-state operating points on larger time-scales, such as minutes or hours. In this context, stability is governed by the existence of a feasible power flow solution where generation meets consumption within the physical limits of the transmission grid [32]. This form of stability assessment is essential for identifying necessary infrastructure upgrades, as it verifies that the system remains robust against the variability of renewable sources and structural changes without explicitly addressing the sub-second frequency containment.

To further ensure system reliability, the transmission grid typically operates under the N-1 safety criterion. This is a fundamental principle in grid planning, and ensures that a power system remains operational under the failure of a single component, such as a line or transformer [53]. In such an event, the system must be capable of handling an automatic redistribution of the power flow across the remaining infrastructure, without exceeding capacity limits. This prevents the grid from overloading and maintains reliability. In contrast, N-0 operation refers to a configuration where the grid lacks this redundancy, and any single component failure can lead to immediate overloads or outages [3].

3.3 Power Flow Analysis

Power flow describes the physical transmission of electrical energy through a power system. The process is determined by fundamental electrical principles, where the interaction of voltage, current, and impedance dictates how the power moves between the system components of generators, transmission lines, transformers, and loads [32].

In any steady-state, balanced three-phase system, the power flow at each bus is characterized by its voltage magnitude and phase angle [32]. As introduced in Section 3.1.1, a bus represents a hub where electrical components interconnect, allowing power to be injected, withdrawn, or transferred. The resulting power flow is described by complex power S, which consists of active power P and reactive power Q. While active power performs physical work, reactive power is required to maintain voltage levels and support the operation of inductive and capacitive components [32]. At each bus, the relationship between these variables is determined by the power flow equations for active and reactive power, expressed as

$$P_k = V_k \sum_{n=1}^{N} V_n (G_{kn} \cos(\theta_k - \theta_n) + B_{kn} \sin(\theta_k - \theta_n)), \tag{3.1}$$

and

$$Q_k = V_k \sum_{n=1}^{N} V_n (G_{kn} \sin(\theta_k - \theta_n) - B_{kn} \cos(\theta_k - \theta_n)), \tag{3.2}$$

where P_k is the active power and Q_k is the reactive power at bus k. V_k, V_n, θ_k, and θ_n are voltage magnitudes and phase angles at buses k and n, respectively. G_{kn} is the conductance between buses k and n, and B_{kn} is the susceptance between them. N is the total number of buses in the system [32]. With these properties defined, the complex power S_k at bus k is given by

$$S_k = P_k + jQ_k, \tag{3.3}$$

where j is the imaginary unit [32]. Note that S_k carry the unit [VA], while P_k and Q_k are denoted by units [W] and [var], respectively. These power flow equations characterize the transfer of electrical energy across system components, typically from generator to load buses. The distribution of active and reactive power is determined by the physical properties of the network, such as line resistance and reactance. These factors dictate the patterns of the power flow, and determine inherent system losses [32].

In order to solve these non-linear power flow equations, the most common tools are built on numerical methods, such as Gauss–Seidel or Newton–Raphson. These numerical methods become strictly necessary for larger number of buses, N, as the power flow equations have no analytical solution in such cases. The iterative techniques are able to accurately approximate the solution of such multi-variable problems, thus providing insights into the power distribution across the network. Gaining these insights on how the power flow is distributed can further highlight potential risks within the system, such as transmission line overloads or voltage drops. Therefore, power flow analysis is a fundamental tool for both operational management and infrastructure planning. In real-time applications, the analysis allows operators to maintain grid stability and optimize solutions for electricity distribution. Additionally, it identifies persistent congestion or under-utilization for the long-term development, thus guiding operators and planners towards optimal expansion and upgrade of the grid [32].

3.4 Introduction to PyPSA

Python for Power System Analysis (PyPSA) is a free and open-source software designed for simulation and optimization of modern power systems. Functionally, it serves as a practical application of the power flow principles outlined in Section 3.3. Rather than modeling continuous operation and sub-second stability, PyPSA performs steady-state calculations over discrete temporal snapshots. Consequently, the main applications of PyPSA are to solve problems of power flow calculations, system optimization, and investment planning. To construct these complex system models, the framework includes components such as conventional generators, vRES, energy storage, and both AC and DC transmission networks. PyPSA also supports sector coupling, which facilitates interconnections between traditionally separate energy sectors like hydrogen generation and storage, heat, and transport [54]. In order to handle these tasks on a large scale, PyPSA is designed to scale efficiently with spatially complex networks and long temporal data series. It serves as an accessible tool for researchers, planners, and utilities. By requiring only basic coding capabilities, it provides a transparent and efficient method of performing complex energy system analysis. A notable application of this framework is PyPSA-Eur, which provides a detailed model of the interconnected European power system [54,55].

3.4.1 PyPSA-Eur

Built on the PyPSA framework, PyPSA-Eur is a focused optimization model of the European power system. It covers the entire area governed by the European Network of Transmission System Operators for Electricity (ENTSO-E), and is designed to facilitate planning and analysis of cost-effective energy systems by minimizing both investment and operational costs [37]. By translating the physical realities of the European power grid into a discrete network of buses and connected components, the model is suitable for both operational studies of the current grid and long-term expansion planning for generation and transmission. Specifically, the dataset within the model includes 7072 transmission lines, representing all HVDC interconnectors and all AC power lines at or above 220 kV. It also incorporates 3803 substations, time series for electricity demand and renewable generation, and geographic potential for the expansion of vRES. Because of its continental scope, the model can capture complex phenomena such as the long-range smoothing effects of renewable power across different resource regions. Furthermore, to ensure computational feasibility, the model is typically clustered down to 50–200 nodes, after which the network is solved as a linearized power flow problem [55,56]. As these data structures and processes are fundamental to the operation of the model, further details of demand, geographic potential, spatial clustering, and optimization are provided in the subsequent subsections.

3.4.2 Data Sources

To accurately represent the physical infrastructure, meteorological conditions, and geographical constraints of the European power system, PyPSA-Eur relies on a compilation of specialized datasets. The structural topology of the grid, including existing power lines and substations, is extracted from OpenStreetMap (OSM) [57]. To simulate the temporal variability of renewable energy generation and electricity demand, the framework utilizes weather profiles from ERA5 [58]. Additionally, the spatial potential for expanding system components is governed by CORINE Land Cover [59], which classifies permissible land use, alongside Natura 2000 [60], which strictly excludes protected environmental zones from infrastructure development. All of these essential datasets are compiled from open sources, and their specific implementations within the model are detailed below.

The base network used within PyPSA-Eur comes from OSM, which provides detailed data regarding the electricity infrastructure of Europe. It includes information on power plant locations, generation types, and transmission lines [57]. The underlying representation of the European high-voltage grid spans from 220 kV to 750 kV, solely constructed from OSM data. Within the dataset, close substations within a radius of 500 m are aggregated to single buses, while exact locations of underlying substations are preserved. Unique identifiers for lines and links are also preserved [61]. By incorporating these elements, the dataset offers a comprehensive view of the inter-

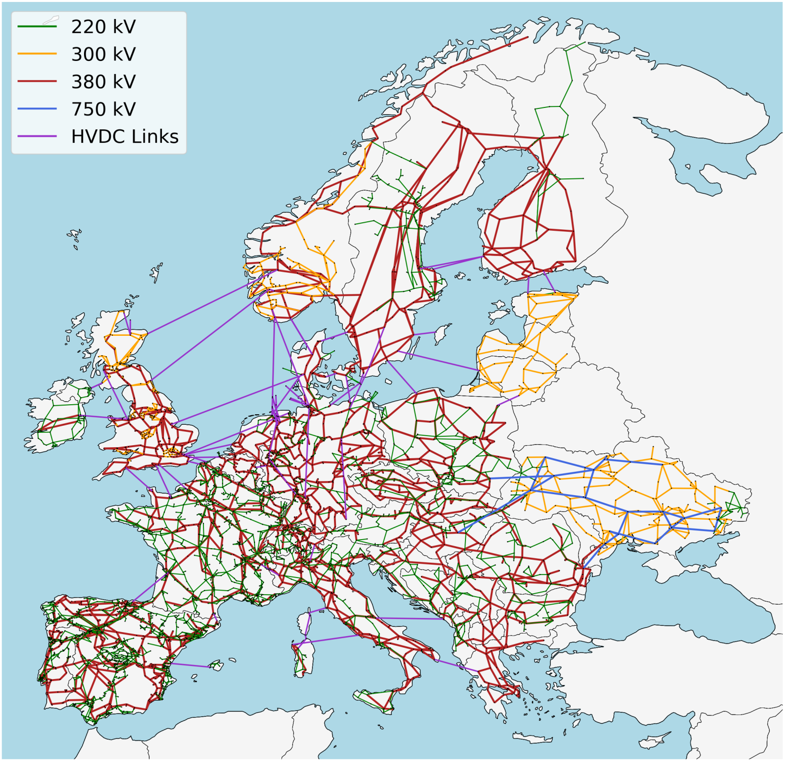

Figure 3.1: Overview of the ENTSO-E transmission network, spanning across Europe. High-voltage AC lines above 220 kV are shown alongside all HVDC cables. These include existing lines/cables, as well as those planned or under construction. The map illustrates the highly interconnected structure of the European network, which facilitates cross-border power flow. Figure reused from [55].

connected European power system. Figure 3.1 visualizes the complete transmission network of this dataset. Note that ENTSO-E provides a separate base network that is available in PyPSA-Eur, and must not be confused with the OSM network which is used as the default base network in PyPSA-Eur.

The weather-dependent data in PyPSA-Eur comes from ERA5, a reanalysis climate dataset produced by the European Centre for Medium-Range Weather Forecasts (ECMWF) [58]. It provides accurate estimations of weather data, such as wind speed and direction, solar irradiation, and temperatures, all with an hourly resolution and estimates of uncertainty. The data is available on a spatial grid with a resolution of $0.25° \times 0.25°$, while atmospheric parameters are provided for 37 distinct pressure levels. This high-resolution mapping allows for a detailed representation of the climatic conditions that are necessary to model vRES profiles accurately.

While ERA5 provides the climatic inputs for renewable generation, the physical infrastructure of the power grid is managed through the Powerplantmatching (PPM) tool [62]. In PyPSA-Eur it is used to clean, standardize, and integrate power plant data from several open-source databases. Specifically, PPM ensures that the power plant data aligns with country-specific capacity statistics, which ultimately prepares the power plant inputs for the framework. The tool matches individual power plants to their correct geographical locations and assigns central attributes such as fuel type, installed capacity, and operational status. By ensuring consistency across multiple datasets, PPM creates a refined and aggregated dataset that is exported directly into the PyPSA-Eur network model. This allows for the precise definition of generation capacities at each bus within the system [37].

The spatial potential for new renewable expansion, and other infrastructural installations, is further constrained by land-use data from the Coordination of Information on the Environment (CORINE) and the Natura 2000 network. CORINE's Land Cover dataset provides detailed mapping of the European landscape by classifying land into 44 distinct thematic categories, such as forests, wetlands, and agricultural areas. While this dataset is stated to be updated every six years, the most recent update was made in 2018 [59]. Additionally, the Natura 2000 dataset identifies protected areas across all EU Member States that are dedicated to preserving threatened species and habitats [60]. As Norway is not an EU member, this dataset does not contain restrictions for Norwegian areas.

In PyPSA-Eur, these datasets are processed together and used to determine where new renewable energy infrastructure can be built. While CORINE identifies urban or industrial zones, Natura 2000 restricts infrastructure from being developed in protected areas. With the utilization of these datasets, PyPSA-Eur is able to exclude unsuitable land and ensure that renewable energy expansion is only modeled within realistic spatial constraints that align with environmental policies [55].

3.4.3 Design

Rather than a ready-made model, PyPSA is designed as a modular toolbox that represents individual power system components as independent objects. This design allows researchers to build custom networks using standardized building blocks such as buses, loads, and generators [63]. The foundation of the PyPSA architecture is the network, which acts as the overall container for the tool. This network connects all attached components and enables the model to run optimization problems, power flow simulations, and network visualization.

There are a wide selection of components available in PyPSA, including buses, loads, generators, storage units, links, and transmission lines. Among these, buses serve as the foundational nodes of the network, with all other components being attached to a bus. They act as hubs for energy flow, ensuring conservation of flow for all elements feeding in and out of a bus at any time step. This ensures that power flows align with the system's operational constraints [63]. Although the main application is energy system analysis, a bus can represent more than an electrical substation. Additional use cases are non-electric energy carriers, such as hydrogen or heat, and non-energy carriers such as CO_2.

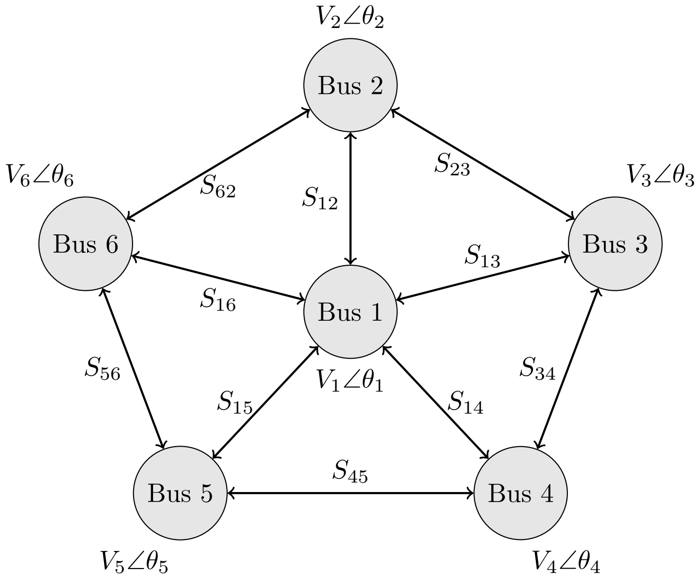

Figure 3.2: A six node representation of a power system. At each bus the voltage magnitudes (V) and phase angles (θ) are shown, as well as the complex power flows (S) between the buses. Reproduced with permission from [6].

Figure 3.2 shows a simplified power system consisting of 6 nodes, illustrating the role of buses in managing power flows. Each node represents a bus, which is defined by its voltage magnitude (V) and phase angle (θ). Connecting the buses, the lines between them represent the transmission lines, which carry the flow of complex power. In PyPSA, these transmission lines model the physical behavior of the AC grid according to Kirchhoff's laws for voltage and current [64]. Another type of transmission carriers in the software are links. These are used to represent controllable, directed flows between buses, such as DC cables, converters, or even cross-sectoral couplings like electrolyzers. While lines are governed by the physical properties of the network, links allow for the inclusion of efficiencies and fixed dispatch limits, providing a bridge between different energy carriers and voltage levels [65].

The power is supplied to the system through generators and discharging storage components. Generation sources are categorized as either conventional plants such as gas, nuclear, and coal, or variable renewable sources like wind and solar [63]. Furthermore, PyPSA makes a distinction between *storage units* and *stores* based on their operational behavior. Storage units, like hydropower and PHS, act similarly to generators because they can actively discharge energy into the system. In contrast, stores represent passive reserves such as batteries, hydrogen, and methanol, which must first be charged before they can supply energy. A complete list of all available technologies can be found in the GitHub repository of PyPSA-Eur [66].

In the modeled power systems, electricity is consumed by loads, PHS, and charging stores. Energy can also be lost in transmission lines, storage units or stores, if the components have efficiencies below 1.0 [63]. With all component types defined, Figure 3.3 displays a simple representation of a bus, with connections to a generator, load and a store and storage unit, alongside the power flow in and out of the bus.

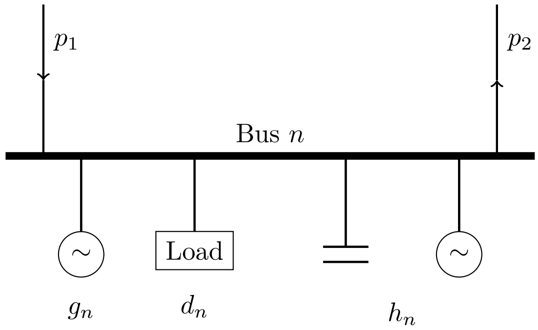

Figure 3.3: A representation of bus n in a power system, displaying power input from a generator (g_n), power supply to a load (d_n), and a store and storage unit (h_n). Power flows (p_1 and p_2), respectively entering and exiting the bus, are also shown. Reproduced with changes from [63].

The primary goal of the design is to solve the power balance at every node. This process ensures that the sum of all power entering and leaving a bus equals zero at every time step [67]. This power balance equation, for a bus n at a specific time t, is given as

$$\sum_s g_{n,s,t} + \sum_s h_{n,s,t} + \sum_l L_{n,l,t} f_{l,t} + \sum_l K_{n,l} p_{l,t} = \sum_s d_{n,s,t}, \tag{3.4}$$

where the term $g_{n,s,t}$ represents the power dispatch of generators while $h_{n,s,t}$ accounts for the net power contribution from storage units and stores at bus n, for each system component s. The electricity demand at the node is captured by $d_{n,s,t}$. The flow of power between nodes is represented by $f_{l,t}$ for links and $p_{l,t}$ for transmission lines and transformers. These network flows are governed by the incidence matrices $L_{n,l,t}$ and $K_{n,l}$, which define the grid topology by assigning values of either -1 or 1 to indicate whether a branch starts or ends at the bus. Furthermore, the time-varying matrix $L_{n,l,t}$ incorporates efficiency factors, $\eta_{n,l,t}$, to account for energy losses or multiple outputs in link components. Equation (3.4) ensures energy balance at each bus, satisfying the energy conservation law by balancing the sum of generation and storage outputs with the demand and losses in the transmission lines and links [67].

3.4.4 System Optimization

This section closely follows the Objective Formulation from the PyPSA documentation [68]. The main objective of the optimization solver in PyPSA is to minimize the total system costs connected to the modeled energy generation, storage, and transmission. This is done by defining the objective function, which represents the sum of all investment and operational costs. To represent this mathematically, the total system costs, $\mathcal{C}_{\text{tot}}$, of the objective function can be formulated as

$$\mathcal{C}_{\text{tot}} = \mathcal{C}_{\text{inv}} + \mathcal{C}_{\text{ops}}, \tag{3.5}$$

where $\mathcal{C}_{\text{inv}}$ represents the annualized investment costs for capacity expansion, while $\mathcal{C}_{\text{ops}}$ denotes the total operational costs for the system.

For extendable components in the system, the investment costs are calculated based on the nominal capacity added to the system. These costs are defined as

$$\mathcal{C}_{\text{inv}} = \sum_{n,s} c_{n,s} G_{n,s} + \sum_{n,s} c_{n,s} H_{n,s} + \sum_{n,s} c_{n,s} E_{n,s} + \sum_{l} c_l F_l + \sum_{l} c_l P_l, \tag{3.6}$$

where c_* represents the annualized capital cost per unit of capacity. The decision variables for nominal power capacity are given by $G_{n,s}$ for generators, $H_{n,s}$ for storage units, F_l for links, and P_l for lines and transformers. Additionally, $E_{n,s}$ represents the nominal energy capacity within the stores of the system. The subscripts n, s, and l label the bus, the technology type, and the network branch, respectively.

The operational portion of the objective function mainly consists of marginal costs related to component dispatch ($\mathcal{C}_d$), supplemented by costs of energy storage ($\mathcal{C}_{\text{sto}}$), spillage ($\mathcal{C}_{\text{spil}}$), and unit commitment ($\mathcal{C}_c$). These costs are weighted by the duration of each snapshot, w_t^o, which reflects their contribution to the total annual cost. The total operational cost can be defined as

$$\mathcal{C}_{\text{ops}} = \mathcal{C}_d + \mathcal{C}_{\text{sto}} + \mathcal{C}_{\text{spil}} + \mathcal{C}_c, \tag{3.7}$$

where the first term, $\mathcal{C}_d$, represents the marginal costs of variable production. It is defined as

$$\mathcal{C}_d = \sum_t w_t^o \left(\sum_{n,s} o_{n,s,t} g_{n,s,t} + \sum_{n,s} o_{n,s,t} h^-_{n,s,t} + \sum_{n,s} o_{n,s,t} h_{n,s,t} + \sum_l o_{l,t} f_{l,t} \right), \tag{3.8}$$

where o_* represents the marginal cost per unit of power for generators ($g_{n,s,t}$), storage unit dispatch ($h^-_{n,s,t}$), store discharge ($h_{n,s,t}$), and link flow ($f_{l,t}$). A key distinction should be noted between storage unit dispatch and store discharge. While the former only incurs costs for discharging, the latter incurs costs for discharging and generates a corresponding revenue for charging. The subscript t indicates the temporal snapshot.

The second operational term, $\mathcal{C}_{\text{sto}}$, accounts for the costs associated with holding energy in storage over time, and is given by

$$\mathcal{C}_{\text{sto}} = \sum_t w_t^o \left(\sum_{n,s} \text{mcs}_{n,s,t} \text{soc}_{n,s,t} + \sum_{n,s} \text{mcs}_{n,s,t} e_{n,s,t} \right), \tag{3.9}$$

where mcs denotes the *marginal costs of storage* per unit of energy. The decision variables $\text{soc}_{n,s,t}$ and $e_{n,s,t}$ represent the State of Charge (SOC) for storage units and the energy level for stores, respectively.

Furthermore, spillage costs can be applied to storage units, particularly for hydro-electric reservoirs where water is released without generating power:

$$\mathcal{C}_{\text{spil}} = \sum_{n,s,t} w_t^o \text{sc}_{n,s,t} \text{spillage}_{n,s,t}, \tag{3.10}$$

where $\text{sc}_{n,s,t}$ is the cost per unit of spilled energy, $\text{spillage}_{n,s,t}$.

Finally, for generators and links where unit commitment is enabled, the model incorporates costs related to the operational status of the assets. These consist of stand-by costs $\text{sbc}_{*,t}$, start-up costs $\text{suc}_{*,t}$ and shut-down costs $\text{sdc}_{*,t}$, which are calculated differently for the two components. For a generator, the operational commitment cost is expressed as

$$\mathcal{C}_c^{gen} = \sum_{n,s,t} w_t^o \text{sbc}_{n,s,t} u_{n,s,t} + \sum_{n,s} \text{suc}_{n,s} su_{n,s,t} + \sum_{n,s} \text{sdc}_{n,s} sd_{n,s,t}, \tag{3.11}$$

while for a link the cost is given as

$$\mathcal{C}_c^{link} = \sum_{l,t} w_t^o \text{sbc}_{l,t} u_{l,t} + \sum_{l,t} \text{suc}_{l,t} su_{l,t} + \sum_{l,t} \text{sdc}_{l,t} sd_{l,t}. \tag{3.12}$$

In these expressions, $\text{sbc}_{*,t}$, $\text{suc}_{*,t}$, and $\text{sdc}_{*,t}$ are linked to the status ($u_{*,t}$), start-up ($su_{*,t}$), and shut-down ($sd_{*,t}$) unit commitment variables. Note that in contrast to the other presented operational costs, only the stand-by costs are weighted by the objective snapshot weightings w_t^o in Equations (3.11) and (3.12). Including these unit commitment variables transitions the optimization problem from the default of linear program to a mixed-integer linear program, significantly increasing the computational complexity to better reflect the technical constraints of thermal plants and converters.

The objective function essentially serves as a balancing mechanism between capital expenditure and operational efficiency. The investment terms in Equation (3.6) represent the fixed costs of expanding infrastructure, such as new generation capacity and transmission reinforcements. In contrast, the operational terms in Equation (3.7) capture the variable costs of running the system across all temporal snapshots. By applying the snapshot weightings w_t^o, the optimization process places greater emphasis on time periods with longer durations or higher strategic importance. Ultimately, the solver minimizes the total system cost by determining the optimal trade-off between the upfront investment costs of building various energy assets and the ongoing expenses of energy production, storage, and transmission [68].

3.4.5 Model Constraints

Within power system modeling, such as PyPSA, model constraints are an essential set of rules that define the operational boundaries for different system components. These rules ensure that the proposed solution from the optimization reflects the physical and operational realities of the energy system [69].

Within PyPSA, capacity limitations for each component in the system can be manually set. For extendable components that are subject to the optimization, the nominal capacity can be limited for each decision variable. For example, the nominal capacity $G_{n,s}$ of a generator will be constrained by

$$\underline{G}_{n,s} \leq G_{n,s} \leq \bar{G}_{n,s}, \tag{3.13}$$

where $\underline{G}_{n,s}$ is the lower boundary for nominal capacity, and $\bar{G}_{n,s}$ is the upper boundary. Equivalent constraints can be set for extendable components of links (F_l), lines and transformers (P_l), stores ($E_{n,s}$), and storage units ($H_{n,s}$) [70]. Additionally, the capacity expansion can be further constrained to be a multiple of a modular capacity, in order to represent fixed sizes of each added component. For a generator, this is expressed as

$$G_{n,s} = G_{n,s}^{\text{mod}} \cdot \tilde{G}_{n,s}, \tag{3.14}$$

where $G_{n,s}^{\text{mod}} \in \mathbb{N}$ is the number of installed modular units with fixed capacity $\tilde{G}_{n,s}$. Similar modularities can apply to links, lines, transformers, stores, and storage units [70]. Furthermore, the nominal capacity can be firmly constrained to hold a fixed value, which is $\tilde{G}_{n,s}$ for generators, $\tilde{F}_l$ for links, $\tilde{P}_l$ for lines and transformers, $\tilde{E}_{n,s}$ for stores, and $\tilde{H}_{n,s}$ for storage units [70]. Beyond these capacity constraints, PyPSA also constrains the power dispatch of relevant components within the system, as well as the stored energy within stores and storage units. Supported by the online PyPSA documentation for these constraints, the remaining part of this section follows closely the respective references [71,72].

Generator constraints are expanded from the pure capacity restrictions by limiting the power dispatch from generators. Each generator within the model has a dispatch variable $g_{n,s,t}$, which is constrained in different ways, depending on the set-up of the model. For a non-extendable generator, the dispatch is limited by

$$\underline{g}_{n,s,t} \cdot \hat{g}_{n,s} \leq g_{n,s,t} \leq \bar{g}_{n,s,t} \cdot \hat{g}_{n,s}, \tag{3.15}$$

where $\underline{g}_{n,s,t}$ and $\bar{g}_{n,s,t}$ are the lower and upper dispatch constraints per unit of nominal capacity, respectively. These factors are time-dependent and account for external factors such as wind availability and solar irradiation. $\hat{g}_{n,s}$ is the nominal capacity of a non-extendable generator. When a generator, or any other component, is defined as extendable, its nominal capacity becomes subject to optimization within the simulation. If so, extendable generators are constrained by

$$\underline{g}_{n,s,t} \cdot G_{n,s} \leq g_{n,s,t} \leq \bar{g}_{n,s,t} \cdot G_{n,s}, \tag{3.16}$$

where $G_{n,s}$ is the nominal capacity to be optimized. Additionally, the dispatch can be set to a fixed value $\tilde{g}_{n,s}$, such that the dispatch is given by

$$g_{n,s,t} = \tilde{g}_{n,s,t}. \tag{3.17}$$

Generators can also be constrained by volume limits, which means that the total energy dispatch over all snapshots must remain within certain limits. These volume limits are governed by the expression

$$\underline{e}_{n,s} \leq \sum_t w_t^g g_{n,s,t} \leq \bar{e}_{n,s} \quad \forall n, s, \tag{3.18}$$

where $\underline{e}_{n,s}$ and $\bar{e}_{n,s}$ are the minimum and maximum limits for the total dispatch, respectively. w_t^g is the snapshot weighting for the generators.

Links are constrained in a similar way to generators, and carry the dispatch variable $f_{l,t}$. The dispatch of a non-extendable link is limited by

$$\underline{f}_{l,t} \cdot \hat{f}_l \leq f_{l,t} \leq \bar{f}_{l,t} \cdot \hat{f}_l, \tag{3.19}$$

where $\underline{f}_{l,t}$ and $\bar{f}_{l,t}$ are the time-dependent lower and upper dispatch constraints per unit of nominal capacity, respectively. $\hat{f}_l$ is the nominal capacity of a non-extendable link. Furthermore, an extendable link is constrained by

$$\underline{f}_{l,t} \cdot F_l \leq f_{l,t} \leq \bar{f}_{l,t} \cdot F_l, \tag{3.20}$$

where F_l is the nominal link capacity to be optimized. As with the generators, a link can be fixed to a certain dispatch value $\tilde{f}_{l,t}$, which locks the dispatch to

$$f_{l,t} = \tilde{f}_{l,t}. \tag{3.21}$$

Furthermore, links can also be constrained by volume limits. If so, these volume limits are constrained by

$$\underline{e}_l \leq \sum_t w_t^g f_{l,t} \leq \bar{e}_l \quad \forall l, \tag{3.22}$$

where $\underline{e}_l$ and $\bar{e}_l$ are the minimum and maximum limits for the total energy dispatch, respectively.

Lines and transformers are also constrained on their power flow. Unlike generators and links, the power flow variable $p_{l,t}$ of these components is constrained by a symmetrical interval around 0. For non-extendable lines or transformers, this constraint is given as

$$-\bar{p}_{l,t} \cdot \hat{p}_l \leq p_{l,t} \leq \bar{p}_{l,t} \cdot \hat{p}_l, \tag{3.23}$$

where $\bar{p}_{l,t}$ is the upper dispatch constraint per unit of nominal capacity, and $\hat{p}_l$ is the nominal capacity of a non-extendable line or transformer. $\bar{p}_{l,t}$ is time-dependent and determined by control mechanisms such as DLR or security margins for lines. Similarly, extendable lines or transformers are constrained by

$$-\bar{p}_{l,t} \cdot P_l \leq p_{l,t} \leq \bar{p}_{l,t} \cdot P_l, \tag{3.24}$$

where P_l is the nominal capacity to be optimized. Due to the nature of the components, lines and transformers cannot be fixed to a certain dispatch value, nor are they restricted by volume limits.

However, the power flow through lines and transformers in AC networks is governed by Kirchhoff's Voltage Law (KVL). In PyPSA, this governing is done through a cycle-based linearized formulation of KVL, given as

$$\sum_l C_{l,c} x_l p_{l,t} = 0 \quad \forall\, c, t, \tag{3.25}$$

where C is a cycle basis matrix of the network graph, in which the independent cycles c are expressed as direct linear combinations of the lines l, and x_l is the series reactance [73].

Stores have two time-dependent variables in PyPSA. They are the store dispatch $h_{n,s,t}$ in MW, and the store energy level $e_{n,s,t}$ in MWh. $h_{n,s,t}$ is unconstrained, allowing it to hold any values, both positive (discharging) and negative (storing). Thus, the limits for store dispatch are given as

$$-\infty \leq h_{n,s,t} \leq +\infty. \tag{3.26}$$

The store energy levels, however, are constrained by minimum and maximum levels. Similar to generators and links, $e_{n,s,t}$ can be defined as non-extendable, extendable or fixed. If defined as non-extendable, the store energy level is limited by

$$\underline{e}_{n,s,t} \cdot \hat{e}_{n,s} \leq e_{n,s,t} \leq \bar{e}_{n,s,t} \cdot \hat{e}_{n,s}, \tag{3.27}$$

where $\hat{e}_{n,s}$ is the nominal energy capacity, while $\underline{e}_{n,s,t}$ and $\bar{e}_{n,s,t}$ are the time-dependent restrictions on the energy level, given per unit of nominal capacity. Furthermore, the energy levels of extendable stores are constrained by

$$\underline{e}_{n,s,t} \cdot E_{n,s} \leq e_{n,s,t} \leq \bar{e}_{n,s,t} \cdot E_{n,s}, \tag{3.28}$$

where $E_{n,s}$ is the energy capacity to be optimized. Lastly, if the energy level is fixed to a certain value $\tilde{e}_{n,s,t}$, it is given as

$$e_{n,s,t} = \tilde{e}_{n,s,t}. \tag{3.29}$$

Additionally, the power and energy variables for stores are governed by the storage consistency equation, expressed as

$$e_{n,s,t} = \eta_{\text{stand},n,s}^{w_t^s} e_{n,s,t-1} - w_t^s h_{n,s,t} \quad \leftrightarrow \quad \lambda_{n,s,t}^{\text{MSV}}, \tag{3.30}$$

where $\eta_{\text{stand},n,s}$ is the storage efficiency after accounting for standing losses, such as thermal dissipation, per hour. w_t^s is the snapshot weighting for stores and storage units, which defaults to 1 hour. The dual variable $\lambda_{n,s,t}^{\text{MSV}}$ represents the marginal storage value, also known as the water value in hydro-storage, as presented in Section 2.4.

Storage units are different from stores, as explained in Section 3.4.3. They also differ from generators, as they link their energy capacity to the power capacity by the SOC, representing the level of energy stored in a unit at any given point in time. In PyPSA, this results in storage units having three time-dependent variables: the discharge $h^-_{n,s,t}$ and charge $h^+_{n,s,t}$, both in MW, and the state of charge variable $\mathrm{soc}_{n,s,t}$ in MWh. For a storage unit, this nominal state of charge cannot be optimized independently of the nominal power output, as these values are coupled through a *max_hours* parameter. Additionally, the nominal charging power is linked to the maximum discharging power, ensuring a fixed relationship between the two variables.

For non-extendable storage units, the three variables are constrained by the expressions

$$0 \leq h^-_{n,s,t} \leq \bar{h}_{n,s,t} \cdot \hat{h}_{n,s}, \tag{3.31}$$

for the discharge,

$$0 \leq h^+_{n,s,t} \leq -\underline{h}_{n,s,t} \cdot \hat{h}_{n,s}, \tag{3.32}$$

for the charge, and the SOC is limited by

$$0 \leq \mathrm{soc}_{n,s,t} \leq r_{n,s} \cdot \hat{h}_{n,s}. \tag{3.33}$$

In these expressions, $\hat{h}_{n,s}$ is the nominal power capacity, $\bar{h}_{n,s,t}$ is a time-dependent restriction on the discharge per unit of nominal capacity, $\underline{h}_{n,s,t}$ is a time-dependent restriction on the maximum charge per unit of nominal capacity, and $r_{n,s}$ is the number of hours at nominal power that will fill the state of charge. Note that $\underline{h}_{n,s,t}$ usually is negative, defaulting to -1, thus ensuring that the upper bound in Equation (3.32) is positive.

Similarly, the discharge and charge variables for extendable storage units are constrained by

$$0 \leq h^-_{n,s,t} \leq \bar{h}_{n,s,t} \cdot H_{n,s}, \tag{3.34}$$

for the discharge, while the charge is limited by

$$0 \leq h^+_{n,s,t} \leq -\underline{h}_{n,s,t} \cdot H_{n,s}, \tag{3.35}$$

where $H_{n,s}$ is the optimized power capacity.

Furthermore, all three variables can be fixed to certain values $\tilde{h}^-_{n,s,t}$, $\tilde{h}^+_{n,s,t}$, and $s\tilde{o}c_{n,s,t}$, which yields the expressions

$$h^-_{n,s,t} = \tilde{h}^-_{n,s,t}, \tag{3.36}$$

$$h^+_{n,s,t} = \tilde{h}^+_{n,s,t}, \tag{3.37}$$

and

$$\mathrm{soc}_{n,s,t} = \tilde{soc}_{n,s,t}, \tag{3.38}$$

for the discharge, charge, and SOC variables, respectively.

Similar to stores, the variables of storage units are connected through a relation expressed as

$$\begin{aligned}\mathrm{soc}_{n,s,t} = \eta^{w_t^s}_{\mathrm{stand};n,s}\, \mathrm{soc}_{n,s,t-1} + \eta_{\mathrm{store};n,s}\, w_t^s\, h^+_{n,s,t} \\ - \eta^{-1}_{\mathrm{dispatch};n,s}\, w_t^s\, h^-_{n,s,t} + w_t^s\, \mathrm{inflow}_{n,s,t} - w_t^s\, \mathrm{spillage}_{n,s,t} \\ \leftrightarrow \quad \lambda^{\mathrm{MSV}}_{n,s,t}\,,\end{aligned} \tag{3.39}$$

where $\eta_{\mathrm{store};n,s}$ and $\eta_{\mathrm{dispatch};n,s}$ are the efficiencies for power going into and out of the storage unit, respectively.

Security constraints are included in PyPSA to allow for proper modeling of the power system behavior after contingencies, such as the outage of particular lines or transformers. To achieve this, N-1 security-constrained optimal power flow can be utilized. This ensures robustness in the system against the outage of a selection of branches [74].

Within the model, this security constraint is ensured by utilizing the Branch Outage Distribution Factor (BODF) matrix, which is constructed by linear power flow assumptions. The BODF matrix captures the effect an outage of branch c has on the flows of all other branches b in a sub-network. If p_b is the flow in branch b before the outage, and $p_b^{(c)}$ is the flow after the outage, the BODF matrix is defined by

$$p_b^{(c)} = p_b + BODF_{bc} p_c. \tag{3.40}$$

In order to ensure no branch exceeds its capacity P_b during a contingency, the optimization problem is limited by

$$|p_{b,t} + BODF_{bc} p_{c,t}| \leq |P_b| \quad \forall b, c, t. \tag{3.41}$$

However, running such security-constrained optimization problems can be computationally expensive, due to the product of lines, outages and snapshots. Therefore, the constructors of PyPSA have proposed several approaches to approximate the security constraints. The simplest of these approaches is to reserve a security margin from all branch capacities for contingencies. This can be done by allowing the optimization to load each line a maximum of 70% of the nominal load capacity. This simplification will ensure system security while significantly improving the computational costs of the simulations [74].

Collectively, these constraints describe the possible operational states the objective function is allowed to minimize within. While capacity and dispatch limits in Equations (3.13) through (3.38) ensure that the power system remains within its technical design limits, the inclusion of KVL in (3.25) and storage consistency relations in (3.30) and (3.39) enforces the fundamental physical and temporal interdependencies of the network. Furthermore, security constraints provide a necessary buffer for real-world contingencies, ensuring that the mathematically optimal solution remains physically robust. Ultimately, the constraints transform the theoretical minimization of costs into a realistic simulation of a reliable, multi-sector power system, where every decision variable is bound by the actual limitations of the component it represents [69]. For a more detailed breakdown of the design and constraints in PyPSA, please refer to the online user-guide [75].

3.4.6 Limitations of the Framework

Although PyPSA-Eur is an open-source, validated model of the European energy system, several limitations persist due to data gaps and necessary approximations. The grid data of the ENTSO-E transmission network is based on a map from OSM, and is known to contain distortions used to enhance map readability. Additionally, the absence of exact line impedances has led to these being approximated based on line lengths and other standard line parameters, rather than specific conductor configurations. The framework also lacks data on distribution network capacities, switch locations, transformer stations, and reactive power compensation facilities. Since local grid constraints are not included in the model, it fails to capture voltage variations and transmission bottlenecks within each node. Furthermore, the spatial distribution of electricity demand within countries is determined using population and Gross Domestic Product (GDP), which may not accurately capture local variations. The model also assumes that the temporal shape of the demand time series is uniform for every node within a country, potentially overlooking regional differences in consumption behavior [76].

4 Methodology

This chapter provides details on the model and methodology used to achieve the results of the study. Section 4.1 presents the utilized version of PyPSA-Eur, while Section 4.2 highlights the data sources used for modeling. Section 4.3 provides details on the specific configuration of key components and parameters in the model that is used within this research. Furthermore, Section 4.4 presents how the results from the modeling is presented and interpreted, alongside the existing power system that the model builds upon. Section 4.5 outlines the limitations of the constructed model, before Section 4.6 presents the study's four scenarios, which are designed to explore how different levels of vRES capacity expansion will affect the Nordic power system. Finally, the usage of Artificial Intelligence (AI) in the creation of this thesis is detailed in Section 4.7.

4.1 Model Version

For the modeling and analysis of the Nordic power system, this study employs PyPSA-Eur version v2025.07.0, specifically release 1.0.5 [55]. System optimization is made possible via the Gurobi solver, which facilitates an exploration and assessment of European and Nordic power system pathways towards 2050.

4.2 Data Sources

The modeling approach in this study relies on a composite dataset that integrates multiple technical and meteorological sources to represent the European power system. This combination of data provides the necessary information on generation capacity, grid topology, and weather patterns required to simulate power flows and renewable energy potential.

The Powerplantmatching (PPM) tool is utilized within the PyPSA-Eur framework to consolidate information from various open-source databases. As detailed in Section 3.4.2, this tool cleans and standardizes the data to align with the specific generation mixes of the included countries. Once processed, the aggregated dataset is exported to the model, where it defines the installed capacities at each bus [37].

In PyPSA, most data sources are unique for their purpose, and thus there is little flexibility in deciding which datasets to use. The only dataset that is subject to manual selection in PyPSA-Eur is the data used to construct the underlying base network. The default option is the OSM network presented in Section 3.4.2, with the possibility to use GridKit or Ten Year Network Development Plan (TYNDP) as alternative bases. GridKit is based on a ENTSO-E web map extract, while TYNDP is a grid topology based on the TYNDP scenarios from the European Network of Transmission System Operators for Electricity and Gas (ENTSO-E / ENTSO-G), which includes planned and existing lines [77]. In this study, the default option of the OSM base network is used.

Additionally, it should be noted that the framework retrieves the latest supported version of all datasets from an archive source, by default [78]. Consequently, transitioning between PyPSA-Eur versions may lead to automatic downloads and usage of updated input data, not necessarily matching this study. Furthermore, some datasets support *primary* or *build* as the source option, meaning that the data can be retrieved from the original data source or built from the latest available data. A full list of the data sources within PyPSA-Eur can be found in the online documentation [77].

4.3 Configuration

While the primary focus of this study is the assessment of a net-zero Nordic power system by 2050, the transition towards this state is modeled using multiple intermediate planning horizons. To capture a realistic development trajectory, the entire power system is simulated in five-year intervals between 2030 and 2050. Within the PyPSA-Eur framework, this approach is implemented as a *myopic* simulation, which ensures a consistent evolution of the system by implementing gradual upgrades at every step. By considering the assets installed in previous periods, the myopic method accounts for pathway dependencies, preventing the model from making a perfect 2050 system that would be unattainable in a real-world transition.

Across all simulations and scenarios, the modeled generation capacities are based on the Nordic grid development plans detailed in Section 2.3. This ensures that the model accurately reflects expected system changes, including the increased electrification of industry, higher shares of vRES, and the phase-out of fossil fuels. Furthermore, to account for changing electricity demand, PyPSA-Eur generates a system load prediction for each planning horizon, based on expected growth in Gross Domestic Product (GDP) and population. To verify that this load development is realistic, the default demand profiles generated by the model are compared against the expectations published by the Nordic TSOs, and adjusted accordingly. The technical steps for this adjustment are further detailed in Section 4.3.3.

The setup of the model primarily focuses on the Nordic synchronous area, specifically targeting Norway, Sweden, Denmark, and Finland as the central objective countries in the simulation. While interconnections to Germany, Belgium, France, the Netherlands, and Great Britain are included to represent cross-border flows, these neighboring regions are modeled as single buses to maintain computational efficiency. To implement this design, spatial focus weights are assigned to each country, as detailed in Table 4.1. Based on the total number of nodes defined for the model, these weights instruct the clustering algorithm to allocate a specific percentage of nodes to the respective countries. By setting these weights to 1% for all countries outside the Nordics, it is ensured that the model is forced to cluster those regions into a single node per country. The only exception is Great Britain, which is allocated two buses to maintain the physical integrity of its underlying network data [79].

Table 4.1: Spatial focus weights for network clustering. These weights determine the percentage-based allocation of nodes across the modeled regions. High weights are assigned to the Nordic countries to ensure high spatial resolution in the primary study area, while a minimal weight of 1% is applied to neighboring countries to simplify them into single-node representations.

Country	**Focus Weight**
Norway	40%
Sweden	30%
Finland	20%
Denmark	5%
Germany	1%
Belgium	1%
France	1%
Netherlands	1%
Great Britain	1%

Within this geographic framework, the model clusters the Nordic power system alongside the interconnected countries into 110 regional buses. To balance computational speed with seasonal accuracy, the simulation data is represented as time series with a temporal resolution of 24 hours. At each bus, various system components are specified, each characterized by distinct physical limitations and operational capabilities. As a whole, this setup is configured to represent the relevant conditions and behavior of the Nordic power system in 2050, including the projected increase in electricity demand and generation capacity.

4.3.1 Generators

The PyPSA-Eur framework includes a range of generator technologies, spanning onshore wind, offshore wind, run of river (RoR), solar PV, nuclear, oil, and gas. To capture specific technical characteristics, offshore wind is categorized into offshore wind DC, offshore wind AC, and floating offshore wind. The main distinction between offshore AC and offshore DC is the connection type to onshore facilities, either by AC or DC transmission. Similarly, solar PV is represented by the three distinct classes solar PV (fixed-tilt), rooftop solar, and horizontal single-axis tracker (HSAT) solar. In order to align with the objectives of this study, only renewable energy technologies are defined as extendable. This configuration allows the model to expand the installed capacities of onshore wind, offshore wind, and solar PV during the optimization. In contrast, all other generation sources, such as RoR, gas turbines and nuclear plants, are modeled with fixed capacities and are not subject to expansion. Under these constraints, the optimal capacity expansion is determined by the objective function (3.5).

The capacity expansion for these extendable generators is further governed by minimum and maximum limits, which are set manually. For all countries included in the model, these constraints are derived from national projections of renewable expansion. While these projections serve as the baseline values in the study, only the capacities within the Nordic region are adjusted between the different scenarios, which is further described in Section 4.6. On the other hand, Table 4.2 shows the sourced projections of vRES capacity expansion for all countries outside the Nordics. Across all simulations and scenarios, the model is forced to install these capacities within a flexibility margin of ± 10%. Additionally, Table 4.5 displays the corresponding baseline values for the Nordic countries.

Table 4.2: Projected installed capacities for renewable generator carriers in non-Nordic countries for 2030, 2040, and 2050, in MW. Across all simulations, the model is forced to install these capacities, with a flexibility margin of ± 10%. Projections are sourced from, or based on [80,81,82,83,84].

Country	**Carrier**	**Installed Capacity 2030 [MW]**	**Installed Capacity 2040 [MW]**	**Installed Capacity 2050 [MW]**
Belgium	Solar PV	17 500	29 500	41 500
	Onshore Wind	5600	7600	9600
	Offshore Wind	5800	5800	5800
France	Solar PV	22 000	46 000	70 000
	Onshore Wind	23 000	33 000	43 000
	Offshore Wind	4400	13 200	25 000
Germany	Solar PV	230 000	400 000	480 000
	Onshore Wind	105 000	165 000	190 000
	Offshore Wind	30 800	61 200	70 000
Great Britain	Solar PV	46 700	77 700	97 000
	Onshore Wind	29 800	42 000	47 500
	Offshore Wind	46 500	93 600	104 400
Netherlands	Solar PV	76 100	124 400	172 600
	Onshore Wind	10 300	15 200	20 000
	Offshore Wind	21 500	46 800	72 000

Furthermore, specific values for spatial capacity density are applied to ensure realistic expansion possibilities. As the default limits in PyPSA-Eur are considered conservative, manual overrides are implemented to better reflect technical potentials. Specifically, the capacity density for onshore wind is set to 6.2 MW/km^2, while it is set to 6.5 MW/km^2 for offshore wind. For fixed-tilt solar PV it is set to 35.0 MW/km^2, and 23 MW/km^2 for HSAT solar [85]. When combined with the land eligibility data provided by the CORINE Land Cover and Natura 2000 datasets [59,60], these density values establish the maximum technical potentials for the expansion of each renewable carrier.

4.3.2 Storage Units and Stores

The storage units included in the model are hydropower and PHS systems. As introduced in Section 3.4, these units are capable of storing energy over extended periods, such as weeks and months. During periods of high system demand, they discharge the stored water from the reservoirs, thus acting as generators. Furthermore, PHS systems can be charged during periods of low system demand by pumping water from their lower outlet back into the reservoir [86]. Due to the limited potential for new hydropower developments in the Nordics, these storage units are set as non-extendable in this study. This decision also aligns with the projections from the Nordic TSOs, which show near-zero expansion for hydropower by 2050, as seen in Figure 2.2. As this is the default option in the configuration of PyPSA-Eur, more comprehensive details on the modeling and characteristics of these units can be found in the PyPSA documentation [87].

Stores mainly consists of different battery types, H_2-stores, biogas, and solid biomass. However, the model also includes a more comprehensive list of carriers, which can be found in the documentation [55]. Within this study, both batteries and H_2-stores are set as extendable, meaning the model is allowed to expand flexible store capacities when optimizing. To implement this in an efficient manner, the stores are configured to optimize their charging and discharging behavior, thus enabling PyPSA to model a flexible power system. Allowing for expanded capacities of these stores is important, as a higher share of these energy carriers is essential for reliable and fast balancing of variable renewable generation in the system, as discussed in Section 2.5.1.

4.3.3 Load

Within PyPSA-Eur, the load components represent all electricity demands across the system. These demands must be met by the supply from the generation sources and storage systems, enabled by power flow through the grid. As previously noted, PyPSA-Eur projects a load profile for the selected system based on expected growth in both GDP and population. The generated profile consists of time-varying data that reflects realistic demand behavior for the Nordic power system. However, the default 2050 demand profile of the Nordics in PyPSA-Eur is underestimated compared to the forecasts provided by the Nordic TSOs. Therefore, a change is made to this profile by scaling the load of all Nordic buses with a factor of 1.7. Importantly, this factor is derived specifically from Nordic demand projections and cannot be arbitrarily applied to the remaining buses in the system. A comparison of simulated loads and official 2050 projections has not been conducted for Continental Europe and the UK, meaning there is no indication that their demand is underestimated to the same extent as the Nordic region. Furthermore, uniformly scaling the remaining continental demand by 1.7 yields an unsolvable problem for the optimizer. Therefore, the load scaling of Nordic buses is manually implemented in the PyPSA-Eur scripts, and the load scaling factor in the PyPSA configuration is kept as 1.0 [87].

The Nordic TSOs anticipate that the electricity demand will nearly double from 2023 levels by 2050 [22,3]. According to their common projections, the annual electricity demand for 2050 is expected to be in the range of 650 TWh to 665 TWh, excluding hydrogen [3]. Since hydrogen demand is highly dependent on specific development paths, it is best to compare the simulated and projected electrical demand in 2050 without accounting for hydrogen. It should however be noted that the TSOs expect significant hydrogen demand by 2050 in their report, increasing the total load projection to roughly 960 TWh. While the default load profile within PyPSA-Eur yields a total Nordic consumption below the projected range, the scaled load profile aligns better. Excluding hydrogen demand, the scaled annual demand amounts to 663 TWh, while the hydrogen demand is highly variable between scenarios. Figure 4.1 illustrates the simulated load profile for the Nordic countries (excluding hydrogen), compared against the 2023 actual load scaled by a factor of two.

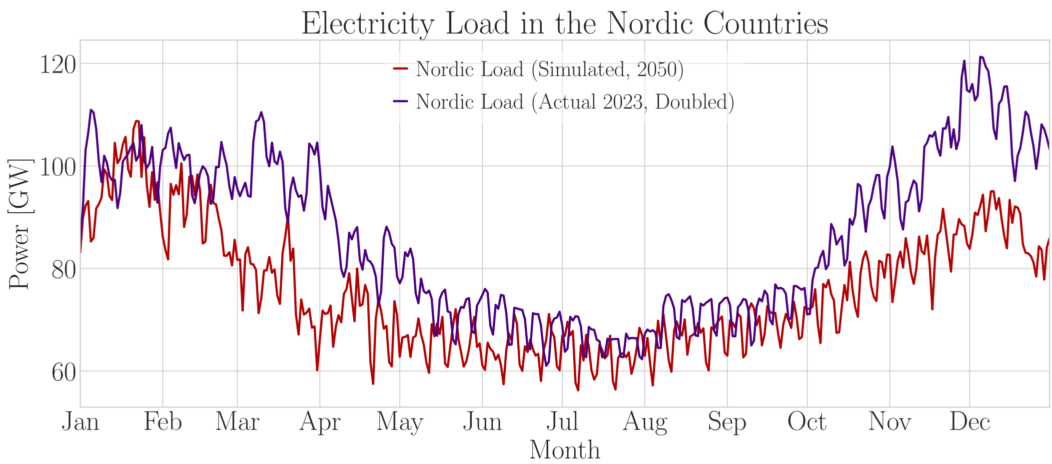

Figure 4.1: Aggregated electricity load across the Nordic countries plotted over the duration of one sample year, in GW. The red line shows the simulated pure electricity load for 2050 in PyPSA-Eur, while the purple line shows the actual load from 2023, doubled for visual comparison of the simulated load and the projections from Nordic TSOs. The simulation in PyPSA-Eur assumes that the load will be slightly lower than doubled 2023-levels, which aligns with TSO projections. Actual load data collected from [88].

The simulated Nordic electricity load reaches a maximum of 109 GW and a minimum of 56 GW. The annual demand amounts to 663 TWh, placing the load profile well within the projected range from the Nordic TSOs. Furthermore, the total annual demand, including hydrogen, is as stated highly variable between scenarios and is therefore elaborated on in the results.

4.3.4 Lines and Links

For the configuration of lines in the simulation, the default PyPSA-Eur settings are used. Because the network is clustered, it is important to note that a simulated line represents an AC connection between two buses rather than actual power lines. With this noted, the optimizer is restricted from constructing new lines. Instead, all existing lines and those currently under development are set as extendable, with a maximum capacity expansion of 20 GW per line. Regarding line loading and security, neither security-constrained optimal power flow nor DLR is implemented in the model. As described in Section 3.4.5, incorporating these features would significantly increase the computational cost of the simulation, Therefore, the computationally efficient alternative of approximating N-1 is applied. The power flow through all lines is limited to a maximum of 70% of their rated capacity. As a result, lines are upgraded when the necessary loading on them exceed 70%, thus ensuring N-1 operation with a low computational cost.

The HVDC interconnectors from the Nordic power system to Europe are included in the model as links. Similar to the lines, the optimizer is kept from constructing new links, meaning only existing and planned links are included, and any required increase in link capacity is achieved through expansion of these. In order to prevent the transmission capacities of these links from becoming bottlenecks of the optimized system, a custom configuration is applied. While the restriction that links are only allowed to carry up to 100% of their rated capacity is kept, the upper limit for expansion per HVDC link is raised from 30 GW to 100 GW.

4.3.5 Costs and Emission Constraints

To accurately optimize the system, the model relies on realistic financial parameters. The cost assumptions used in this model are retrieved for 2050, for the whole system and across planning horizons. To ensure realistic cost comparisons for different investment periods, a social discount rate of 2% is applied, which is a standard rate for long-term public infrastructure projects. For more information and details on how this discount rate functions, please refer to Ref. [89].

The contributors to PyPSA have gathered cost assumptions for various technologies as a basis for the framework, from a range of sources. This study uses the default cost assumptions for 2050, found in [90]. Table 4.3 shows the relevant costs for the generator technologies set at extendable in this study, which are used by the optimizer when solving the objective function (3.5) for the cost-optimal solution that meets the technical requirements for the modeled system.

Table 4.3: Investment cost assumptions for the extendable generators in the model, and the assumed lifetimes. Costs are given in EUR per installed capacity, and lifetimes in years. Data is sourced from [90].

Technology	Investment cost 2050	Lifetime [Years]
Solar HSAT	353 EUR/kW$_p$	40
Solar PV	409 EUR/kW$_p$	40
Solar Rooftop	524 EUR/kW$_p$	40
Onshore Wind	1019 EUR/kW	30
Offshore Wind	1524 EUR/kW	30
Floating Offshore Wind	1580 EUR/kW	20

Regarding emission constraints, decreasing CO_2 limits are applied for every planning horizon until they reach zero for 2050. This means no net emissions are allowed for the final system, which forces the model to reduce fossil-fuel-based generation, and increase generation from renewable sources. By integrating these constraints, the model ensures that the energy system aligns with the EU's long-term climate goals of net-zero emissions, while balancing economic and operational considerations.

4.3.6 Weather Data

For all simulations and scenarios presented in this study, a fixed dataset for the referenced weather is used. The meteorological data is sourced from the ERA5 reanalysis database [58], with 2013 serving as the reference year. 2013 is the default year in PyPSA-Eur primarily because it serves as a well-tested, representative, and complete historical baseline for European weather data. Using this year enables automatic, reliable use of pre-compiled weather data, ensuring consistent simulations of renewable energy generation. Additionally, the ERA5 data is supplemented by SARAH-3, a satellite-based climate data record of surface solar radiation [91]. In combination, these datasets provide the model with the necessary inputs to simulate generation profiles for the weather dependent assets in the model, such as vRES and hydropower. Furthermore, using this data as fixed input ensures that the generation profiles remain consistent for all installed components across planning horizons and scenarios. While removing all weather-dependent uncertainty is a notable simplification of the system, this method enables direct comparability of the power system across different scenarios, which is the primary scope of this study.

4.4 Interpreting the System Model

In order to analyze the modeled power system in this study, focus is put on the representation of generators, storage units, stores, and transmission carriers. This methodology closely follows the analysis in [6], so that the results from this study are easily comparable. Figure 4.2 displays a representation of the current Nordic power system, while the corresponding map for the entire simulated system is shown in Figure A.2 in Appendix A. The figures show the existing installed capacities of renewable and nuclear generators and storage units in the Nordic countries, from 2025. Additionally, existing transmission capacities of both AC lines and HVDC links between buses are shown.

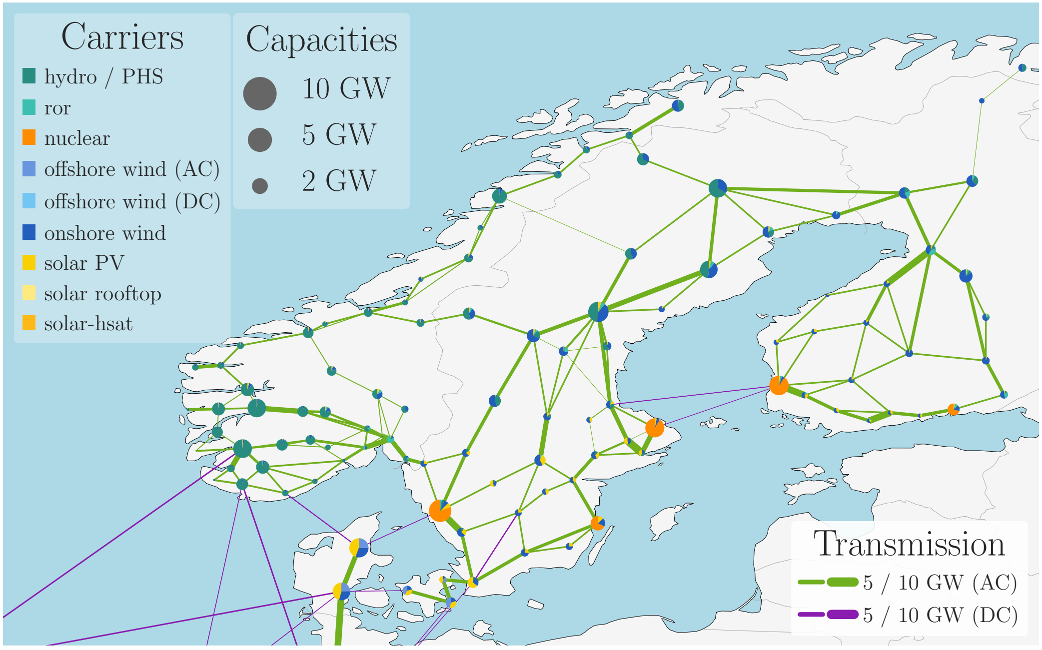

Figure 4.2: Existing installed capacities of generators, transmission lines and HVDC links in the model, for 2025. The system is clustered into 110 nodes, connected by lines and HVDC links. Hydropower is seen to be dominating generation in Norway, while onshore wind and solar has larger shares in the Danish and Swedish regions. Nuclear generation is only present in Sweden and Finland, while Denmark is the only country with noticeable offshore wind capacity. The figure focuses on the Nordic area as this is the main scope of the study, and the remaining interconnected countries are outside of the map borders.

As introduced in Section 3.4, PyPSA-Eur utilizes spatial clustering of buses and their connected components to reduce system complexity and computational cost. To achieve this, the model simplifies the grid by transforming it into a 380 kV-only equivalent network. Subsequently, k-means clustering is used to group all network components into 110 zones, with one bus per zone. Thus, each bus represents a realistic geographic cluster of network components such as generators, loads, and transmission lines [92]. In the network maps throughout this thesis, such as Figure 4.2, the size of each bus corresponds to the total installed generation capacity, while the internal segments illustrate the share of each generation source.

Between the buses, transmission lines and HVDC links are shown as the connections. The displayed width of these connections represents the aggregated capacity of all the underlying, actual transmission components. Consequently, it must be noted that the shown lines and links are not necessarily real components in the network, and do not correspond to precise geographic locations or capacities. Color-coding is used to make a clear distinction between AC transmission lines and HVDC links, with AC lines shown in green and HVDC links shown in purple. Such a simplified representation of the Nordic power system enables a clear visualization of generation and transmission capacities. In turn, this facilitates a strong understanding of the aggregate system design and necessary transmission capacities.

4.5 Model Limitations

Building on the general constraints presented in Section 3.4.6, the specific implementation used in this study introduces additional constraints. Clustering the Northern-European power system into 110 nodes using the focus weights shown in Table 4.1 reduces system complexity and thus the computational cost. However, this spatial aggregation necessarily limits the model's ability to accurately capture regional demand variations and local grid constraints. Furthermore, the exclusion of distribution grids below 220 kV prevents the model from accounting for local flexibility challenges, which are important under vRES integration. Moreover, because Norway is not part of the Natura 2000 network, the model does not restrict vRES installations on protected Norwegian areas. Additionally, to reduce scope complexity, the model excludes HVDC connections to Poland and the Baltic countries, which simplifies the modeled power flows but limits the simulation accuracy of the actual 2050 Nordic power system.

Table 4.4: Existing generator capacities in the Nordics, comparing modeled assumptions against actual installations. To maintain comparability, RoR and floating offshore wind from PyPSA-Eur are merged into hydropower and offshore wind, respectively, while all solar PV technologies are aggregated. In both columns, hydropower and onshore wind are seen as the dominant capacities.

Carrier	Installed Capacity in the Model [GW]	Actual Installed Capacity [GW]
Hydropower	46.0	53.2
Onshore Wind	31.9	33.1
Offshore Wind	2.9	2.7
Nuclear Power	13.0	11.5
Solar PV	10.4	10.6
Total	**104.2**	**111.1**

In addition to spatial constraints, the model assumptions for existing installed generator capacities contain inaccuracies. Table 4.4 shows the existing installed capacities in the Nordic countries within the model alongside actual numbers, sourced from [93,94,95,96,97,98]. Both are aggregated for all Nordic countries. The numbers highlight that hydropower and onshore wind are the main providers in the system, while nuclear power and solar PV contribute with significant capacities. However, comparing the model capacities with the actual values reveals notable deviations. In particular, the installed hydropower capacity is underestimated by 7.2 GW in the model, and nuclear power is overestimated by 1.5 GW. While the installed capacities for vRES are more accurate, these deviations indicate that the input dataset to PyPSA-Eur of existing capacities has room for improvement.

Building on the misalignment of hydropower capacity, Figure 4.3 shows the model's simulated total SOC in the Nordics compared to actual values. The simulated data includes SOC from the storage units `hydro` and `PHS` from the model, which corresponds to the actual SOC values collected from [88]. While both the simulated and actual data show similar trends, the figure clearly exhibits that the model underestimates the reservoir levels of Nordic hydropower throughout the year. The difference is smallest in the winter, and largest in the spring/summer. From the middle of April until the middle of August, the deviation is 30 TWh or greater, with a maximum difference of 37 TWh at the end of June. Knowing that hydropower has the biggest total installed capacity in the Nordics, this is a significant limitation for the study. The large deviation could indicate that the model is simulating a worst-case scenario with low availability of hydropower, e.g. due to low precipitation in the chosen weather-referenced year, or due to missing data on specific hydropower plants in the model.

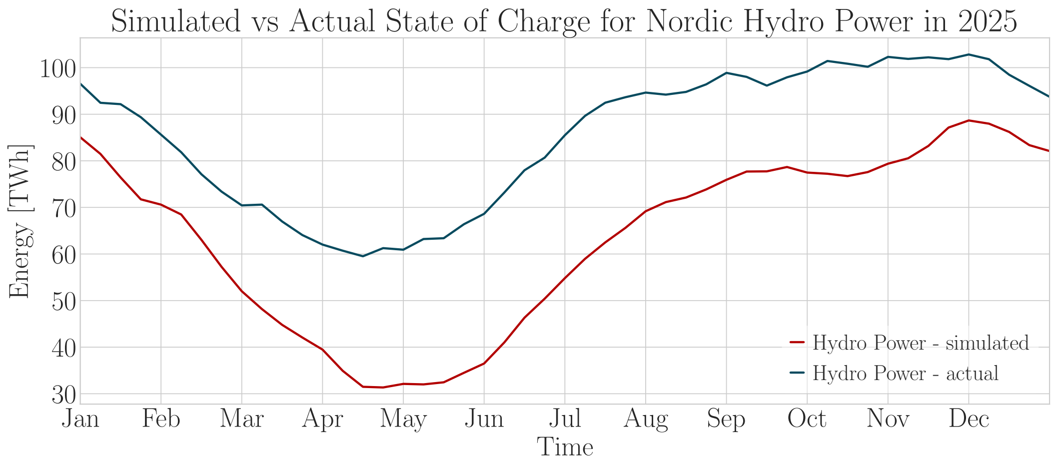

Figure 4.3: Aggregated SOC for all Nordic hydropower storage units throughout 2025. The red line shows the simulated SOC from the model, while the blue line shows the actual SOC. Clearly, the model underestimates the SOC compared to the actual values. Data on actual SOC collected from [88].

Additionally, actual SOC-profiles for hydropower can vary significantly from year to year, due to precipitation and other weather conditions. In this study, however, the referenced weather data presented in Section 4.3.6 is constant for all simulations. Also taking into account that neither hydropower nor PHS is set as extendable, this means that the simulated SOC profile seen in Figure 4.3 will be constant across all planning horizons and all presented scenarios.

4.6 Scenarios

This section outlines the four scenarios investigated by this study. The scenarios are all built around a set of baseline values, which represent the most likely development path for the capacity expansion of vRES in the Nordic power system. Since the study utilizes a myopic simulation method, baseline values are defined for the years 2030, 2040, and 2050, and are sourced from the grid development plans of the Nordic TSOs [3]. Table 4.5 presents these baseline values, which are the only capacity values that are subject to change across the different scenarios.

Table 4.5: Baseline values for installed capacities of renewable generators in 2030, 2040, and 2050, in MW. Solar PV represents an aggregate of solar generation from solar PV, HSAT Solar and Solar Rooftop. The table shows the baseline values for each carrier within all of the Nordic countries Norway, Sweden, Denmark, and Finland, which are based on projections gathered from [3].

Country	Carrier	Baseline Values 2030 [MW]	Baseline Values 2040 [MW]	Baseline Values 2050 [MW]
Norway	Solar PV	5800	13 200	21 800
	Onshore Wind	4800	6400	7800
	Offshore Wind	1600	4000	6000
Sweden	Solar PV	4800	11 000	17 200
	Onshore Wind	20 600	25 200	28 000
	Offshore Wind	0	1600	1800
Denmark	Solar PV	21 000	37 300	44 700
	Onshore Wind	6400	6400	6400
	Offshore Wind	4200	24 400	44 500
Finland	Solar PV	9600	20 600	28 000
	Onshore Wind	18 600	46 100	50 100
	Offshore Wind	0	0	0

Furthermore, the scenario-specific adjustments to the installed capacity limits presented in this section apply uniformly to the 2030, 2040, and 2050 horizons, and are also applied to the intermediate horizons of 2035 and 2045. While the percentage-wise adjustments are consistent across these investment periods, only the capacity ranges for 2050 are illustrated in the figures. This is done because the primary scope of this study is to analyze the Nordic power system in the target year 2050. The range adjustments for the preceding years are implemented to ensure a gradual development path towards 2050 for each scenario, providing the necessary boundary conditions for the myopic optimization.

While other generation sources are included both in the PyPSA-Eur model and the projections from the Nordic TSOs, the scope for the scenarios is to discover varying expansion levels of solar PV, onshore wind, and offshore wind, as well as their impact on the Nordic power system. Therefore, the installed capacities of all other generation sources remain fixed, as detailed in Section 4.3.1. Based on the baseline values and varying capacity limits for these technologies, the study defines four specific scenarios, with their abbreviations in parentheses:

- Scenario: **Baseline Values ± 10%** (BV)
- Scenario: **Solar Expansion** (SE)
- Scenario: **Wind Expansion** (WE)
- Scenario: **Flexible Expansion** (FE)

4.6.1 Baseline Values ± 10%

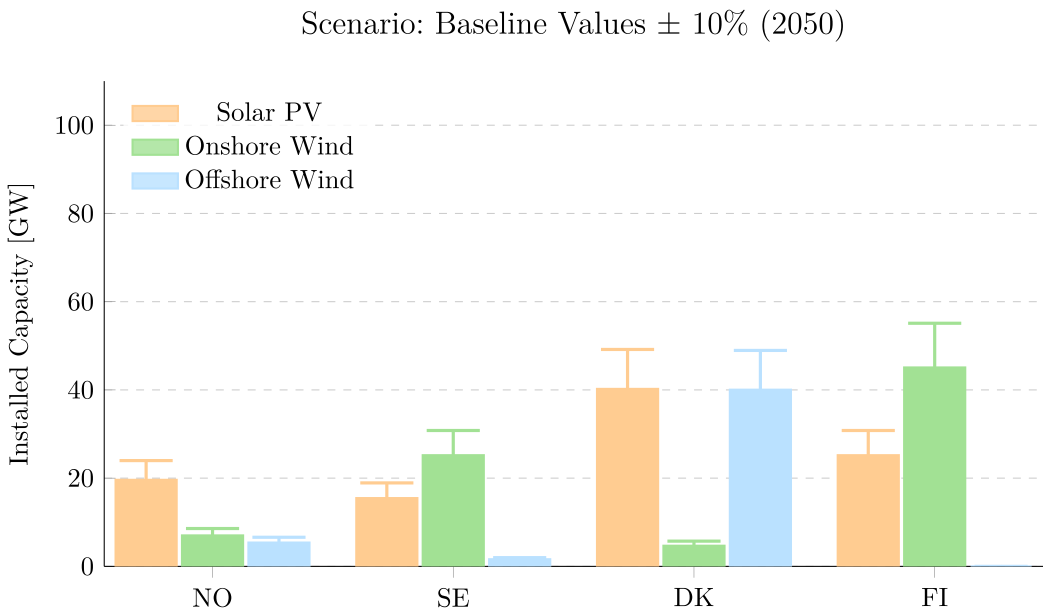

Figure 4.4: Installed capacity ranges for each generation carrier and country in 2050 under the Baseline ± 10% scenario, displayed in GW. The solid bars indicate the minimum installed capacities, while the error bars display the range in which the capacities must remain. No bar is shown for offshore wind in Finland, as the baseline value is 0 GW.

The Baseline Values ± 10% scenario seeks to explore a Nordic power system where the projections from the Nordic TSOs are realized. However, imposing hard constraints to match the predictions exactly would not allow for any flexibility in the optimization. Therefore, some flexibility margins are applied, and the installed capacities must be within ± 10% of the baseline values. This provides sufficient leeway for the solver to optimize without straying too far from realistic policy expectations. Figure 4.4 illustrates the range of these margins for 2050, with installed capacities shown per country and carrier. The bars represent the minimum installed capacity in GW, while the error bars display the allowed range between the minimum and maximum values, in which the solver can search for the optimized system design.

4.6.2 Solar Expansion

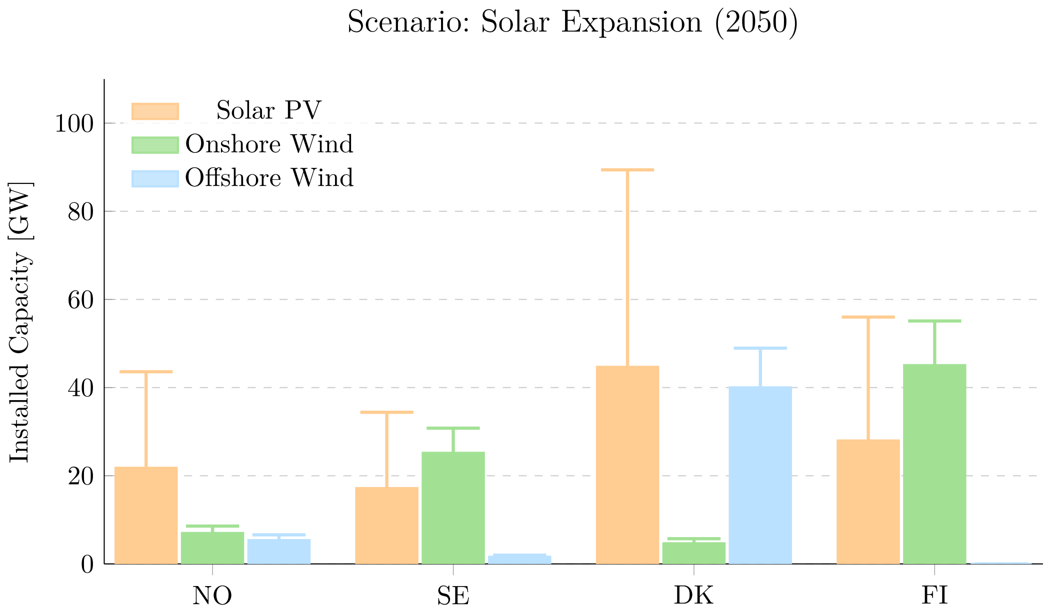

Figure 4.5: Installed capacity ranges for each generation carrier and country in 2050 under the Solar Expansion scenario, displayed in GW. The solid bars indicate the minimum installed capacities, while the error bars display the range in which the capacities must remain. No bar is shown for offshore wind in Finland, as the baseline value is 0 GW.

In this scenario, the limits for Solar PV expansion are extended. While the limits for both onshore wind and offshore wind expansion are kept identical to the Baseline Values ± 10% scenario, the upper limits for solar PV are increased to be 200% of the baseline values, for all countries. The lower limits for solar PV are set to be the baseline values from Table 4.5. Figure 4.5 illustrates the ranges of these limits for the target year 2050. This scenario allows the optimizer to model a large expansion of solar capacity if it finds that as the optimal solution. Allowing for this simulation enables exploration of how such a high integration of solar PV would affect the power system, highlighting both potential benefits and challenges.

4.6.3 Wind Expansion

The Wind Expansion scenario follows the same logic of capacity range adjustment as Solar Expansion, only focused on the installed capacities of wind power. The solar PV limits are identical to the Baseline Values ± 10% ranges. For both onshore wind and offshore wind in all countries, the maximum limits are set to 200% of the baseline values, and the minimum limits are set to be the baseline values. The resulting capacity ranges for 2050 are displayed in Figure 4.6. This scenario allows the optimizer to simulate a 2050 Nordic power system with a large expansion of installed wind capacity, if it finds that as the optimal solution. Similar to the Solar Expansion, this simulation enables exploration of how such a high integration of wind power would affect the power system, potentially highlighting both benefits and challenges.

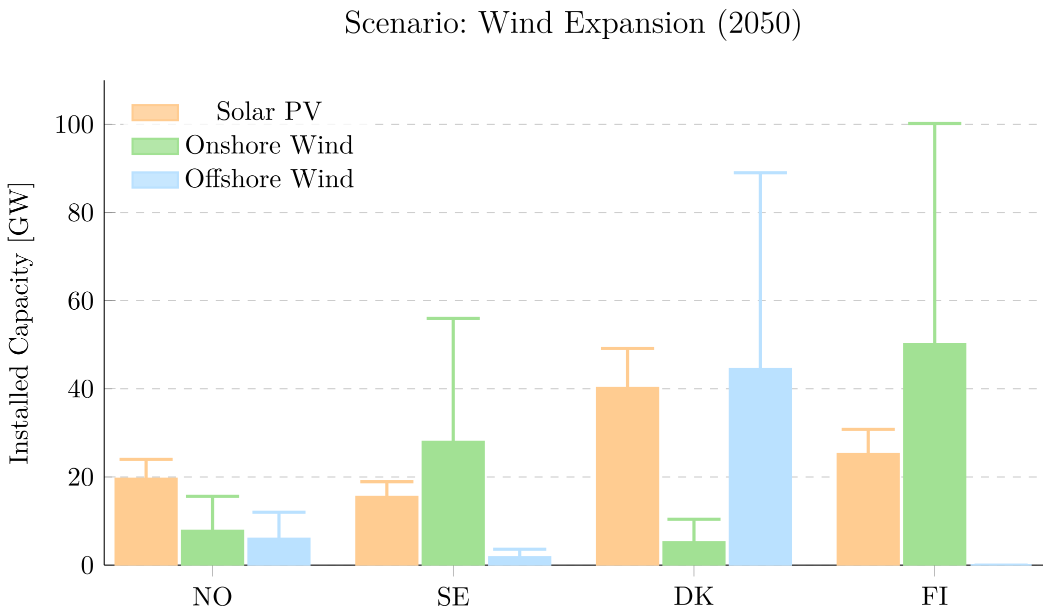

Figure 4.6: Installed capacity ranges for each generation carrier and country in 2050 under the Wind Expansion scenario, displayed in GW. The solid bars indicate the minimum installed capacities, while the error bars display the range in which the capacities must remain. No bar is shown for offshore wind in Finland, as the baseline value is 0 GW.

4.6.4 Flexible Expansion

The Flexible Expansion scenario seeks to explore an optimized system found by the model. To achieve this, all minimum limits are removed for solar PV, onshore wind and offshore wind within the Nordics. To prevent unrealistic expansion of single carriers, the maximum limits are set to 200% of the baseline values. Additionally, the fixed capacity limits for all other countries are kept to ensure that the scenario strictly explores a flexible solution for the Nordic power system. By giving the model freedom to determine the expansion of the extendable carriers within this framework, this scenario identifies the most cost-effective and efficient expansion of vRES capacity in the Nordics, without being restricted by TSO projections.

4.7 Use of Generative Artificial Intelligence

Various AI tools have been utilized to support different stages of the research and writing process for this thesis. Language improvement and help with the explanation of theoretical concepts were facilitated through the use of ChatGPT and Google Gemini. In addition to these tasks, Google Gemini was used for content and structure revision, as well as for brainstorming ideas. To streamline the literature review and theoretical background, NotebookLM assisted with identifying relevant references, summarizing academic papers, and improving the understanding of their content. Finally, technical tasks involving the development and implementation of the PyPSA model were supported by GitHub Copilot. This tool assisted in understanding error messages, improving the quality of the code, and achieving the final analysis results presented in this study.

5 Results

This chapter presents the results of the four different scenarios introduced in Section 4.6. These results provide insight into how different pathways for vRES expansion affect the performance and economy of the Nordic power system. Section 5.1 gives an overview of the installed capacities of extendable generators alongside the expansion of transmission infrastructure across all scenarios. The annual energy balances of the Nordic countries are presented in Section 5.2, before the system costs for the different scenarios are given in Section 5.3. Section 5.4 illustrates the optimized installed capacities in maps for each scenario. Finally, the chapter finishes with charts of the power balances of the Nordic power system in Section 5.5.

5.1 Installed Capacities and Transmission Expansion

The optimized installed capacities for vRES in the Nordic countries are presented in Table 5.2. This table compares existing capacities with the optimal 2050 configurations determined by the model across all four scenarios. For the aggregated Nordic system, the installed capacities of vRES vary from 251.5 GW in the Baseline Values $\pm$ 10% scenario, to 423.7 GW in the Flexible Expansion scenario. Capacities for non-Nordic countries are provided in Table A.1 in Appendix A. Since hydropower and nuclear generation were defined as non-extendable, their installed capacities remain fixed at the levels specified in Table 4.4.

Additionally, Table 5.1 presents the simulated capacity expansion of both AC lines and HVDC links, for each scenario. The expansions are given in percentages, with respect to the existing transmission capacities in the Nordic power system, and include both internal transmission infrastructure and interconnectors to the European synchronous power system. The current capacities of AC lines and HVDC links within the model are 421.8 GVA and 24.4 GW, respectively.

Table 5.1: Capacity expansion of AC lines and HVDC links, for all scenarios. Expansions are given in percentages with respect to the existing transmission capacities in the model. This includes both the internal transmission infrastructure in the Nordic power system, as well as interconnectors to Europe.

Transmission Type	Baseline Values $\pm$ 10%	Solar Expansion	Wind Expansion	Flexible Expansion
AC Line Expansion	49.0% (206 GVA)	42.1% (177 GVA)	72.8% (307 GVA)	72.2% (305 GVA)
HVDC Link Expansion	319.3% (78 GW)	257.8% (63 GW)	662.0% (162 GW)	597.1% (146 GW)

Table 5.2: Installed capacities of extendable, renewable generation carriers in 2050. The capacities are shown for all four scenarios, in addition to the existing capacities within the model. Offshore wind AC and DC have been aggregated to *Offshore Wind*, and solar PV has been renamed *Solar Fixed* for clarity. The scenarios are abbreviated as Existing Capacities (EC), Baseline Values ± 10% (BV), Solar Expansion (SE), Wind Expansion (WE), and Flexible Expansion (FE). All values are given in GW.

Country/ Scenario		**Solar Fixed**	**Solar Rooftop**	**Solar HSAT**	**Onshore Wind**	**Offshore Wind**	**Total**
Norway	EC	0.6	0.0	0.0	4.5	0.0	**5.1**
	BV	0.6	7.3	11.8	8.6	6.6	**34.9**
	SE	0.6	4.6	22.6	8.6	5.8	**42.2**
	WE	0.6	7.7	11.3	15.6	8.0	**43.2**
	FE	0.6	5.6	22.8	15.6	8.4	**53.0**
Sweden	EC	4.8	0.0	0.0	16.7	0.1	**21.6**
	BV	4.8	9.1	5.0	30.8	1.8	**51.5**
	SE	4.8	17.4	6.7	30.8	1.8	**61.5**
	WE	4.8	11.1	3.0	56.0	3.2	**78.1**
	FE	4.8	17.7	11.6	56.0	3.2	**93.3**
Denmark	EC	3.9	0.0	0.0	2.5	2.8	**9.2**
	BV	3.9	8.2	30.1	7.0	42.0	**91.2**
	SE	3.9	8.2	62.4	7.0	40.1	**121.6**
	WE	3.9	8.2	31.4	12.8	47.9	**104.2**
	FE	3.9	8.2	64.0	12.8	56.1	**145.0**
Finland	EC	1.1	0.0	0.0	8.2	0.0	**9.3**
	BV	1.1	8.3	16.1	48.4	0.0	**73.9**
	SE	1.1	6.6	33.8	48.3	0.0	**89.8**
	WE	1.1	8.1	16.0	89.8	0.0	**115.0**
	FE	1.1	7.2	34.1	89.8	0.0	**132.2**
Nordic Total	EC	**10.4**	**0.0**	**0.0**	**31.9**	**2.9**	**45.2**
	BV	**10.4**	**32.9**	**63.0**	**94.8**	**50.4**	**251.5**
	SE	**10.4**	**36.8**	**125.5**	**94.7**	**47.7**	**315.1**
	WE	**10.4**	**35.1**	**61.7**	**171.2**	**59.1**	**340.5**
	FE	**10.4**	**38.7**	**132.5**	**174.4**	**67.7**	**423.7**

5.2 Energy Balances

The annual energy balances for the Nordic power system in 2050 are illustrated in Figure 5.1. This figure provides an aggregated overview of the total electrical supply and demand for each country across the four expansion scenarios, while Figure A.1 in Appendix A shows the same balances for all planning horizons. Electrical supply is shown as positive values, and demand as negative values.

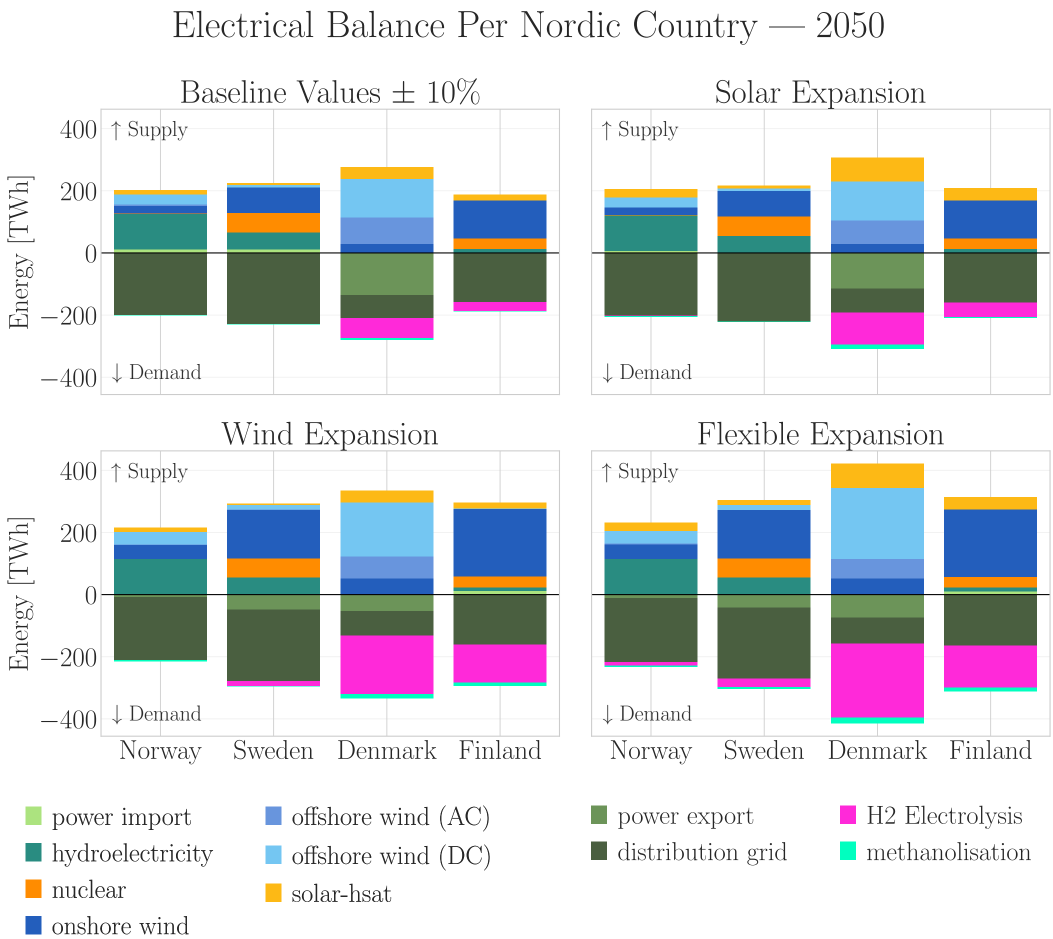

Figure 5.1: Total electrical balance of each country in the Nordics for all of 2050, in TWh. Electrical supply is shown as positive values, and demand as negative values. Solar PV is not included, because the annual generation is too low to be visible in the plotted bars. Solar rooftop is not included, as it is modeled to provide power directly to local demand, and does not supply power to the AC grid. Across scenarios, Denmark is seen as a substantial power producer, feeding most of the generated energy to power export and H_2 electrolysis.

The balance accounts for the installed generation carriers that supply power to the AC grid, and the sources of electrical demand. Additionally, the figure captures the net energy exchange via transmission lines, shown as either net import or export of electricity. Of the modeled generation carriers, solar rooftop is not included, as it is modeled to provide power directly to local demand and does not supply power to the high-voltage AC grid. Furthermore, hydroelectricity is an aggregate of RoR and power generation from the storage units, hydro and PHS.

The pure electrical demand is consistent in the range of 659 TWh to 671 TWh across scenarios, with the exception of the Flexible Expansion, which has 682 TWh. However, the total system load varies significantly more because of the hydrogen demand. The lowest amount of H_2 demand is seen in the Baseline Values ± 10% scenario, with a value of 92 TWh, giving a total load for the Nordic power system of 756 TWh. The Solar Expansion scenario is simulated with an H_2 demand of 151 TWh, yielding a total load of 810 TWh. The Wind Expansion and Flexible Expansion scenarios show higher hydrogen demands of 330 TWh and 412 TWh, pushing the total load to 1001 TWh and 1094 TWh, respectively. For comparison, the Nordic TSO projection is a total 2050 demand of 960 TWh, including a hydrogen demand of roughly 300 TWh [3].

The supplied electricity from Figure 5.1 is detailed in Table 5.3. This table shows the generated energy in 2050 of all the included generation carriers, for all the scenarios. Total generation of each scenario is also included, and shows that Baseline Values ± 10% has the lowest generation of 878.9 TWh, while Flexible Expansion has the highest generation of 1269.6 TWh. Across scenarios, hydroelectricity and onshore wind are the top suppliers.

Table 5.3: Generated electrical energy in the Nordics, per generation source, within each scenario. Hydroelectricity shows the aggregate production from RoR and the storage units, hydro and PHS. All data is given for 2050, in TWh.

Generation Carrier	**Baseline Values ± 10%**	**Solar Expansion**	**Wind Expansion**	**Flexible Expansion**
Hydroelectricity	182.5	182.5	182.5	182.4
Nuclear	97.0	97.0	96.4	96.2
Onshore Wind	259.5	259.8	474.1	472.2
Offshore Wind (AC)	87.7	76.1	71.2	68.1
Offshore Wind (DC)	165.8	164.7	228.6	281.2
Solar PV	10.1	10.1	10.1	10.1
Solar-HSAT	76.3	150.9	74.3	159.4
Total	**878.9**	**941.1**	**1137.2**	**1269.6**

5.3 System Cost

The annualized system costs for all scenarios are summarized in Table 5.4. These values account for both investment and operational costs for generators, storage units, and transmission infrastructure. The table distinguishes between the costs of the Nordic power system and the entire modeled system, both given in BEUR/year.

Since the objective function (3.5) is formulated to minimize the total cost of the entire modeled system, the reported costs for the Nordic system are a result of this global optimization, rather than an isolated cost-minimization specifically for the Nordic region.

Table 5.4: Simulated cost of the Nordic power system and the entire modeled system, across all scenarios. The Nordic system cost includes both investment and operational costs for all components connected to Nordic buses, while the total system cost represents the global minimum calculated by optimizing the objective function (3.5). All costs are annualized, and given in BEUR/year.

System Cost	Baseline Values ± 10%	Solar Expansion	Wind Expansion	Flexible Expansion
Nordic Power System [BEUR/year]	14.0	13.6	12.6	15.6
Entire Modeled System [BEUR/year]	83.5	81.7	82.5	80.0

5.4 Maps of the Optimized Nordic Power System

Figures 5.2 and 5.3 illustrate the simulated Nordic power system under all four scenarios Baseline Values ± 10%, Solar Expansion, Wind Expansion, and Flexible Expansion. The maps display installed generation capacities for all nodes alongside transmission capacities between nodes. The transmission branches are color-coded to make a clear distinction between AC lines and HVDC links, and the figure shows both the total transmission capacities and the simulated upgrade of each branch. Thus, the figures showcase how the transmission infrastructure in the Nordic power system must adapt to each specific expansion scenario. The corresponding figures of the whole modeled system can be found in Appendix A.

Across scenarios, significant expansion of both transmission and generation capacities are seen compared to the 2025 system displayed in Figure 4.2. Solar installation is seen in the southern part of the Nordic region, while both offshore and onshore wind expansion is seen mainly along the coastal lines. Substantial line expansion is shown across the system, especially in Sweden, and the majority of HVDC links are expanded.

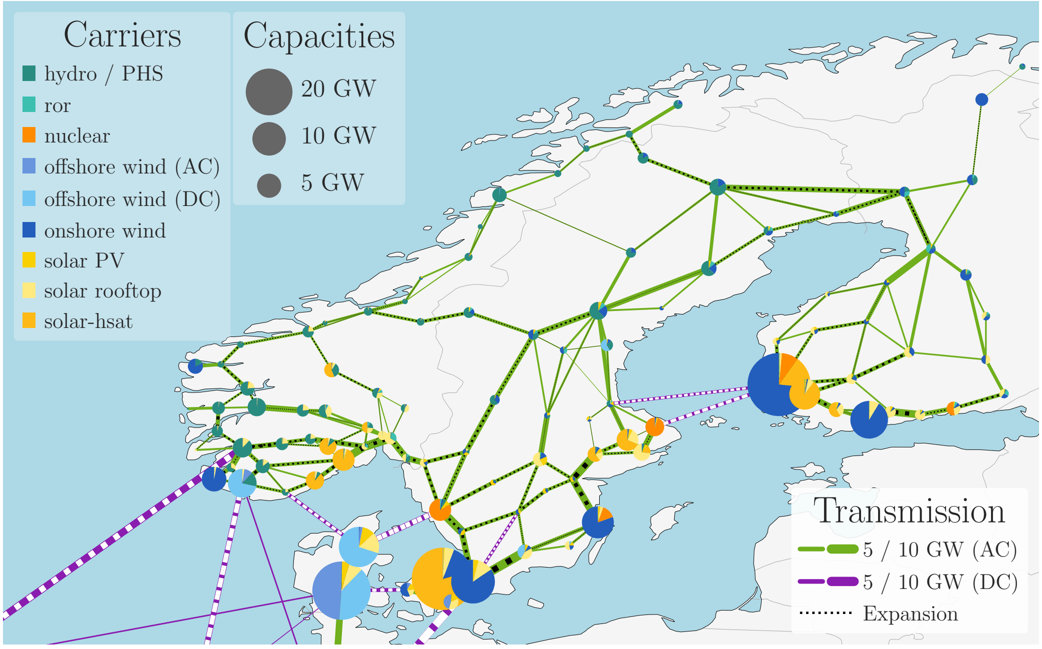

(a) Baseline Values ± 10%

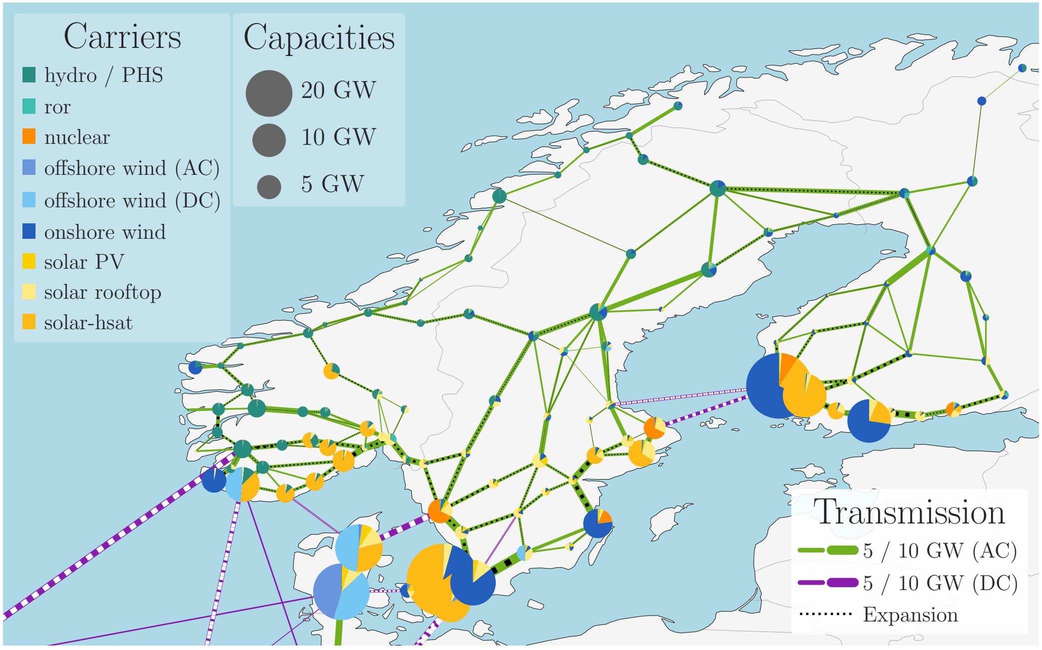

(b) Solar Expansion

Figure 5.2: Installed capacities of generation and transmission in the Nordic power system, under the scenarios Baseline Values ± 10% (a) and Solar Expansion (b). The size of each bus represents the total installed capacity, and is illustrated as a pie chart consisting of the capacities of each generation source. Similarly, the width of both lines and links corresponds to their transmission capacities. The dotted lines for both AC and DC represent the expansion of these branches. HVDC links are shown in purple with expansion in white, and AC lines are shown in green with expansion in black.

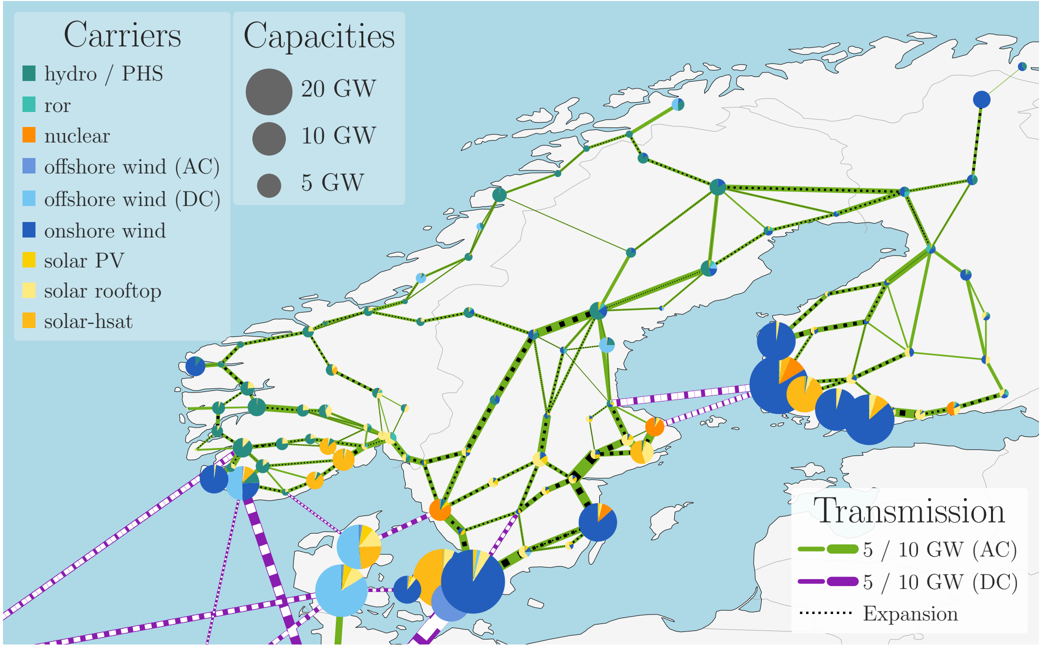

(a) Wind Expansion

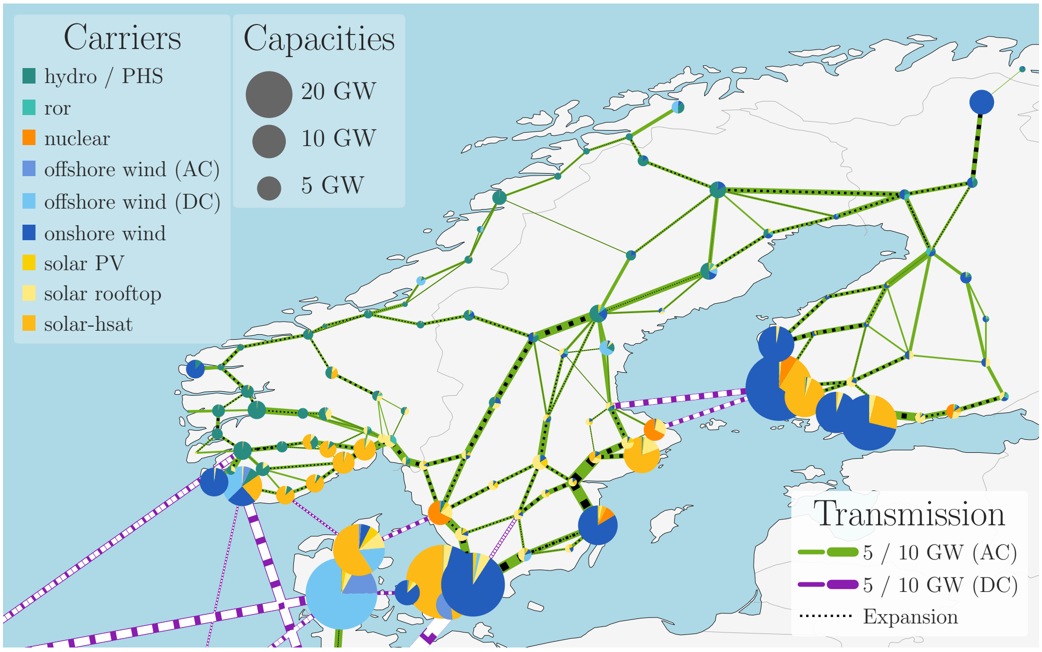

(b) Flexible Expansion

Figure 5.3: Installed capacities of generation and transmission in the Nordic power system, under the scenarios Wind Expansion (a) and Flexible Expansion (b). The size of each bus represents the total installed capacity, and is illustrated as a pie chart consisting of the capacities of each generation source. Similarly, the width of both lines and links corresponds to their transmission capacities. The dotted lines for both AC and DC represent the expansion of these branches. HVDC links are shown in purple with expansion in white, and AC lines are shown in green with expansion in black.

5.5 Power Balances

Beyond the annual energy balances, this section provides charts displaying temporal power balances between Nordic generation and load at every simulated timestep, while equivalent charts for the entire system is found in Appendix A.

Figures 5.4, 5.5, 5.6, and 5.7 present the temporal Nordic power balance for the scenarios Baseline Values ± 10%, Solar Expansion, Wind Expansion, and Flexible Expansion, respectively, throughout the year 2050. In these three-panel figures, the top panel shows the aggregated generation from all generators and storage units plotted against the electrical load, including demand from H_2 electrolysis. The middle panel displays the net power of all Nordic stores, where positive values indicate net discharge and power supplied to the system, while negative values indicate net charging. The bottom panel combines the load and the stores, resulting in a direct comparison of all power flowing in and out of buses in the Nordic system.

5.5.1 Baseline Values ± 10%

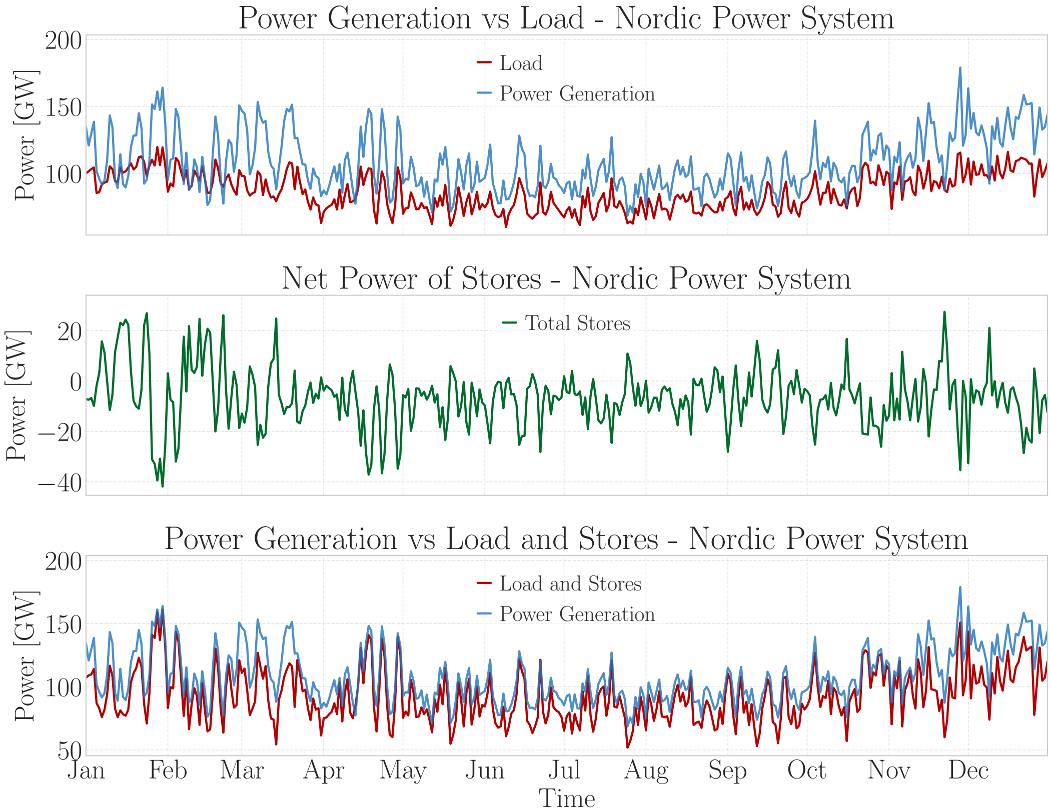

Figure 5.4: Generation, load, and net power of stores for the Nordic simulated system in 2050, under the Baseline Values ± 10% scenario. Given in GW. The top panel illustrates the generation in blue and the load in red, the middle panel shows the net power output of the stores, and the bottom panel displays the generation alongside the combination of system load and net power of stores.

[Figure 5.4](#) illustrates that the generation is higher than the combination of load and net power of stores for the majority of the year. This behavior indicates a general power surplus in the Nordic region, and thus a net export of power from the aggregated region. The generation peaks at 178.9 GW, which is 57.6% of the total installed capacity. The stores are actively discharging and charging throughout the year, improving the balance and providing stability to the system. Collectively, they have a maximum discharge of 27.5 GW and a maximum charge of 41.9 GW. Combining the load and net power of stores, the maximum loading on the system is 161.3 GW. Since the difference in generation and the combined power of load and stores represent power trade with external countries, the system in this scenario is seen to be stable, with a majority of days with noticeable power export.

5.5.2 Solar Expansion

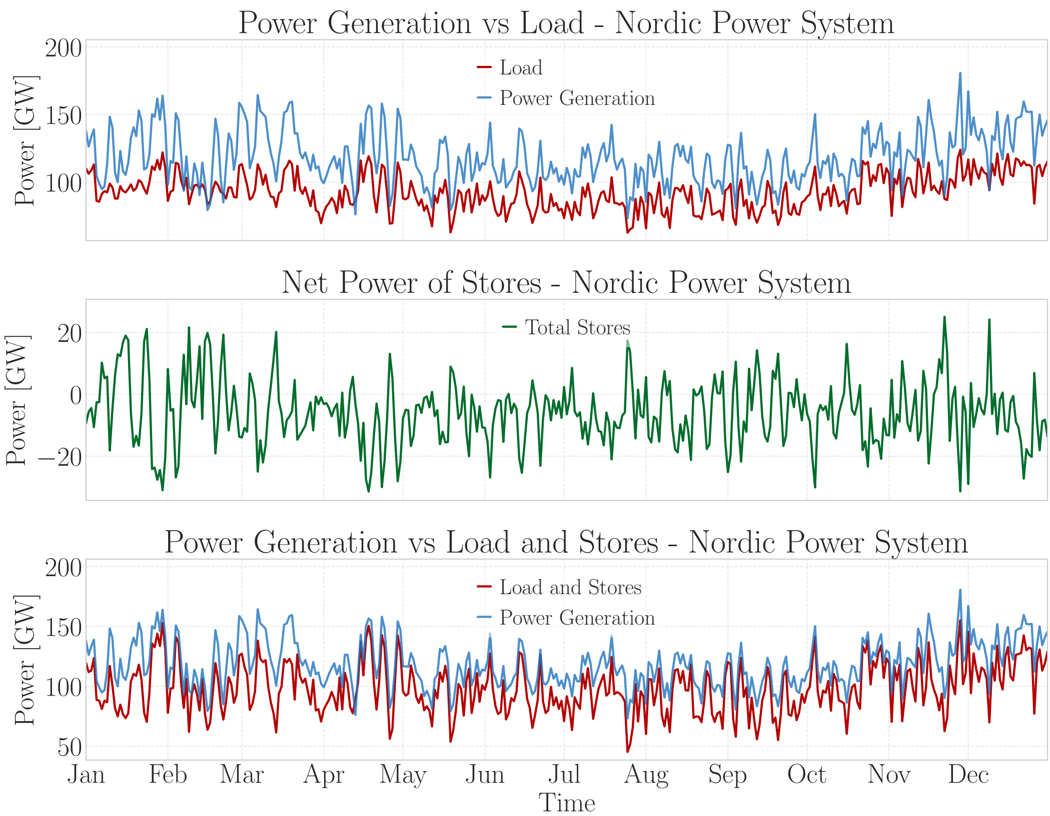

Figure 5.5: Generation, load, and net power of stores for the Nordic simulated system in 2050, under the Solar Expansion scenario. Given in GW. The top panel illustrates the generation in blue and the load in red, the middle panel shows the net power output of the stores, and the bottom panel displays the generation alongside the combination of system load and net power of stores.

Similar to Figure 5.4, Figure 5.5 displays generation levels higher than the combination of load and net power of stores for the majority of the year in the Solar

Expansion scenario, indicating net power export during most days. The generation peaks at 180.8 GW, which is 48.3% of the total installed capacity. The stores are seen to play a smaller role, as they show lower extreme values, with a maximum discharge of 25.1 GW and a maximum charge of 31.4 GW. Combining the load and net power of stores, the maximum loading on the system is 155.1 GW.

5.5.3 Wind Expansion

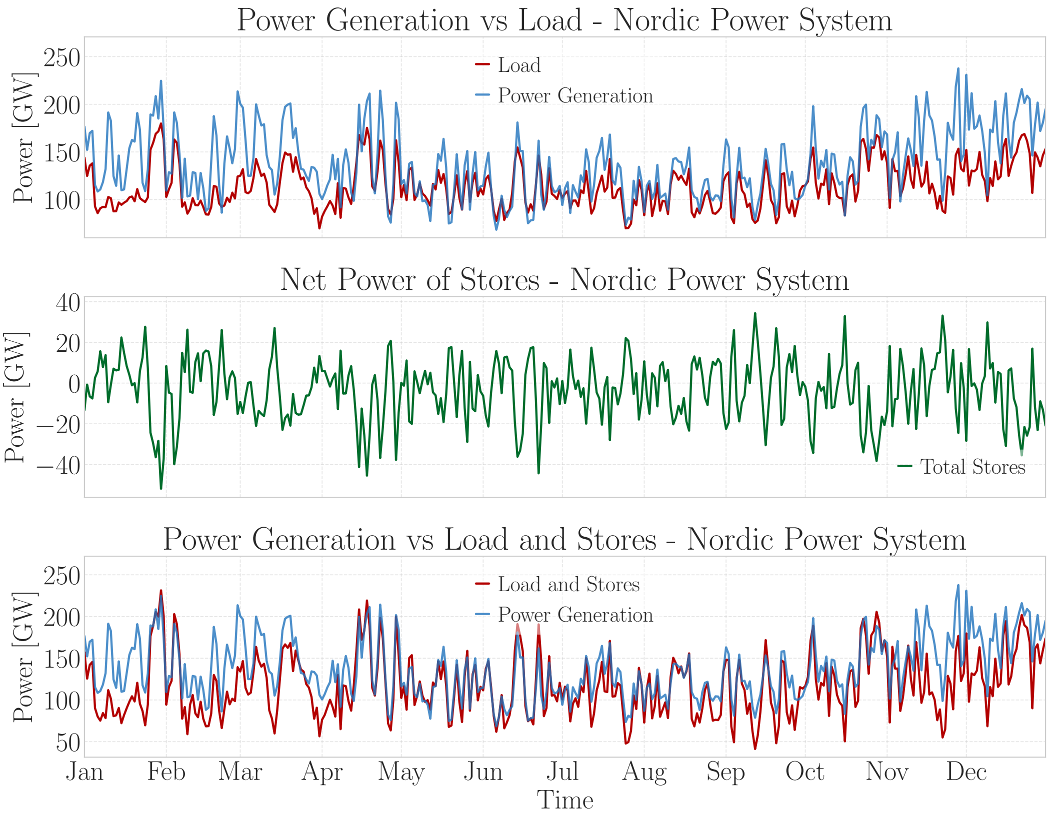

Figure 5.6: Generation, load, and net power of stores for the Nordic simulated system in 2050, under the Wind Expansion scenario. Given in GW. The top panel illustrates the generation in blue and the load in red, the middle panel shows the net power output of the stores, and the bottom panel displays the generation alongside the combination of system load and net power of stores.

For the Wind Expansion scenario, Figure 5.6 illustrates an internally balanced power system, with less deviations between the generation and combination of load and stores. The generation closely follows the combined series of load and stores, with some exceptions. Alongside this balance, which indicates lower power export compared to other scenarios, more volatile generation and load profiles are seen. Since H_2 electrolysis is included in the demand, this scenario displays a load profile that tracks wind availability, with some of the excess power directed to electrolysis instead of power export, as seen in Figure 5.1. The generation peaks at 237.7 GW, which is 59.5% of the total installed capacity. The stores are also actively utilized in this scenario, as they display high extreme values, with a maximum discharge of 34.4 GW and a maximum charge of 51.9 GW. Combining the load and net power of stores, the maximum loading on the system is 231.4 GW, the highest of all scenarios.

5.5.4 Flexible Expansion

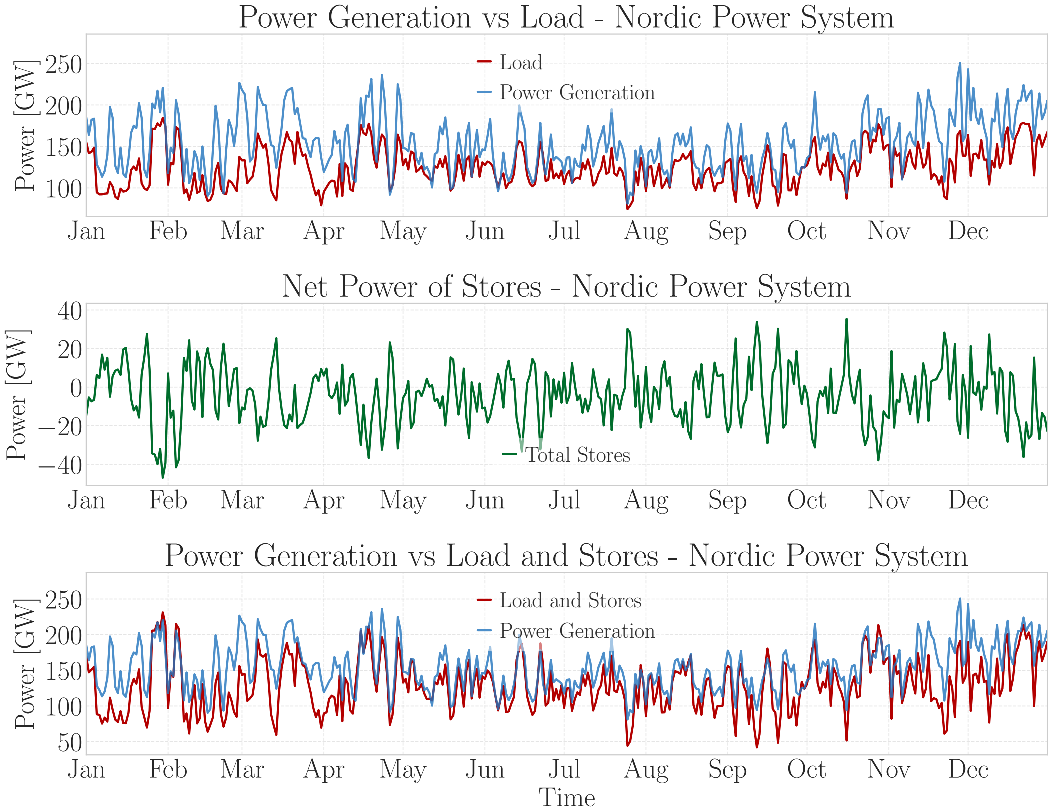

Figure 5.7: Generation, load, and net power of stores for the Nordic simulated system in 2050, under the Flexible Expansion scenario. The load includes both pure electrical demand and H_2 electrolysis. With all data given in GW, the top panel illustrates the generation in blue and the load in red, the middle panel shows the net power output of the stores, and the bottom panel displays the generation alongside the combination of system load and net power of stores.

The Flexible Expansion scenario displays a unique power balance profile. As illustrated in Figure 5.6, the demand profiles are notably volatile. Similar to the Wind Expansion scenario, this visual pattern indicates that the electrical demand from H_2 electrolysis closely tracks the availability of wind generation. Additionally, the generation is also observed to be higher than the combined power of load and stores for the majority of the year. This sustained surplus points to a steady net export of power from the Nordic system, occurring alongside the electrolysis demand. This scenario has a generation peak of 250.7 GW, which is 51.9% of the total installed capacity. The stores are also here actively utilized, with a maximum discharge of 35.4 GW and a maximum charge of 47.0 GW. Combining the load and net power of stores, the maximum loading on the system is 231.2 GW.

6 Discussion

This chapter evaluates the results presented in Chapter 5. It begins by comparing key parameters across the simulated scenarios in Section 6.1, followed by an analysis of the role of hydrogen in the simulated systems in Section 6.2. Section 6.3 then examines the alignment of this study with Nordic TSO projections and existing literature. Finally, Section 6.4 outlines the relevant limitations of the specific model employed in this study, providing context for the future research areas proposed in Section 6.5.

6.1 Comparison of Scenarios

While all simulated scenarios successfully model a net-zero power system, they present varying pathways to achieving that target. In general, the optimizer tends to favor large expansions of vRES in the Nordic countries when allowed to do so. This tendency is seen both from the installed capacities and total generated electricity across the scenarios. In the Nordics, the most restricted scenario, Baseline Values ± 10%, displays a vRES expansion of 205.9 GW and a total generation of 878.9 TWh. While both the Solar Expansion and Wind Expansion yield greater installed capacities and annual generation, the Flexible Expansion is the most aggressive scenario with a vRES expansion of 363.5 GW and an annual generation reaching 1185 TWh.

6.1.1 Installed Capacities

Reviewing Table 5.2 reveals several notable trends. Firstly, the onshore wind capacity hits the respective maximum limit in all scenarios and countries, except Finland, indicating that the model generally wants to maximize onshore wind capacity. Although wind power expansion has the highest investment costs and lowest lifetimes according to Table 4.3, this significant favoritism might be due to high-quality simulation of the wind resources of the Nordic region. It is likely that the model simulates superior energy potential for onshore wind in the Nordic region, backed by Figures 5.2 and 5.3, showing extensive wind expansion in costal areas across the region. Consequently, the framework establishes onshore wind not only as a supplementary technology, but as a major provider of energy to the future Nordic energy system. The critical implication of this result is that the cost-optimal 2050 transition is highly sensitive to this specific capacity constraint, and unconstrained simulations would likely simulate even higher, unrealistic expansions of onshore wind in the Nordics. However, real-world socio-political barriers, such as land-use conflicts or unmodeled local grid congestion, will prevent onshore wind from reaching these theoretical optimal solutions, and the system will inevitably be forced to rely on alternative energy sources or storage solutions.

It is also found that across all scenarios, fixed-tilt solar experiences no expansion. All expansion of solar PV comes in the form of solar rooftop or HSAT, clearly signaling that the model favors HSAT technology for utility-scale solar plants. With the investment cost being lower for HSAT than fixed-tilt, this is an expected outcome. Additionally, the high latitudes of the Nordic region means that the sun stays low on the horizon in winter and covers wide angles of the sky in the summer. While HSAT technology is able to track this behavior, fixed-tilt panels would miss more of the irradiant sunlight. However, this optimal configuration of solar expansion carries practical limitations. Relying entirely on HSAT demands a vastly greater land use, as tracking the spatial capacity density for HSAT is substantially lower than for fixed-tilt, as introduced in Section 4.3.1. HSAT technology also increases the mechanical complexity of the solar PV plants, as they are relying on moving tracking motors that require more maintenance than fixed-tilt PV panels.

Furthermore, the model shows no significant reduction of capacities in the Solar Expansion and Wind Expansion scenarios. Instead, additional solar and wind capacities are added respectively compared to the Baseline Values ± 10% scenario, resulting in an increased total installed capacity. Similarly, when the model is allowed to expand all carriers in the Flexible Expansion scenario, it chooses to expand all carriers above the baseline values without reaching their respective upper limits. This indicates that the model prefers a larger expansion of vRES in the Nordic power system than the TSOs have projected, facilitating greater power export to the European market. Consequently, it is found that the overall cost-optimal solution for the collective European system is to expand vRES capacity in the Nordics, and utilize the region as a green energy supplier for Continental Europe and the UK. This goes beyond the scope of optimizing the Nordic system in isolation, and suggests that cooperation and cost-sharing of power system development across country borders will facilitate a cheaper pathway to an overall carbon-neutral system for the whole European continent.

Additionally, the Wind Expansion and Flexible Expansion scenarios highlight that the optimizer strongly prioritizes the expansion of wind power when capacity constraints are relaxed. In these scenarios, both onshore and offshore wind capacities experience significant expansion compared to the Baseline Values ± 10%, especially in Denmark and Finland. These results indicate that the model identifies a large expansion of wind power in the Nordic power system as advantageous, allowing for high power generation during periods of abundant wind availability. Instead of curtailing this generation, the excess power is exported directly through the power transmission system or converted via H_2 electrolysis for subsequent export through hydrogen pipelines. As noted before, this finding highlights that the model suggests high utilization of available Nordic wind energy, not only supplying domestic demand for electricity and hydrogen, but serving as an export hub of clean energy to the broader European system.

The transmission expansion results presented in Table 5.1 demonstrate that all scenarios require substantial additional capacity for both AC lines and HVDC links.

The finding that AC line expansion is between 49.0% and 72.8% across scenarios clearly indicates that a widespread upgrade of the Nordic transmission system will be essential to achieve a carbon-neutral power grid, regardless of the specific expansion pathway chosen. Furthermore, the Wind Expansion and Flexible Expansion scenarios show a pronounced increase in the required capacity for HVDC links compared to the other scenarios, as also seen in Figures 5.2 and 5.3. This significant HVDC expansion from 24.4 GW up to 162 GW is driven by the need to export large amounts of energy to the European continent due to the extensive power generation installed in the Nordics. Especially during periods of high wind generation, this green electricity is exported to European countries, alongside the H_2 electrolysis that can capture remaining energy. This finding essentially highlights that the cost optimal European transition is dependent on a realization of vast HVDC expansion. If these interconnectors for some reason cannot be built, such as supply chain constraints of social opposition, this simulated export strategy becomes unattainable.

6.1.2 System Costs

An evaluation of the Nordic system costs against the entire modeled system costs presented in Table 5.4 highlights that the optimizer solves the objective function (3.5) for the entire interconnected network rather than the Nordic region in isolation. Because of this global optimization, a cheaper solution for the Nordic power system would likely exist if it were optimized independently. Instead, the model allocates large generation capacities in the Nordics, utilizing the renewable resources of this region to minimize overall costs and facilitate power export to Europe. For the Nordic system specifically, the Baseline Values ± 10% scenario shows a high annualized cost of 14.0 BEUR/year, and the Wind Expansion scenario results in the lowest Nordic cost of 12.6 BEUR/year. Furthermore, although the Flexible Expansion scenario represents the most cost-effective solution globally, it yields the highest Nordic cost of 15.6 BEUR/year. This cost distribution reveals a notable political consequence of this study. While utilizing the Nordic region as a green energy provider represents the cost-optimal pathway to a carbon neutral Europe, it requires the Nordic system to take on a disproportionate share of the expansion cost. Without an implementation of trans-national cost sharing agreements and market redesigns to compensate the Nordic regions for their expansion costs, this optimal solution remains politically unattractive.

6.1.3 Energy and Power Balances

Looking into the energy balances from Section 5.2 reveals clear variations in electricity production between the scenarios. Both the Baseline Values ± 10% and Solar Expansion scenarios demonstrate moderate generation totals of 878.9 TWh and 941.1 TWh, resulting in respective power exports of 122.9 TWh and 131.1 TWh. On the other hand, the Wind Expansion and Flexible Expansion scenarios present substantially larger energy generation, mainly driven by a significant increase in generation from both onshore and offshore wind. In the Flexible Expansion scenario, the generation reaches an overall maximum of 1269.6 TWh, which is a significant 44.5% increase from the Baseline Values ± 10% scenario. The net power exports of the Wind Expansion and Flexible Expansion scenarios are 136.2 TWh and 175.6 TWh, respectively, excluding the energy export through H_2 electrolysis and subsequent transport to Europe. Notably, the net export of electricity observed across all scenarios aligns well with expectations from the Norwegian TSO, which also projects a net electricity surplus for the Nordic region in 2050 [22]. Additionally, these results further emphasize that the model favors high wind generation in the Nordics when capacity constraints are relaxed, facilitating such large amounts of energy export to the European system.

The temporal power balances presented in Section 5.5 reveal significant variations in power peaks across the scenarios. The generation peak in the Baseline Values ± 10% scenario reaches 178.9 GW, while it increases to 250.7 GW under the Flexible Expansion scenario. However, the simultaneous generation share is notably higher in the former scenario. In the Baseline Values ± 10% scenario, the peak represents 57.6% of the total installed capacity, whereas it accounts for 51.9% in the Flexible Expansion scenario. The lowest simultaneous generation percentage is observed in the Solar Expansion scenario at 48.3%, while the Wind Expansion scenario reaches 59.5%. These findings indicate that different renewable mixes utilize their maximum installed capacities to varying degrees during peak production, and the grid infrastructure is utilized more efficiently with high wind integration. Furthermore, these results indicate that the strategy of excessively integrating vRES in the Nordics to supply continental Europe with green energy necessitates greater capacity expansion of the transmission system, as seen in Table 5.1. Yet again, this increase in required transmission expansion highlights the need for trans-national agreements and cost-sharing in order for these scenarios to be politically viable.

The charts in Figures 5.4 through 5.7 further illustrate that the power stores are actively utilized across all modeled scenarios. Regardless of the expansion pathway, stores are essential additions to the power system to ensure stability. However, contrasting the power profiles from the Baseline Values ± 10% and Solar Expansion scenarios with the Wind Expansion and Flexible Expansion scenarios highlights distinct operational challenges. A large share of wind generation is seen to create volatile power generation profiles, especially during the winter months. Because excess power is directed to H_2 electrolysis instead of being curtailed, the load also follows this fluctuating profile. This rapid fluctuation in generation requires substantial storage and export capabilities. Thus, the stores are seen to play a bigger part in the Nordic system in these latter two scenarios. In addition, a strong reliance is placed on large transmission capacities and hydrogen electrolysis, which collectively manage the surplus energy in the system and maintains a balanced grid.

6.2 The Role of Hydrogen

The substantial variation in hydrogen demand across the modeled scenarios represents a critical finding in this study. The particularly high demand observed in Denmark and Finland is considered to be a simulation-specific result of the model treating these regions as major green hydrogen export hubs, rather than a modeling error. Especially in the Wind Expansion and Flexible Expansion scenarios, hydrogen electrolysis acts as a crucial absorber of excess wind power. When onshore and offshore wind production exceeds the regional electrical load, and power export demand, the surplus energy is fed directly into hydrogen electrolyzers. After the electrolysis, the hydrogen is exported out of the Nordics through H_2 pipelines, supplying sector-coupled industries. By operating the system in this manner, the overall demand profile, including hydrogen, closely tracks wind availability. Ultimately, this operational flexibility allows the grid to remain balanced without having to curtail large amounts of wind generation. Furthermore, some sources, such as [84], highlight specific applications for offshore wind that are dedicated entirely to hydrogen production rather than a combination with electricity generation.

Building upon this established link between wind generation and hydrogen production, the simulated annual demand for hydrogen exhibits a broad range across the modeled pathways. The Baseline Values $\pm$ 10% scenario results in a H_2 demand of 92 TWh, while the Solar Expansion scenario reaches 151 TWh. Because the model computes hydrogen demand dynamically as a response to available surplus energy, these lower figures fall significantly short of the corresponding projection from the Nordic TSOs, which is approximately 300 TWh [3]. This shortfall indicates that the wind capacities installed under the Baseline Values $\pm$ 10% and Wind Expansion scenarios are likely insufficient to supply the anticipated hydrogen market, suggesting that a greater expansion of wind energy could be necessary to meet these projected targets.

In contrast, the simulated hydrogen demand increases substantially in the Wind Expansion scenario to 330 TWh, before reaching a maximum of 412 TWh in the Flexible Expansion scenario. With the hydrogen demand not having any upper constraints in the simulations, and seemingly being modeled as an unbounded sink of excess energy, these scenarios thus project H_2 demands which exceed the TSO projections. This discrepancy suggests that such extensive installed capacities of wind power in the Nordic region might be unrealistic. If actual hydrogen demand aligns closer to the TSO projections, the high wind capacities observed in these scenarios would likely lead to high curtailment rates and reduced profitability for the wind power plants. Consequently, it can be assumed that the high installed capacities of wind power in the Wind Expansion and Flexible Expansion scenarios are optimistic and should be interpreted with this consideration of hydrogen demand in mind.

6.3 Alignment with TSO Projections and Previous Work

This section discusses the alignment of the results from this study with the expected development from the Nordic TSOs. Furthermore, the results are compared to similar studies presented in Section 2.7.

6.3.1 Alignment with Outlook from Nordic TSOs

A comparison of the 2050 installed capacities from Table 5.2 with the projections from the Nordic TSOs in Table 4.5 reveals several deviations, which collectively highlight a structural difference between the pure mathematical optimization in this study and policy-driven planning. While the modeled framework maximizes capacity based on resource availability and system costs, the TSO projections inherently account for the practical limitations of social acceptance, municipal land use restrictions, and permitting delays. Most notably, the onshore wind capacities substantially exceed the TSO projections in this study. As discussed, all scenarios display installed capacities of onshore wind that reach their maximum allowable limits in all countries except Finland. Contrarily, the onshore wind capacity in Finland falls below the baseline value under the Baseline Values $\pm$ 10% and Solar Expansion scenarios, likely due to the substantially large baseline value of 50.1 GW. Although the onshore wind capacities surpass the baseline in the Wind Expansion and Flexible Expansion scenarios, they are not close to reaching their Finnish limits for maximum expansion.

Additional trends are found when looking more closely at the Baseline Values $\pm$ 10% scenario. The simulated installed solar capacities in Norway, Denmark, and Finland are all below the baseline capacities, while it is above in Sweden. Furthermore, the offshore wind capacity is only simulated to exceed the baseline value in Norway, while it matches the baseline value in Sweden and is below in Denmark. Across the entire Nordic region, this scenario yields installed capacities slightly below the baseline values for solar and offshore wind, with respective deviations of 5.4 GW and 1.9 GW. On the contrary, onshore wind reaches an installed capacity that is 2.5 GW above the baseline. When viewed collectively, these results show that the aggregate simulated system in the Baseline Values $\pm$ 10% scenario closely replicates the projection from [3], even with the 20% flexibility margin given to the model. However, this is also the scenario with the lowest installed capacity and annual electricity generation, with all other scenarios resulting in higher generation and higher energy export to the broader European system. This suggests that the projections from [3] reflect a strong expansion pathway for the isolated Nordic system, while this study indicates that a broader perspective and international collaboration on system development ultimately yields the overall cost-optimal solution.

This indication is further clarified by the Flexible Expansion scenario, which presents a distinctly different development path for the Nordic power system. The aggregated installed capacities of all energy carriers exceed the baseline projections. As noted, this extensive expansion incurs the highest Nordic annualized cost in the study at 15.6 BEUR/year. However, it simultaneously represents the most cost-effective solution for the entire modeled European system, with an annualized system cost of 80.0 BEUR/year, revealing an interesting trade-off. An extensive expansion of vRES across the Nordic countries might be costly for the region in isolation. Yet, this approach is modeled to become the cost-optimal solution for Europe as a whole, when excess power from the Nordics is efficiently exported to the European continental grid. Ultimately, this finding suggests that the decision-makers of the Nordic power system development should not focus on the technical and cost optimization of the Nordic system isolated, but instead collaborate with European entities to advance the overall optimal pathway. In the end, the net-zero goal is a shared European objective, and international cooperation and robust agreements is likely the most efficient way to accelerate the broader energy transition. As previously noted, such cooperation does however depend on cost-sharing alternatives that yield an efficient distribution of the financial burden this pathway would put on the Nordic system. Without this, it is unlikely that Nordic TSOs are willing to indirectly pay for the decarbonization of continental Europe.

6.3.2 Comparison with Previous Work

The findings of this study offer an interesting contrast to the literature reviewed in Section 2.7. Malum [6] identified a cost-effective Nordic system with a total installed capacity of 130.4 GW, and a total system cost of 33.9 BEUR. In contrast, the current model invests in significantly higher installed capacities between 251.5 GW and 423.7 GW, and yields annualized costs ranging from 12.6 BEUR/year to 15.6 BEUR/year. Since [6] reported total system costs, it is logical that the annualized Nordic system costs found by the current setup are lower. However, the annualized costs in this study are roughly 40% of the total costs reported by Malum, essentially meaning significantly higher total costs in the current study. This relationship becomes even clearer when considering the geographical scope of the two models. In [6], Denmark was excluded entirely, which naturally resulted in a smaller system with lower cumulative costs. In this study, the integration of the Danish power system alone accounts for roughly 100 GW to 140 GW of installed vRES capacity in 2050. Removing Denmark from this study, alongside all the interconnections to Continental Europe and the UK, would ultimately result in lower costs. Finally, the increase in overall capacity expansion is also driven by the application of updated projections from the Nordic TSOs, which yielded higher baseline values than those used by [6].

Beyond costs and capacity, the inclusion of the broader European system fundamentally shifts the optimal system in this study from that simulated by [6]. While Malum concluded that a carbon-neutral Nordic system could be achieved with a transmission expansion of under 5%, and solely relying on existing hydropower and storage systems for balancing, the current study contradicts this finding. By modeling the European interconnectors, the results demonstrate that the cost-optimal European transition benefits from the Nordic power system functioning as an energy export hub, which is a fundamental finding that differs from [6]. This wider European optimization requires a Nordic AC line expansion of up to 72.8%, and heavily depends on HVDC interconnectors and hydrogen electrolysis to export energy and to balance the volatile electricity generation. Ultimately, the comparison shows that modeling the Nordics in isolation does not fully capture the infrastructural and flexibility requirements necessary to support an interconnected European energy transition.

A different economic dynamic emerges when comparing the current results with the findings of Saleem [7]. While Saleem focused on the infrastructure required to integrate 30 GW of offshore wind in Norway by 2040, concluding that this specific technology pathway demands high system costs, the current study demonstrates that a cost-optimized technology mix prioritizing onshore wind and international export yields a more economical transition. Although their study utilized annualized costs, it reported a significantly higher cost of 27.1 BEUR/year. However, their methodology differs from the current study in several key aspects. Firstly, their model did not include hydropower as a power generation source, while still increasing the electrical demand for the Nordic region by 50%. This omission represents a major structural difference that likely inflates the required capacity expansion and associated costs. Additionally, [7] simulated the year 2040 instead of 2050. Assuming a consistent discount rate of 2%, projected technology investment costs are generally higher in 2040 than in 2050. Another reason for this discrepancy could be that cost assumptions within the PyPSA-Eur framework have been updated in newer versions, influencing the final economic outcomes. Furthermore, the cost difference is likely a result of expanding the study scope to include more European countries. This broader geographic boundary may allow the model to distribute fixed system costs and leverage cost-efficient resources across a wider area.

Besides system costs, the results of transmission expansion further highlight the differences in modeling approaches. This study finds an AC line expansion of 49.0% and 42.1% in the Baseline Values ± 10% and Solar Expansion scenarios, respectively. While these results align well with the 48.3% required transmission expansion reported by [7], they greatly exceed the conservative expansion of 3.66% to 4.97% simulated by [6]. However, the apparent alignment with [7] likely stems from fundamentally different system dynamics. Since Saleem's model forced a high expansion by excluding hydropower while increasing electricity demand, a domestic energy deficit that required internal rerouting was likely simulated. In contrast, the current study triggers a similar expansion rate because the Nordic grid is optimized as an export hub. To utilize the HVDC links for European export, the internal AC backbone must also be upgraded to route generation from northern and coastal regions to the southern export nodes. As previously noted, this establishes the clear structural consequence of cross-border power trade being dependent on domestic, Nordic infrastructure. If social opposition and permitting delays prevent these widespread upgrades to the internal AC grid, the capacity to supply the European market becomes unachievable.

The inclusion of European interconnectors seems to fundamentally change the optimization results compared to studies that modeled the Nordic region in isolation. While previous isolated models naturally excludes European interconnectors, this study reveals a substantial expansion of such HVDC interconnectors ranging from 257.8% to 662.0% across the simulated scenarios. This significant growth indicates a heavy dependence on power trade and integration with the European market, regardless of specific development pathways. Additionally, coupling the Nordic power system to Europe appears to lower the overall need for domestic flexibility assets, as power can be exported or imported as needed. This effect becomes evident when comparing the net power of stores in this study with the equivalent results in [6]. Although the installed capacities in this study are at least doubled from [6], the store profiles display similar behaviors. By relying on cross-border trade to manage short-term fluctuations in supply and demand, the Nordic power system avoids the need to build excessive local storage, resulting in a more cost-efficient development of the regional grid. This operational shift in utilization of HVDC interconnectors aligns well with Nordic TSO expectations [3], which states the same use-case for HVDC cables towards 2050. This alignment highlights a compelling argument for their role as structural support of both the Nordic and broader European power systems, as they compliment the systems with both export and balancing capabilities.

6.4 Model and Methodology Limitations

As introduced in previous sections, the model employed in this study has several limitations, which are further discussed in the following sections. Additionally, they also discuss some of the choices and trade-offs made during the simulation process that directly affect the results.

6.4.1 Underestimation of Hydropower

A notable limitation of the model, as presented in Section 4.5, is the underestimation of Nordic hydropower capacity and its SOC. Beyond the simple reduction in installed capacity and the available energy, the model relies on a single fixed historical weather year. This gives the model very little flexibility to adjust the reservoir level across simulated scenarios and planning horizons, ultimately yielding a nearly fixed SOC profile throughout any simulated year. This constant profile is unrealistic because actual water inflow to the reservoirs fluctuates significantly from year to year depending on precipitation levels. Consequently, the rigid profile prevents the model from flexibly dispatching the stored hydro energy when the specific power system in question needs it to balance variable generation from vRES. On the other hand, the used weather year is the same for both precipitation, wind availability, and solar irradiation, making it reasonable to assume that the simulated dispatch of hydropower is consistent with low vRES production.

Despite this inaccuracy, the underestimation also yields a valuable analytical perspective by simulating a conservative hydrological scenario regarding hydropower availability. By modeling a general low SOC of hydropower alongside reduced water inflow, the system is forced to become resilient while more dependency is put on the supply from vRES. This constraint leads the simulation to identify the levels of installed capacities the system requires to maintain system reliability during a dry year, an event that will be inevitable in the long run. However, the lack of simulated hydropower flexibility has direct consequences for the overall optimization results. Because the model cannot rely on fully charged hydro reservoirs to help balance the grid, it may over-invest in alternative balancing technologies or transmission capacities in HVDC interconnectors. Ultimately, there are both benefits and drawbacks to the different ways of simulating the SOC of hydropower in such a fixed way. Since an overestimation could have lead to underestimation of necessary components in the system, the default inclusion of hydropower in the PyPSA-Eur framework was kept.

6.4.2 Temporal Resolution

An additional methodological constraint within the simulation setup involves the trade-off between temporal and spatial resolution. Given limited computational resources, achieving high granularity in both aspects is not feasible. For this study, the available computational power for the simulation was limited, forcing a compromise in one of the two resolutions. To ensure the model could accurately represent the complex transmission infrastructure, its required expansion, and the geographic distribution of different energy carriers across the system, spatial resolution was prioritized while the temporal resolution was set to 24-hour intervals. While a finer temporal resolution, such as 1 hour, would inherently capture short-term weather fluctuations more precisely, the achieved results are deemed to provide a robust representation of long-term system dynamics. It is therefore not expected that an increased temporal resolution would yield significantly different results regarding the capacity expansion pathways and overall system costs.

6.4.3 Spatial Clustering

As introduced in Section 3.4.5, a notable limitation of the PyPSA-Eur framework is the exclusion of distribution grids and their local constraints. This exclusion generally prevents the model from capturing local transmission bottlenecks and voltage variations within individual nodes, making this limitation particularly relevant for this study. Figures 5.2 and 5.3 illustrate that significant rooftop solar capacity is installed in Denmark and the southern regions of the other Nordic countries, across all scenarios. However, this rooftop solar generation is not presented in Section 5.2 because it is modeled on low-voltage buses that are directly connected to the distribution grid. Thus, rooftop solar generation is not included in the AC buses of the model. Ultimately, this means that the model is incapable of capturing local grid challenges typically introduced by high rooftop solar penetration, such as voltage fluctuations, power quality issues, and grid overloading [99].

Furthermore, the clustering of transmission lines introduces an additional limitation to the results. Since all actual lines between two nodes are aggregated into a single representation, the model fails to identify specific lines that require expansion. However, this study is intended as a high-level pathway exploration, and such granular details are beyond its scope. The employed method effectively identifies the need for regional transmission capacity expansion, ultimately providing a clear indication of where grid reinforcements should be prioritized. In practice, TSOs possess the detailed network data required to plan and execute specific line expansions.

6.4.4 Weather Data

Relying entirely on weather data extracted from the single year of 2013 presents a notable limitation of the model employed in this study, as any individual year will contain certain climate deviations that can skew wind and solar generation profiles away from long-term averages. While it could be suspected that such an anomaly caused the optimizer to favor extensive wind power expansion, historical reports indicate that 2013 actually experienced below-average wind speeds in the Nordics [100,101]. This suggests that the model's preference for wind expansion is instead driven by other factors, such as large-scale cost efficiency.

To mitigate the impact of annual weather variations, a more robust approach would be to create a Typical Meteorological Year (TMY) by averaging 30 years of historical data. Alternatively, the entire simulation could be run across multiple weather years, and then averaged to obtain the final results. However, creating and implementing a TMY as the weather reference requires complex extraction and treatment of the weather data incorporated in the PyPSA-Eur framework. The second option would require the number of simulations in the study to be multiplied by 30, followed by significantly advanced data processing to extract the results correctly. Therefore, both options were considered beyond the scope of this study, although a TMY might have been utilized if it were a ready-to-use option within the PyPSA-Eur framework.

6.4.5 Non-Nordic Countries

In this study, modeling non-Nordic countries as singular nodes ensures a realistic simulation of the Nordic power system and its key HVDC interconnectors without exceeding available computational resources. However, this spatial aggregation forces the model to neglect internal regional differences within these countries, reducing the representational accuracy of their power systems. Expanding the model to have a finer spatial resolution for those regions would ultimately allow for a more realistic simulation, consequently improving the accuracy of the power trade profiles across the HVDC interconnectors.

Additionally, the setup used in this study excludes multiple countries that are interconnected to the Nordic system, as introduced in Section 2.2. While this simplification was made to reduce the complexity of the study and computational demand of the simulation, restructuring the model to include Poland and the Baltic countries would yield a more realistic representation of the Nordic power system. By incorporating these additional energy markets, the optimization would likely simulate an even higher expansion of HVDC interconnectors to manage the increased cross border power flow. Consequently, such an inclusion would further emphasize the role of such interconnectors in providing balancing power to the Nordic system, alongside additional power export to the European continent.

6.4.6 Exclusion of Nuclear Power Expansion

The current model configuration does not allow for the expansion of nuclear power. This exclusion of nuclear as an extendable technology is a specific modeling choice made to align with current, official projections [3], which state no expansion of this technology towards 2050. While the technology has gained increasing public support in Norway over recent years [27], official reports do not indicate that nuclear capacity will be expanded in the Nordic power system, as seen in Figures 2.2 and 2.4. Furthermore, the expansion of nuclear generation in Italy was explored by [43], but the study found it not cost-efficient under current capital and operational expenditure assumptions. Ultimately, this led the optimization to neglect it entirely. However, the power system dynamics in Italy differ from those in the Nordics, and the fundamental economics and system needs could vary in the Nordic context. By providing stable, weather independent generation, allowing nuclear expansion could potentially reduce the system's reliance on high volumes of vRES and their associated transmission upgrades. Therefore, exploring nuclear capacity expansion within the Nordic power system remains a relevant area and represents a strong candidate for future research.

6.4.7 Lack of Policies

As with most technical optimizations of similar scope, a major limitation of this study is that the PyPSA-Eur framework does not incorporate political considerations, beyond the overarching target of carbon-neutrality. While this limitation is partially addressed by basing the simulation scenarios on official capacity projections from the TSOs, complex real-world factors such as public support and political decision-making cannot be directly modeled within the framework. Therefore, this research constitutes a purely technical and economic analysis of the pathways toward a net-zero Nordic power system in 2050. Ultimately, whether these scenarios are realistic or achievable will depend heavily on future political decisions, rather than solely being based on technical possibilities and cost-optimal configurations.

6.5 Future Research

While this study addresses the identified research gap of a simulated Nordic power system that accounts for power trade through HVDC interconnectors, several areas remain for future work. A direct extension of this work would be to replicate the analysis using a finer temporal resolution. With sufficient computational resources, a simulation with a granularity of 1 hour would yield more accurate results. This approach would accurately capture the hourly variability of weather resources, enabling a more realistic representation of renewable generation profiles. Although the general trends of the results are expected to remain consistent, future research should explore how higher temporal accuracy impacts the model's decisions for capacity expansion in the Nordics.

In addition to increasing the temporal resolution, another valuable extension of this research would be to explore a simulation where the model is allowed to construct entirely new transmission infrastructure. By permitting the creation of new AC lines under realistic cost assumptions, the model would be free to identify the true cost-optimal solution for both power flow and the simulated system expansion. This approach would offer valuable insights into future transmission strategies and improve the accuracy of long-term grid planning. However, granting this freedom to the model would further highlight the challenge of modeling public acceptance. Since new transmission lines at higher voltage levels are frequently opposed by local residents or municipalities [102], a purely technical optimization might propose infrastructure developments that face significant practical and political barriers.

Building on the limitations of spatial aggregation and geographical scope in Section 6.4.5, future research could also investigate expansion of the model by using multiple nodes for the connected European countries. Since modeling the entire continent at high resolution is computationally restrictive, a logical next step is a regional split of 2–5 buses per connected country. This enhancement would allow for a more realistic simulation of their internal power systems, consequently improving the accuracy of the simulated power trade profiles across the HVDC interconnectors. By capturing internal European transmission bottlenecks, this more accurate profile would likely constrain cross border power trade, potentially altering the optimal generation mix and storage requirements in the Nordics. Furthermore, the geographical scope of the model should also be broadened to include Poland and the Baltic countries. Incorporating these missing regions would ensure that all relevant HVDC links are actively modeled, thus yielding a more comprehensive and realistic representation of the Nordic power system and its integration with the broader European market.

Finally, another interesting field for future research could involve a configuration of the model which allows nuclear power expansion in the Nordics. Although this technology was excluded from the current study, simulating nuclear capacity additions would provide valuable insights into how this added generation affects overall system behavior and costs. Specifically, future optimization studies should investigate whether introducing nuclear power could reduce the need for extensive expansion of vRES, energy storage, and associated transmission infrastructure. Given the ongoing political evaluations and shifting public support for nuclear energy, modeling its integration could be valuable for a thorough assessment of all viable pathways to a reliable, net-zero power system.

7 Conclusion

This study identifies cost-optimal pathways for the Nordic power system to achieve carbon neutrality by 2050. Specifically, it determines how the expansion of renewable energy and transmission infrastructure can be optimized to ensure a cost-efficient transition away from fossil fuels. The findings demonstrate that a net-zero system requires a large-scale expansion of vRES, coupled with significant capacity upgrades of both internal and cross-border transmission networks.

To achieve this, the study utilizes the PyPSA-Eur modeling framework to simulate four distinct capacity expansion scenarios for the target year 2050. A central departure from previous research is that this model does not evaluate the Nordic region in isolation. Instead, it accounts for interconnections to Continental Europe and the UK, and the consequential power trade. By incorporating these cross-border dynamics, the simulations reveal that there is a great potential of the Nordic power system to function as an interconnected green energy export hub for the broader European market.

To successfully meet future electricity demands, the optimized scenarios require a total installed vRES capacity in the Nordics between 251.5 GW and 423.7 GW by 2050, which must be supported by substantial infrastructure upgrades. The simulations indicate that the internal AC transmission grid requires capacity expansions of up to 72.8%, while cross-border HVDC interconnectors must be expanded by up to 662.0%. Crucially, modeling the Nordic region's coupling to the European continent demonstrates that this reliance on cross-border power trade reduces the system's need for domestic energy storage. By exporting and importing power as needed, the Nordic grid can maintain system stability while minimizing the need for extensive local storage facilities, such as batteries or hydrogen stores.

The evaluation of cost-efficiency reveals an important trade-off between regional and continental optimization. The Flexible Expansion scenario, which allows for expanded vRES growth, provides the most cost-effective solution for the whole European power system, reaching the lowest annualized costs of 80.0 BEUR/year. However, this configuration also pushes the annualized costs for the Nordic region to the highest simulated level of 15.6 BEUR/year. This duality suggests that future Nordic grid investments should be planned in close cooperation with European decision-makers to achieve the lowest overall costs.

In scenarios with extensive wind power expansion, hydrogen electrolysis emerges as a central mechanism for grid balancing. Electrolyzers act as large, flexible loads that can absorb excess wind generation, making Denmark and Finland suitable regions for green hydrogen export. However, the simulated hydrogen demand for the Nordics in the Flexible Expansion scenario reaches up to 412 TWh, which exceeds the current projection from Nordic TSOs of approximately 300 TWh by 2050. This deviation suggests that the highest wind capacities in the results of this study may be overly optimistic, as they depend on a hydrogen export market that may not be in place.

While this study provides a robust technical and economic foundation for the development of a carbon-neutral Nordic grid, translating these optimized pathways into reality will require navigation through socio-political landscapes and local distribution constraints. Rather than viewing these as pure modeling limitations, future research should build upon this study by incorporating multi-year weather variations and addressing public acceptance to simulate actual infrastructure development. Nevertheless, the fundamental finding of the performed study remains clear. Achieving a net-zero Nordic power system by 2050 is feasible through strategic expansion of wind and solar power, alongside essential upgrades of the transmission network.

Ultimately, the transition away from fossil fuels is not just a regional infrastructural challenge, but a critical component of the broader European response to the global climate crisis. Large-scale energy system modeling is an essential tool for navigating the complexities of strict CO_2-emission constraints and high vRES integration. By embracing a highly interconnected power system, the Nordic region can move beyond isolated optimization and serve as a central green energy hub for the European continent. This collaborative approach secures the most cost-optimal pathway for the energy transition, drives the sustainable transformation of our society, and proves that a clean, resilient, and carbon-neutral European energy system is well within reach.

References

[1] Environmental and Energy Study Institute (EESI). Fossil Fuels. Accessed: 2026-01-15. URL: https://www.eesi.org/topics/fossil-fuels/description.

[2] European Commission and Directorate-General for Climate Action. Going climate-neutral by 2050 – A strategic long-term vision for a prosperous, modern, competitive and climate-neutral EU economy. Tech. rep. Accessed: 2026-03-12. Publications Office of the European Union, 2019. URL: https://op.europa.eu/publication-detail/-/publication/92f6d5bc-76bc-11e9-9f05-01aa75ed71a1.

[3] Energinet, Fingrid, Statnett, and Svenska kraftnät. Nordic Grid Development Perspective 2025. Tech. rep. Accessed: 2026-03-12. Nordic Council of Ministers, 2025. URL: https://www.statnett.no/globalassets/for-aktorer-i-kraftsystemet/planer-og-analyser/nordic-grid-development-perspective-2025.pdf.

[4] Statnett SF. Systemutviklingsplan 2025. Tech. rep. Accessed: 2026-03-12. Statnett SF, 2025. URL: https://www.statnett.no/globalassets/for-aktorer-i-kraftsystemet/planer-og-analyser/sup/systemutviklingsplan-2025.pdf.

[5] T. Brown, D. Schlachtberger, A. Kies, S. Schramm, and M. Greiner. Synergies of sector coupling and transmission reinforcement in a cost-optimised, highly renewable European energy system. *Energy* **160**, 720–739, 2018. DOI: 10.1016/j.energy.2018.06.222.

[6] V. Malum. *Large-Scale Optimization of the Nordic Power System in Connection with Statnett's Grid Development Plans using PyPSA*. Master's thesis. Norwegian University of Life Sciences (NMBU), 2024. URL: https://hdl.handle.net/11250/3188543.

[7] M. Saleem. *Exploring Offshore Wind Development in Norway Through Heuristic Modelling*. Master's thesis. Norwegian University of Life Sciences (NMBU), 2024. URL: https://hdl.handle.net/11250/3154057.

[8] World Wide Fund for Nature (WWF). Klimaendringer. Accessed: 2026-01-15. URL: https://www.wwf.no/klima-og-energi/klimaendringer.

[9] International Energy Agency (IEA). World Energy Outlook 2025. Tech. rep. Accessed: 2026-03-12. International Energy Agency, 2025. URL: https://iea.blob.core.windows.net/assets/81980a53-9716-47f1-904e-b92a2c4d2ea4/WorldEnergyOutlook2025.pdf.

[10] United Nations Framework Convention on Climate Change (UNFCCC). The Paris Agreement. Tech. rep. Accessed: 2026-03-12. UNFCC, 2016. URL: https://unfccc.int/sites/default/files/resource/parisagreement_publication.pdf.

[11] World Meteorological Organization (WMO). WMO confirms 2024 as warmest year on record at about 1.55°C above pre-industrial level. Accessed: 2026-02-02. URL: https://wmo.int/news/media-centre/wmo-confirms-2024-warmest-year-record-about-155degc-above-pre-industrial-level.

[12] N. Modig, R. Eriksson, P. Ruokolainen, J. N. Ødegård, S. Weizenegger, and T. D. Fechtenburg. Overview of frequency control in the nordic power system. Tech. rep. Accessed: 2026-03-12. European Network of Transmission System Operators for Electricity (ENTSO-E), 2024. URL: https://eepublicdownloads.blob.core.windows.net/public-cdn-container/clean-documents/SOC%20documents/Nordic/2024/Overview_of_Frequency_Control_in_the_Nordic_Power_System.pdf.
[13] K. Brunak, A. Kofoed-Wiuff, T. Lindroos, and K. Bozhkova. Tracking Nordic Clean Energy Progress 2025. Tech. rep. Accessed: 2026-03-12. Nordic Energy Research, 2025. URL: https://pub.norden.org/nordicenergyresearch2024-05/nordicenergyresearch2024-05.pdf.
[14] International Energy Agency (IEA). Electricity — Europe. Accessed: 2026-01-15. URL: https://www.iea.org/regions/europe/electricity.
[15] K. Hofstad, J. H. Halleraker, and T. H. Bakken for Store Norske Leksikon (SNL). Vannkraft. Accessed: 2026-01-15. URL: https://snl.no/vannkraft.
[16] International Energy Agency (IEA). Energy System of Norway. Accessed: 2026-01-15. URL: https://www.iea.org/countries/norway.
[17] International Energy Agency (IEA). Energy System of Finland. Accessed: 2026-01-15. URL: https://www.iea.org/countries/finland.
[18] International Energy Agency (IEA). Energy System of Denmark. Accessed: 2026-01-15. URL: https://www.iea.org/countries/denmark.
[19] International Energy Agency (IEA). Energy System of Sweden. Accessed: 2026-01-15. URL: https://www.iea.org/countries/sweden.
[20] National Grid and Statnett. North Sea Link. Accessed: 2026-03-10. URL: https://www.northsealink.com/.
[21] E. Nycander and L. Söder. An open dispatch model for the Nordic power system. *Energy Strategy Reviews* **39**, 100775, 2022. DOI: 10.1016/j.esr.2021.100775.
[22] Statnett SF. Langsiktig Markedsanalyse 2024–2050. Tech. rep. Accessed: 2026-03-12. Statnett SF, 2025. URL: https://www.statnett.no/globalassets/for-aktorer-i-kraftsystemet/planer-og-analyser/lma/langsiktig-markedsanalyse-2024-50.pdf.
[23] G. M. Njoka, L. Mogaka, and A. Wangai. Impact of variable renewable energy sources on the power system frequency stability and system inertia. *Energy Reports* **12**, 4983–4997, 2024. DOI: 10.1016/j.egyr.2024.10.057.
[24] European Network of Transmission System Operators for Electricity (ENTSO-E). Dynamic Line Rating (DLR). Accessed: 2026-02-03. URL: https://www.entsoe.eu/technopedia/techsheets/dynamic-line-rating-dlr/.
[25] O. Babatunde, J. Munda, and Y. Hamam. Power system flexibility: A review. *Energy Reports* **6**, 101–106, 2020. DOI: 10.1016/j.egyr.2019.11.048.
[26] Norwegian Water Resources and Energy Directorate (NVE). Tilstanden i kraftsystemet 2025: Kraftåret 2024 og utviklingen fram mot 2029. Tech. rep.

Accessed: 2026-03-12. Norges vassdrags- og energidirektorat (NVE), 2025. URL: https://publikasjoner.nve.no/rapport/2025/rapport2025_10.pdf.

[27] M. Aasen. Nordmenn mer positive til kjernekraft enn vindkraft. Accessed: 2026-01-19. URL: https://cicero.oslo.no/no/artikler/nordmenn-mer-positive-til-kjernekraft-enn-vindkraft.

[28] The Norwegian Energy Regulatory Authority (RME). Water values - how do we ensure that we utilize hydropower in the best possible way? Accessed: 2026-01-20. URL: https://www.nve.no/norwegian-energy-regulatory-authority/the-norwegian-energy-regulatory-authority/water-values-how-do-we-ensure-that-we-utilize-hydropower-in-the-best-possible-way/.

[29] International Energy Agency (IEA). Electricity Market Report - July 2022. Accessed: 2026-01-20. URL: https://www.iea.org/reports/electricity-market-report-july-2022/executive-summary.

[30] Statistisk Sentralbyrå (SSB). Statistics on Electricity prices. Accessed: 2026-03-09. URL: https://www.ssb.no/en/energi-og-industri/energi/statistikk/elektrisitetspriser.

[31] Statnett SF. Kortsiktig Markedsanalyse 2025–2030. Tech. rep. Accessed: 2026-03-12. Statnett SF, 2025. URL: https://www.statnett.no/globalassets/for-aktorer-i-kraftsystemet/planer-og-analyser/kma/kortsiktig-markedsanalyse-2025---2030.pdf.

[32] J. D. Glover and T. J. Overbye. Power System Analysis & Design, SI. 7th ed. Cengage Learning, 2017. ISBN: 978-0-357-67619-6.

[33] J. Graham, E. Heylen, Y. Bian, and F. Teng. Benchmarking explanatory models for inertia forecasting using public data of the Nordic area. *2022 17th International Conference on Probabilistic Methods Applied to Power Systems (PMAPS)* IEEE, 1–6, 2022. DOI: 10.1109/PMAPS53380.2022.9810572.

[34] International Renewable Energy Agency (IRENA). Power System Flexibility for the Energy Transition, Part 1: Overview for policy makers. Tech. rep. Accessed: 2026-03-12. International Renewable Energy Agency, 2018. URL: https://www.irena.org/-/media/Files/IRENA/Agency/%20%20%20%20Publication/2018/Nov/IRENA_Power_system_flexibility_1_2018.pdf.

[35] J. DeCarolis, H. Daly, P. Dodds, I. Keppo, F. Li, W. McDowall, S. Pye, N. Strachan, E. Trutnevyte, W. Usher, M. Winning, S. Yeh, and M. Zeyringer. Formalizing best practice for energy system optimization modelling. *Applied Energy* **194**, 184–198, 2017. DOI: 10.1016/j.apenergy.2017.03.001.

[36] S. Pfenninger, A. Hawkes, and J. Keirstead. Energy systems modeling for twenty-first century energy challenges. *Renewable and Sustainable Energy Reviews* **33**, 74–86, 2014. DOI: 10.1016/j.rser.2014.02.003.

[37] J. Hörsch, F. Hofmann, D. Schlachtberger, and T. Brown. PyPSA-Eur: An open optimisation model of the European transmission system. *Energy Strategy Reviews* **22**, 207–215, 2018. DOI: 10.1016/j.esr.2018.08.012.

[38] Statistisk sentralbyrå (SSB). Elektrisitet. Accessed: 2026-01-08. URL: https://www.ssb.no/energi-og-industri/energi/statistikk/elektrisitet.

[39] H. Eide. *Exploring Offshore Wind Development in Norway Through Heuristic Modelling*. Master's thesis. Norwegian University of Life Sciences (NMBU), 2024. URL: https://hdl.handle.net/11250/3209207.

[40] I. A. Bermejo, H. Foretić, and V. Kopustinskas. Modelling Power Disruption Scenarios and Assessing Resilience of a Power System. 1st ed. Research Publishing, Singapore, 2025. ISBN: 978-981-94-3281-3. DOI: 10.3850/978-981-94-3281-3_ESREL-SRA-E2025-P4584-cd.

[41] A. D. Bella, T. Seibold, T. Brown, and M. Tavoni. Pursuing decarbonization and competitiveness: a narrow corridor for European green industrial transformation. Accessed: 2026-03-12. URL: https://arxiv.org/pdf/2510.08199.

[42] P. Glaum, F. Neumann, and T. Brown. Offshore power and hydrogen networks for Europe's North Sea. *Applied Energy* **369**, 123530, 2024. DOI: 10.1016/j.apenergy.2024.123530.

[43] A. Pampado, D. Fioriti, and D. Poli. Exploring Uncertainties in Future Power Systems: Methodology and Analysis for Italy 2040. *2025 IEEE International Conference on Environment and Electrical Engineering and 2025 IEEE Industrial and Commercial Power Systems Europe (EEEIC / ICPS Europe)* 1–6, 2025. DOI: 10.1109/EEEIC/ICPSEurope64998.2025.11169239.

[44] Terna SpA and Snam SpA. Documento di descrizione degli scenari 2024. Tech. rep. Accessed: 2026-03-12. Terna SpA, 2024. URL: https://download.terna.it/terna/Documento_Descrizione_Scenari_2024_8dce2430d44d101.pdf.

[45] F. Fristed, S. Tønning, Z. Xie, L. Langer, and G. B. Andresen. Early cross-sector decarbonisation for Europe's hard-to-abate sectors: Insights from Denmark's 2030 target. *Applied Energy* **401**, 126568, 2025. DOI: 10.1016/j.apenergy.2025.126568.

[46] E. F. Bødal, S. E. Holm, A. Subramanian, G. Durakovic, D. Pinel, L. Hellemo, M. M. Ortiz, B. R. Knudsen, and J. Straus. Hydrogen for harvesting the potential of offshore wind: A North Sea case study. *Applied Energy* **357**, 122484, 2024. DOI: 10.1016/j.apenergy.2023.122484.

[47] L. Mæhlum and K. A. Rosvold for Store Norske Leksikon (SNL). Overføringsnett. Accessed: 2026-01-22. URL: https://snl.no/overf%C3%B8ringsnett.

[48] K. A. Rosvold for Store Norske Leksikon (SNL). Nettfrekvens. Accessed: 2026-01-23. URL: https://snl.no/frekvens_-_nettfrekvens.

[49] K. Hostad for Store Norske Leksikon (SNL). Transmission System Operators. Accessed: 2026-01-22. URL: https://snl.no/Transmission_System_Operators.

[50] Energifakta Norge. Strømnettet. Accessed: 2026-01-22. URL: https://energifaktanorge.no/norsk-energiforsyning/kraftnett/.

[51] Institute of Electrical and Electronics Engineers, Power and Energy Society (IEEE-PES). Stability definitions and characterization of dynamic behavior in systems with high penetration of power electronic interfaced technologies. Tech. rep. Accessed: 2026-03-12. Institute of Electrical and Electronics Engineers, 2020. DOI: 10.17023/zwwp-vv02.
[52] T. Wildi. Electrical Machines, Drives and Power Systems. 6th ed. Pearson Prentice Hall, 2006. ISBN: 978-1-292-02458-5.
[53] K. Mermer for Envelio. N-1 contingency analysis in modern power grids. Accessed: 2026-01-23. URL: https://envelio.com/insights/n-1-contingency-analysis-automation-software-medium-voltage-grids.
[54] PyPSA Contributors. PyPSA - Python for Power System Analysis. Accessed: 2026-01-26. URL: https://github.com/PyPSA/PyPSA.
[55] PyPSA Contributors. PyPSA-Eur: A Sector-Coupled Open Optimisation Model of the European Energy System. Accessed: 2026-01-26. URL: https://github.com/PyPSA/pypsa-eur.
[56] PyPSA Contributors. Linear Power Flow. Accessed: 2026-01-30. URL: https://docs.pypsa.org/latest/user-guide/linear-power-flow/.
[57] B. Xiong, D. Fioriti, F. Neumann, I. Riepin, and T. Brown. Prebuilt Electricity Network for PyPSA-Eur based on OpenStreetMap Data. Accessed: 2026-03-12. URL: https://zenodo.org/records/14144752.
[58] Copernicus. Climate Reanalysis. Accessed: 2026-01-26. URL: https://climate.copernicus.eu/climate-reanalysis#.
[59] Copernicus. CORINE Land Cover. Accessed: 2026-01-26. URL: https://land.copernicus.eu/en/products/corine-land-cover.
[60] European Environment Agency (EEA). Natura 2000 Viewer. Accessed: 2026-01-26. URL: https://natura2000.eea.europa.eu/.
[61] PyPSA Contributors. Base Network. Accessed: 2026-02-04. URL: https://pypsa-eur.readthedocs.io/en/latest/data-base-network.html.
[62] F. Gotzens, H. Heinrichs, J. Hörsch, and F. Hofmann. Performing energy modelling exercises in a transparent way - The issue of data quality in power plant databases. *Energy Strategy Reviews* **23**, 1–12, 2019. DOI: 10.1016/j.esr.2018.11.004.
[63] PyPSA Contributors. Design - Documentation. Accessed: 2026-01-28. URL: https://docs.pypsa.org/latest/user-guide/design/.
[64] PyPSA Contributors. Line - Documentation. Accessed: 2026-01-28. URL: https://docs.pypsa.org/latest/user-guide/components/lines/.
[65] PyPSA Contributors. Link - Documentation. Accessed: 2026-01-28. URL: https://docs.pypsa.org/latest/user-guide/components/links/.
[66] PyPSA Contributors. pypsa-eur/config /config.default.yaml at master PyPSA/pypsa-eur. Accessed: 2026-01-28. URL: https://github.com/PyPSA/pypsa-eur/blob/master/config/config.default.yaml.

[67] PyPSA Contributors. Energy Balances. Accessed: 2026-01-28. URL: https://docs.pypsa.org/latest/user-guide/optimization/energy-balance/.

[68] PyPSA Contributors. Optimization - Objective. Accessed: 2026-01-28. URL: https://docs.pypsa.org/latest/user-guide/optimization/objective/.

[69] PyPSA Contributors. Optimization - Overview. Accessed: 2026-01-29. URL: https://docs.pypsa.org/latest/user-guide/optimization/overview/.

[70] PyPSA Contributors. Optimization - Capacity Limits. Accessed: 2026-01-29. URL: https://docs.pypsa.org/latest/user-guide/optimization/capacity-limits/.

[71] PyPSA Contributors. Optimization - Dispatch Limits. Accessed: 2026-01-29. URL: https://docs.pypsa.org/latest/user-guide/optimization/dispatch-limits/.

[72] PyPSA Contributors. Optimization - Storage. Accessed: 2026-01-29. URL: https://docs.pypsa.org/latest/user-guide/optimization/storage/.

[73] PyPSA Contributors. Optimization - Power Flow. Accessed: 2026-01-29. URL: https://docs.pypsa.org/latest/user-guide/optimization/power-flow/.

[74] PyPSA Contributors. Optimization - Contingencies. Accessed: 2026-01-30. URL: https://docs.pypsa.org/latest/user-guide/optimization/contingencies/.

[75] PyPSA Contributors. Documentation - Overview. Accessed: 2026-01-30. URL: https://docs.pypsa.org/latest/user-guide/user-guide/.

[76] PyPSA Contributors. Limitations. Accessed: 2026-02-13. URL: https://pypsa-eur.readthedocs.io/en/latest/limitations.html.

[77] PyPSA Contributors. Data Sources - Data Inventory. Accessed: 2026-02-04. URL: https://pypsa-eur.readthedocs.io/en/latest/data_sources.html#data-inventory.

[78] PyPSA Contributors. Configuration - Data. Accessed: 2026-02-04. URL: https://pypsa-eur.readthedocs.io/en/latest/configuration.html#data.

[79] F. Neumann and J. Hörsch. One-node-per-country clustering becomes infeasible. Accessed: 2026-02-05. URL: https://github.com/PyPSA/pypsa-eur/issues/24.

[80] Elia Transmission Belgium (ETB). Belgian Electricity System Blueprint for 2035-2050. Tech. rep. Accessed: 2026-03-12. ETB, 2024. URL: https://www.elia.be/en/newsroom/2024/09/20240924_elia-publishes-blueprint-for-the-belgian-electricity-system-2035-2050.

[81] Le Réseau de Transport d'Électricité (RTE). Energy Pathways to 2050. Tech. rep. Accessed: 2026-03-12. RTE, 2021. URL: https://assets.rte-france.com/prod/public/2022-01/Energy%20pathways%202050_Key%20results.pdf.

[82] 50Hertz Transmission GmbH, Amprion GmbH, TenneT TSO GmbH, and TransnetBW GmbH. Netzentwicklungsplan Strom 2037 mit Ausblick 2045, Version 2025, Erster Entwurf. Tech. rep. Accessed: 2026-03-12. Übertragungsnetzbetreiber (ÜNB), 2025. URL: https://www.netzentwicklungsplan.de/sites/default/files/2025-12/NEP_2037_2045_V2025_1_Entwurf.pdf.

[83] National Energy System Operator (NESO). Future Energy Scenarios: Pathways to Net Zero. Tech. rep. Accessed: 2026-03-12. NESO, 2025. URL: https://www.neso.energy/document/364541/download.

[84] J. Warnaars, M. Kellner, and R. Martens. 2030-2050 Integrated Infrastructure Outlook. Tech. rep. Accessed: 2026-03-12. Netbeheer Nederland, 2023. URL: https://www.energiekompas2050.nl/wp-content/uploads/2024/01/II3050-Main-Report-20240118-1.pdf.

[85] A. Covey, R. Pupa, M. Lai, A. Gole, N. Randazzo, B. Lee, S. Litvin, S. MacGregor, L. Mau, E. Stone, Y. Xue, E. Takekawa, M. Huy, G. Wu, and R. Deshmukh. Empirical estimates of installed capacity density for solar photovoltaic and onshore and offshore wind power plants. *Environmental Research: Infrastructure and Sustainability* **6**, 015005, 2026. DOI: 10.1088/2634-4505/ae437f.

[86] European Association for Storage of Energy (EASE). Pumped hydro Storage. Tech. rep. Accessed: 2026-03-12. EASE, 2016. URL: https://energystorageeurope.eu/wp-content/uploads/2016/07/EASE_TD_Mechanical_PHS.pdf.

[87] PyPSA Contributors. Configuration. Accessed: 2026-02-12. URL: https://pypsa-eur.readthedocs.io/en/latest/configuration.html.

[88] European Network of Transmission System Operators for Electricity (ENTSO-E). Transparency Platform. Accessed: 2026-02-12. URL: https://transparency.entsoe.eu/.

[89] M. Harrison. Valuing the Future: the social discount rate in cost-benefit analysis. Tech. rep. Accessed: 2026-03-12. Productivity Commission, 2010. URL: https://assets.pc.gov.au/research/supporting/cost-benefit-discount/cost-benefit-discount.pdf.

[90] PyPSA Contributors. Technology Data - Outputs. Accessed: 2026-02-13. URL: https://github.com/PyPSA/technology-data/blob/master/outputs/costs_2050.csv.

[91] U. Pfeifroth, J. Drücke, S. Kothe, J. Trentmann, M. Schröder, and R. Hollmann. SARAH-3 – satellite-based climate data records of surface solar radiation. *Earth System Science Data* **16**(11), 5243–5265, 2024. DOI: 10.5194/essd-16-5243-2024.

[92] PyPSA Contributors. Limitations. Accessed: 2026-02-16. URL: https://pypsa-eur.readthedocs.io/en/latest/preparation.html.

[93] Norwegian Water Resources and Energy Directorate (NVE). Kraftproduksjon. Accessed: 2026-02-16. URL: https://www.nve.no/energi/energisystem/kraftproduksjon/.

[94] Statistical Database (SCB). Gross generation, installed generator capacity and number of plants. Year 2015 – 2024. Accessed: 2026-02-16. URL: https://www.statistikdatabasen.scb.se/pxweb/en/ssd/START__EN__EN0105__EN0105A/AnlInstEffBrProd/.

[95] International Renewable Energy Agency (IRENA). Energy Profile Denmark. Tech. rep. Accessed: 2026-03-12. IRENA, 2025. URL: https://www.irena.org/-/media/Files/IRENA/Agency/Statistics/Statistical_Profiles/Europe/Denmark_Europe_RE_SP.pdf.

[96] Offshore Coalition for Energy and Nature (OCEaN). Accelerating Offshore Wind and Nature Protection – Country Profile Denmark. Tech. rep. Accessed: 2026-03-12. OCEaN, 2024. URL: https://offshore-coalition.eu/wp-content/uploads/2025/03/Denmark_Factsheet_FINAL_country-profile.pdf.

[97] International Renewable Energy Agency (IRENA). Energy Profile Finland. Tech. rep. Accessed: 2026-03-12. IRENA, 2025. URL: https://www.irena.org/-/media/Files/IRENA/Agency/Statistics/Statistical_Profiles/Europe/Finland_Europe_RE_SP.pdf.

[98] Renewables Finland. Offshore wind power. Accessed: 2026-02-16. URL: https://suomenuusiutuvat.fi/en/wind-power/offshore-wind-power/.

[99] D. W. Almeida, A. H. M. S. M. S. Abeysinghe, and J. B. Ekanayake. Analysis of Rooftop Solar Impacts on Distribution Networks. *Ceylon Journal of Science* **48**(2), 103–112, 2019. DOI: 10.4038/cjs.v48i2.7614.

[100] P. Nielsen. Danish Wind energy index ver.13 update. Tech. rep. Accessed: 2026-03-12. EMD International AS, 2013. URL: https://www.vindstat.dk/PDF_sider/Windindex_DK_ver%2013_update.pdf.

[101] Arise AB. Year-End Report 1 January – 31 December 2013. Tech. rep. Accessed: 2026-03-12. Arise AB, 2014. URL: https://www.arise.se/sites/default/files/pr/201402133321-1.pdf?ts=1708702035.

[102] Ø. Aas, M. Qvenild, L. C. Wold, G. B. Jacobsen, and A. Ruud. Local opposition against high-voltage grids: public responses to agency-caused science–policy trolls. *Journal of Environmental Policy & Planning* **19**(4), 347–359, 2017. DOI: 10.1080/1523908X.2016.1213625.

A Additional Results

Table A.1: Installed capacities of extendable, renewable generation carriers in non-Nordic countries in 2050. The capacities are shown for all four scenarios, in addition to the existing capacities within the model. At the end, the system total is listed, which includes the Nordic capacities from Table 5.2. The scenarios are abbreviated as existing capacities (EC), Baseline Values ± 10% (BV), Solar Expansion (SE), Wind Expansion (WE), and Flexible Expansion (FE). All values are given in GW.

Country/ Scenario		**Solar**	**Solar Rooftop**	**Solar HSAT**	**Onshore Wind**	**Offshore Wind**	**Total**
Belgium	EC	9.8	0.0	0.0	3.3	2.3	**15.4**
	BV	8.9	23.2	9.5	8.6	5.5	**55.7**
	SE	8.9	23.2	9.5	8.6	5.2	**55.4**
	WE	8.9	23.2	7.7	8.6	5.2	**53.6**
	FE	8.9	23.2	5.3	8.6	5.5	**51.5**
Germany	EC	89.9	0.0	0.0	57.5	9.2	**156.6**
	BV	71.9	162.5	197.5	171.0	63.0	**665.9**
	SE	71.9	162.5	197.5	171.0	63.0	**665.9**
	WE	71.9	162.5	197.5	171.0	63.0	**665.9**
	FE	71.9	162.5	197.5	171.0	63.0	**665.9**
France	EC	21.5	0.0	0.0	23.1	1.5	**46.1**
	BV	20.5	53.8	2.7	38.7	22.5	**138.2**
	SE	20.5	53.8	2.7	38.7	22.5	**138.2**
	WE	20.5	53.8	2.7	38.7	22.5	**138.2**
	FE	20.5	53.8	2.7	38.7	23.9	**139.6**
Great Britain	EC	17.9	0.0	0.0	15.8	15.9	**49.6**
	BV	17.8	55.4	33.5	52.2	114.8	**273.7**
	SE	17.8	55.4	33.5	52.2	114.4	**273.3**
	WE	17.8	55.4	33.5	52.2	114.3	**273.2**
	FE	17.8	88.9	0.0	52.2	114.8	**273.7**
Nether-lands	EC	24.0	0.0	0.0	6.5	4.7	**35.2**
	BV	24.0	30.6	100.8	22.0	64.8	**242.2**
	SE	24.0	30.6	100.8	22.0	64.8	**242.2**
	WE	42.5	30.6	82.2	22.0	64.8	**242.1**
	FE	42.5	30.6	82.2	22.0	64.8	**242.1**
System Total	EC	**163.1**	**0.0**	**0.0**	**106.2**	**33.6**	**302.9**
	BV	**153.5**	**358.4**	**407.1**	**387.3**	**321.0**	**1627.3**
	SE	**153.5**	**362.3**	**469.5**	**387.2**	**317.6**	**1690.1**
	WE	**172.0**	**360.6**	**385.3**	**466.7**	**328.9**	**1713.5**
	FE	**172.0**	**397.7**	**420.2**	**466.7**	**339.7**	**1796.3**

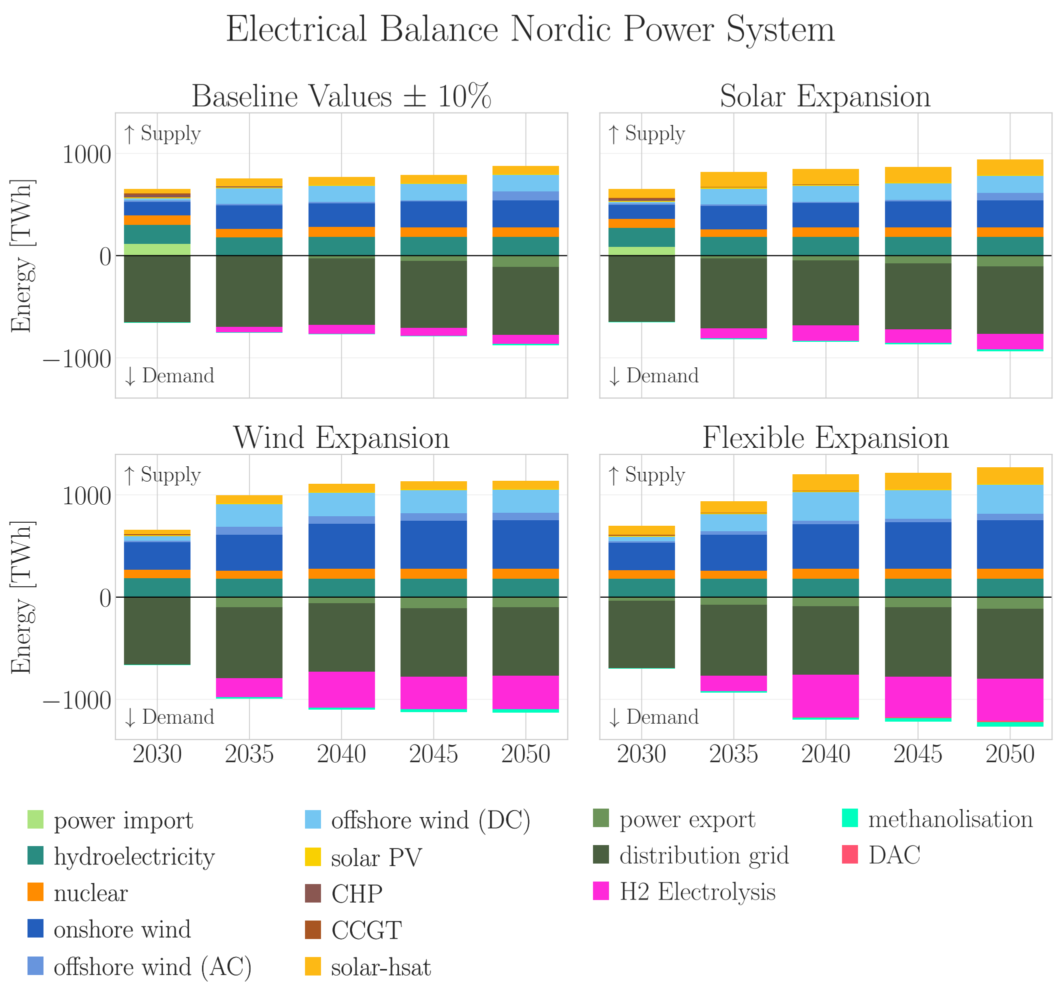

Figure A.1: Electrical balance of the Nordic power system for all planning horizons. Electrical supply is shown as positive values and demand is shown as negative values, and the Nordic power system is balanced in all horizons.

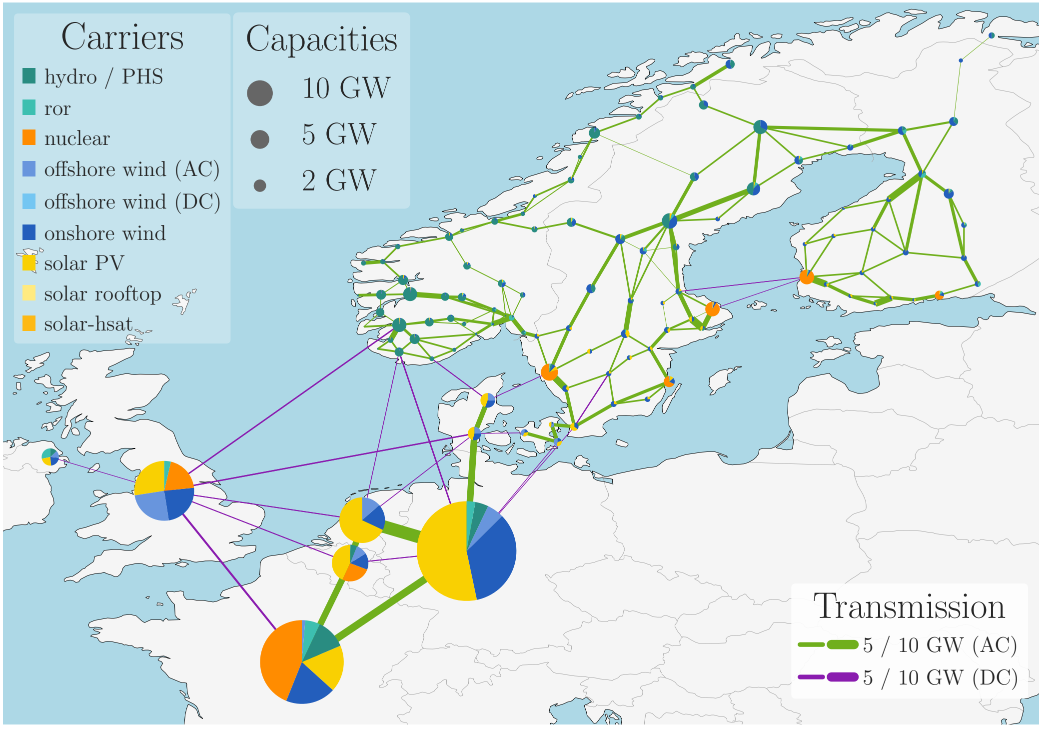

Figure A.2: Existing installed capacities of renewable generators, transmission lines and HVDC links in the model, for 2025. The system is clustered into 110 nodes, connected by lines and HVDC links. All countries outside the Nordic region are clustered into one node per country, resulting in very large buses for these countries and their connecting lines and links.

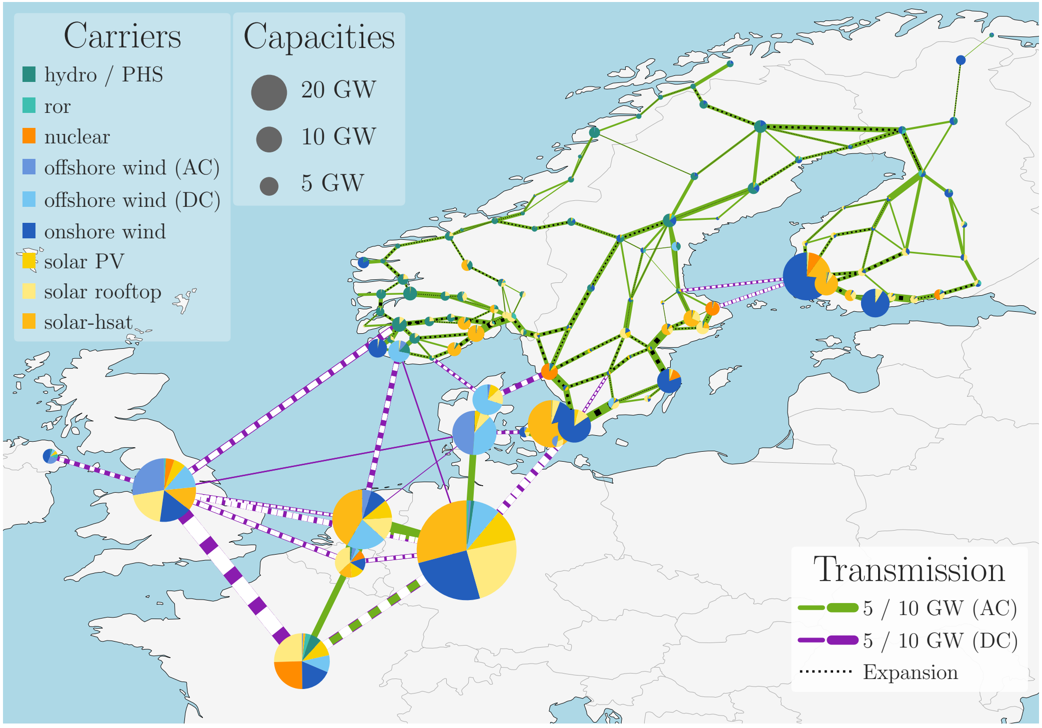

(a) Baseline Values ± 10%

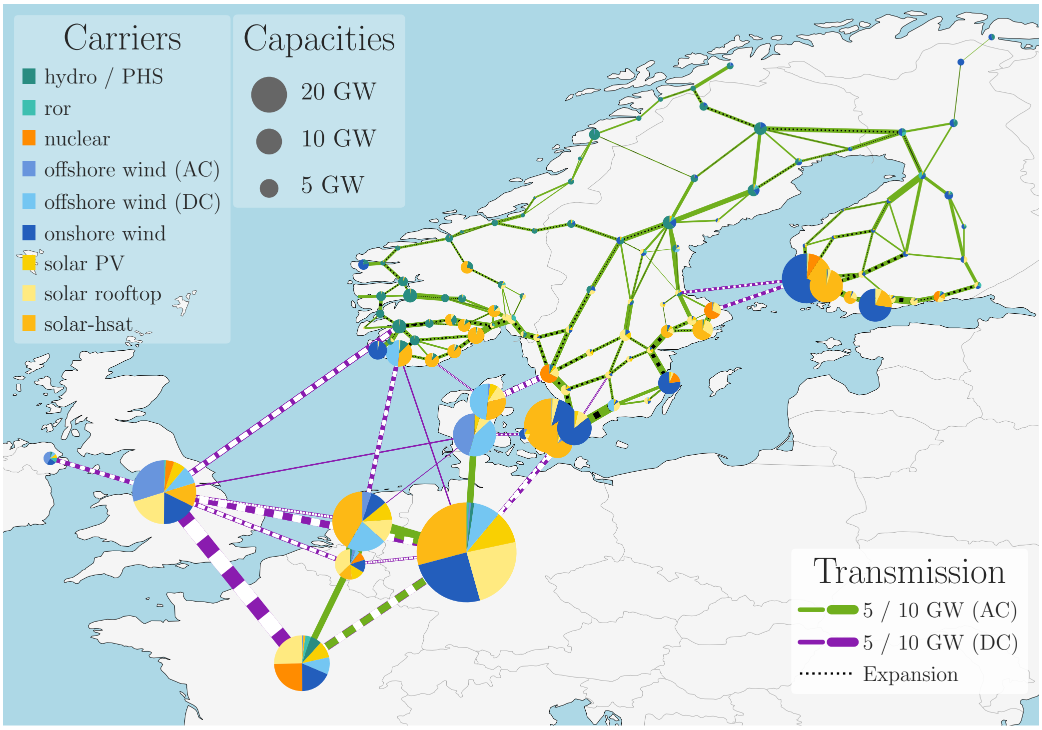

(b) Solar Expansion

Figure A.3: Installed capacities of generation and transmission in the modeled system, under the scenarios Baseline Values ± 10% (a) and Solar Expansion (b). The sizes of non-Nordic buses have been scaled down to 25% for visibility purposes, and thus the legend does not apply to these.

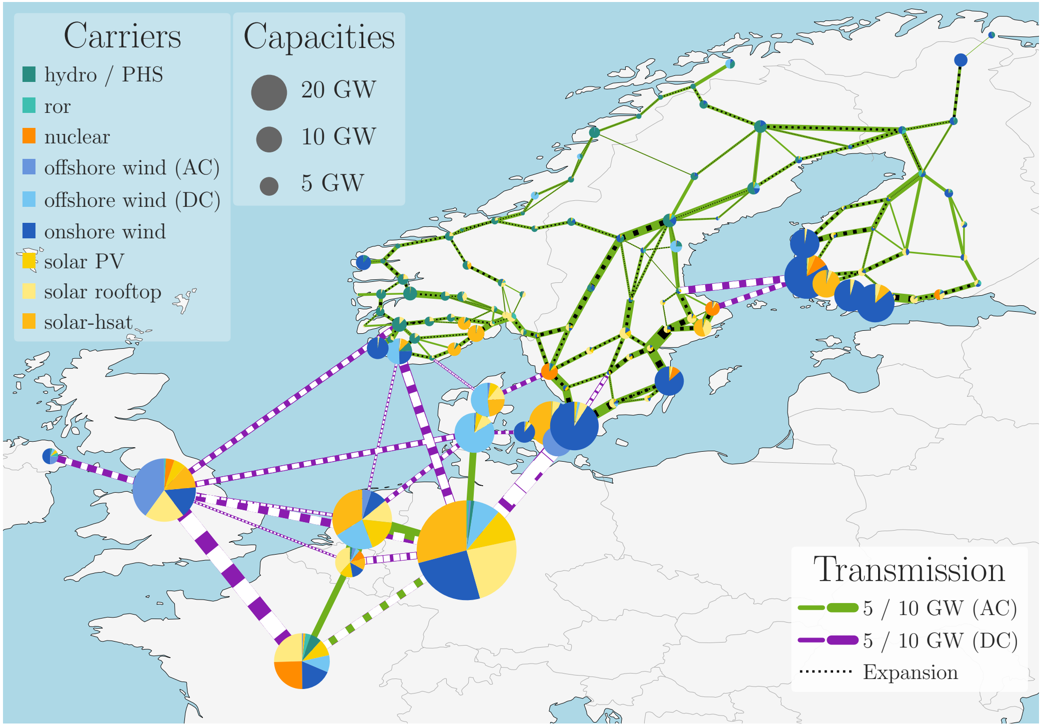

(a) Wind Expansion

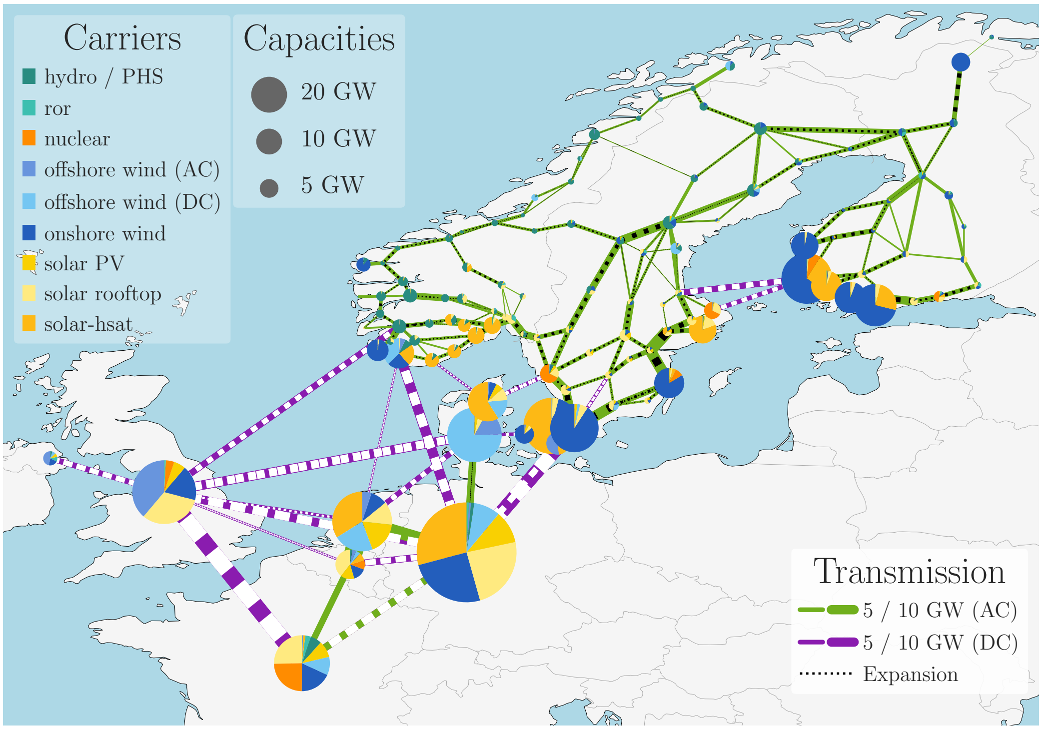

(b) Flexible Expansion

Figure A.4: Installed capacities of generation and transmission in the modeled system, under the scenarios Wind Expansion (a) and Flexible Expansion (b). The sizes of non-Nordic buses have been scaled down to 25% for visibility purposes, and thus the legend does not apply to these.

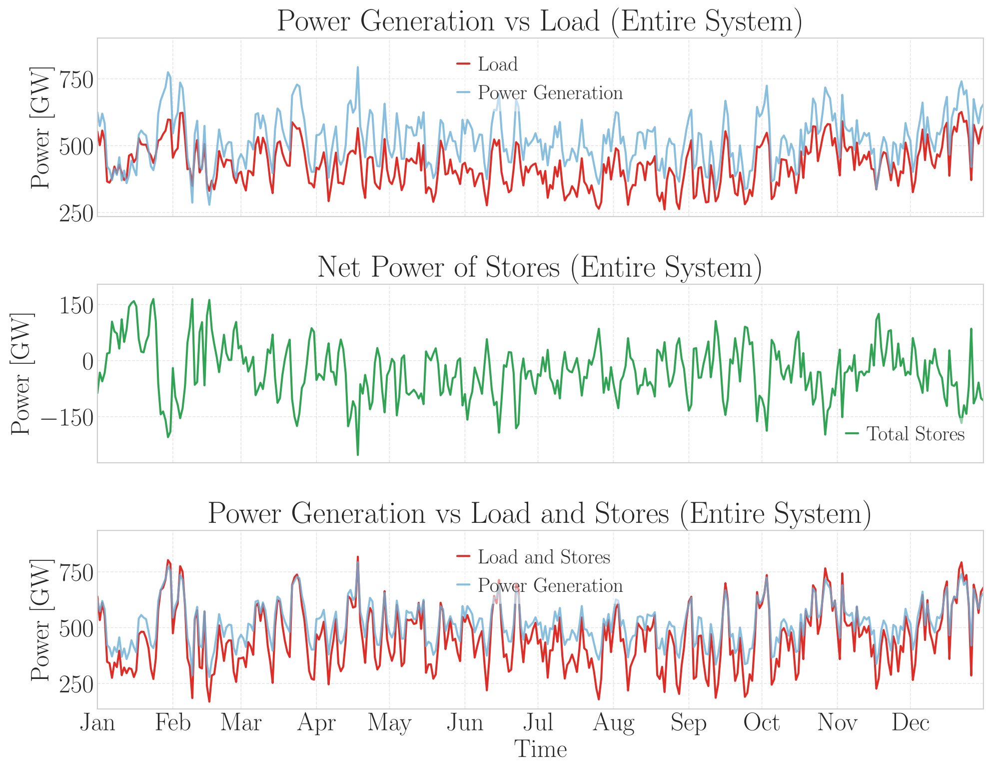

Figure A.5: Power generation, load, and net power of stores for the entire simulated system in 2050, under the Baseline Values ± 10% scenario.

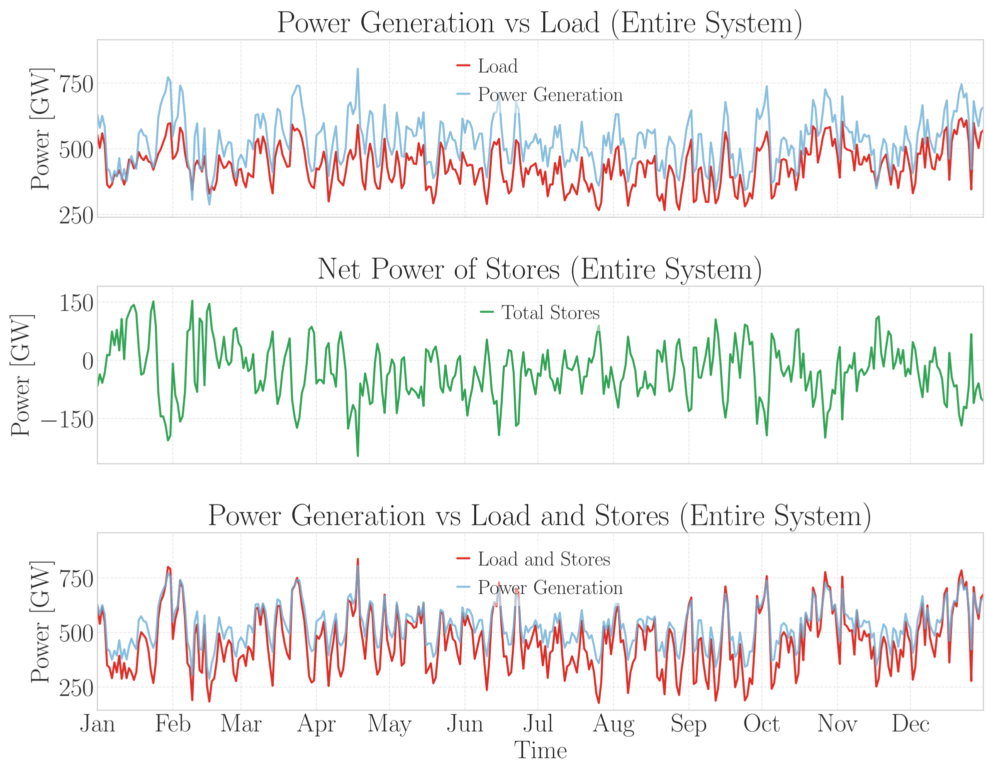

Figure A.6: Power generation, load, and net power of stores for the entire simulated system in 2050, under the Solar Expansion scenario.

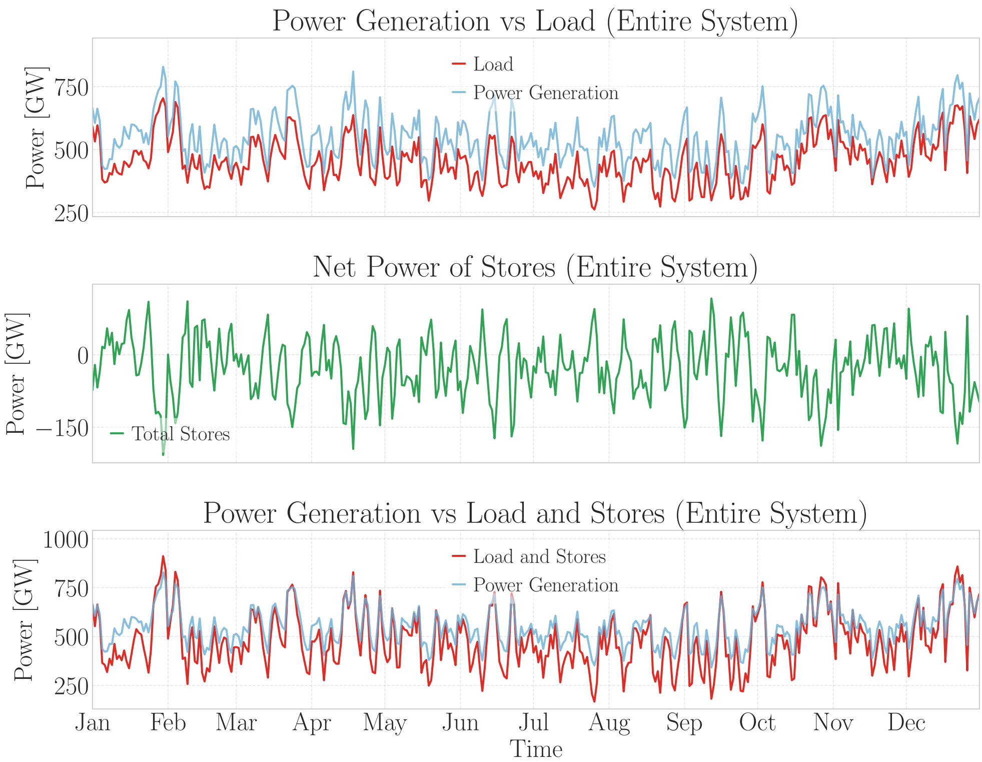

Figure A.7: Power generation, load, and net power of stores for the entire simulated system in 2050, under the Wind Expansion scenario.

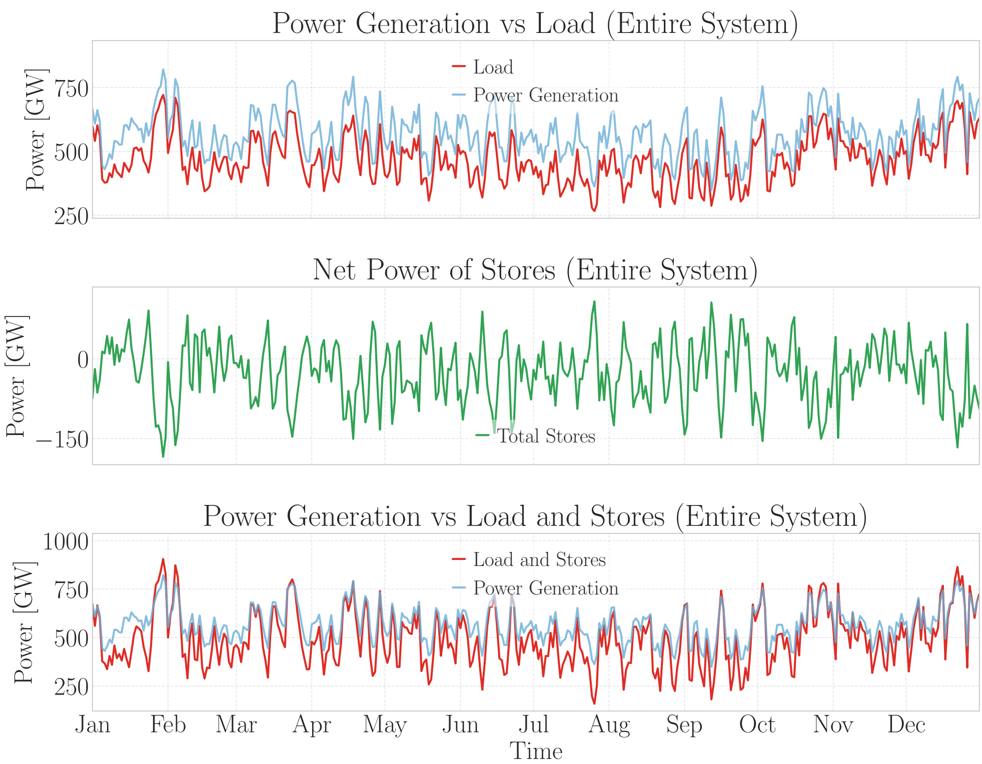

Figure A.8: Power generation, load, and net power of stores for the entire simulated system in 2050, under the Flexible Expansion scenario.

Norges miljø- og biovitenskapelige universitet
Noregs miljø- og biovitskaplege universitet
Norwegian University of Life Sciences

Postboks 5003
NO-1432 Ås
Norway